Towards Fluorinated Substrate Analogs and N-Acylated 2-Aminopyrimidine Inhibitors of Lipoxygenases

By
Meghan Lynn Haycock

Thesis submitted to the Department of Chemistry in conformity with the requirements for

the degree of Master of Science

University of Ottawa
Ottawa, Ontario, Canada
(May 2014)

Abstract

Cyclooxygenase (COX) and lipoxygenase (LOX) catalyze the rate-determining step in the production of arachidonic acid- derived signaling molecules (eicosanoids) within the body. COX has been extensively investigated, which has enabled the design of non-steroidal inflammatory drugs (NSAIDs) such as aspirin, acetaminophen (ApAP) and ibuprofen. However, there are still fundamental questions surrounding the LOX family of enzymes, which has limited the development of isoform specific inhibitors. The structural basis and regio- and stereoselectivity of the LOX isoforms are not known. Herein, we describe two strategies to develop isoform-specific inhibitors of lipoxygenase.

Efforts were focused on the synthesis of unnatural lipid derivatives, in which the methylene hydrogen atoms on the substrate were replaced with a moiety lacking a labile hydrogen atom, such as fluorine. This would allow the LOX enzyme to remain in an active form, while preventing enzyme turnover. This preliminary work will enable the assessment of their activity as inhibitors and attempts at their co-crystallization might provide the first insight into the binding mode of these fatty acid substrates.

The preparation of a small library of acylated 2-aminopyrimidines and their efficacy as inhibitors of soybean lipoxygenase-1 was explored. Preliminary studies suggest the mode of action occurs through a bi-dentate coordination of the ferric iron atom. Modifications of the acylated 2-aminopyrimidines to make it more substrate-like and to increase its lipophilicity, yielded inhibitors with low micromolar IC_{50} values. With further optimization, acyl 2-aminopyrimidines could serve as a useful platform for the discovery of safe and efficient isoform specific inhibitors.

Acknowledgements

I would like to thank my supervisor, Dr. Derek Pratt, for giving me the opportunity to be a part of his research group. Your guidance and patience was much appreciated. Your enthusiasm and knowledge for chemistry is admirable.

I would also like to thank the members of the Pratt group past and present. To Dr. Jason Hanthorn for showing me how to become a "master" at flash column chromatography. To Dr. Gavin Zheng for being patient and reminding me that, "It's okay, it's okay". Evan Haidasz and Ron Shah for their vast knowledge about our compounds. JP Chauvin for countless laughs and arguments on pronunciation. To Zosia Zielinski and Shelby Allison for being such supportive lab mates and friends. To the rest of my lab comrades, thanks for making the past two years fun. I know each and every one of you will miss my great country tunes!!!

Thank you to the Ottawa Swans for having my back both on and off the field. To my three amigos Holly, Amanda and Cat, the support, laughs, and car rides made everything better!

A special thank you to all of my friends. Your visits and encouraging words and understanding have been much appreciated.

Finally, I need to give a huge shout out to my wonderful and incredibly supportive family. A big thank you to my parents, Sharon and Keith without their help and encouragement this would not be possible. To my little brother Matty, for his impeccably timed visits and continuous comic relief. To my pops, for always being so proud of whatever I do. And to my "sister" Jenna who is always reminding me to keep my stick on the ice. Thanks folks…. I went from Get 'er done, to got 'er did!!!

Statement of Originality

I hereby certify that all of the work described within this thesis is the original work of the author. Any published (or unpublished) ideas and/or techniques from the work of others are fully acknowledged in accordance with the standard referencing practices.

Meghan Haycock

May, 2014

Table of Contents

Title Page i

Abstract ii

Acknowledgements iii

Statement of Originality iv

Table of Contents v

List of Tables ix

List of Schemes x

List of Figures xiv

Chapter 1-Introduction 1

1.0 Introduction 2

1.1 Polyunsaturated Fatty Acids 3

1.2 Lipid Autoxidation 5

1.3 Enzyme Mediated Lipid Peroxidation 10

1.4 Prostaglandins 12

1.5 Leukotrienes 14

1.6 Cyclooxygenase: Structure and Mechanism 16

1.7 Lipoxygenases: Structure and Mechanism 18

1.7.1 Human 5-Lipoxygenase 21

1.7.2. 15*S*-Lipoxygenase 25

1.7.3. 12-Lipoxygenase 25

1.7.4. Other Isoforms 26

1.8. Discovery of Inhibitors for COX and LOX Activity 28

1.8.1 Cyclooxygenase Inhibition by NSAIDs 28

1.8.2. Lipoxygenase Inhibition 32

1.9 Project Proposal 34

1.10. References 35

Chapter 2- Towards Fluorinated Substrate Analogs for Lipoxygenases 39

2.0 Introduction 40

2.1 Proposed Synthesis of 11,11-Difluorolinoleic acid 45

2.2 Synthesis of the C1-C9 Phosphonium Salt **2.6** 48

2.3 Synthesis of the C10-C18 α,α-Difluoroaldehyde **2.5** 50

2.4 A Cu-Catalyzed Cross Coupling Approach to the C10-C18 Fragment 57

2.5 Reduction of the Ester Moiety of **2.11** 61

2.6 Polarity Reversal of the Triphenylphosphonium Ylide 65

2.7 Alternative Approaches to Ester **2.11** 67

2.8 Conclusion & Future Work 76

2.9 Reference 81

Chapter 3- N-Acylated 2-Aminopyrimidines as Potential Inhibitors of Lipoxygenase 83

3.0 Introduction 84

3.1 Results and Discussion 91

3.1.1 Synthesis of O-Benzylated Pyri(mi)dine Analog of Acetaminophen 92

3.1.2 pK_a Measurements of O-Benzylated Pyri(mi)dine Analog of Acetaminophen 94

3.1.3 Synthesis of 5-Hydroxy N-Acylated 2-Aminopyrimidines 97

3.1.3.1 Bromination of 2-Aminopyrimidine 98
3.1.3.2 Addition of a 2,4-Dimethylpyrrole Protecting Group 98
3.1.3.3 Copper-catalyzed C-O Coupling 99
3.1.3.4 Removal of 2,4-Dimethylpyrrole Protecting Group 100
3.1.3.5 Acylation of 2-Aminopyrimidines 101
3.1.3.6 Hydrogenation of the N-Acetylated 2-Aminopyrimidines 103
3.1.4. The sLOX-1 Catalyzed Oxidation of Linoleic Acid to give 13-HPODE 104
3.1.4.1. Kinetics of sLOX-1 Catalyzed Oxidation of Linoleic Acid 104
3.1.4.2 Inhibition of sLOX-1 with N-Acylated 2-Aminopyrimidinols 106
3.1.4.3. Inhibition of sLOX-1 with N-Acylated 2-amino-5-Benzoxylpyrimidines 108
3.1.4.4 Stability Studies of Lipophilic N-Acylated 2-Aminopyrimidinols 110
3.1.5. Synthesis of 5-Alkyloxy N-Acylated 2-Aminopyrimidines 113
3.1.5.1 General Reaction Conditions to Introduce an Alkyl Chain in Position 5 113
3.1.5.2 New Synthetic Approach to Introduce Alkyl Groups 114

3.1.5.3 Deprotection of the 2,4-Dimethylpyrrole Group on the Alkoxy Compounds 116
3.1.6. Synthesis of 5-Alkyl N-Acylated 2-Aminopyrimidines 117
3.1.6.1 Sonagashira Cross Coupling to Produce 5-Alkynyl 2-Aminopyrimidines 118
3.1.6.2 Hydrogenation of 5-Alkynyl 2-Aminopyrimidines 119
3.1.6.3 Acylation of 5-alkyl-2-aminopyrimidines 120
3.1.7 Inhibition Studies on sLOX-1 activity with acylated 5-hexyl-2-aminopyrimidines 120
3.2 Conclusions 122
3.3 References 127
Chapter 4-Experimental Methods **129**
4.1 General 130
4.2 Preparation of Compounds Described in Chapter 2 130
4.3 Preparation of Compounds Described in Chapter 3 150
4.4 Spectrophotometric Determination of pK_a Values 165
4.5 Inhibition of sLOX-1 165
4.6 Oxidative Stability Experiments 166
4.6.1 Under Air 166
4.6.2 Under Argon 166
4.7 References 167

List of Tables:

Table 1.1. Structures of common saturated and unsaturated fatty acids. 2

Table 2.1. A list of palladium sources and ligands tested in a Negishi type cross coupling reactions. 56

List of Schemes:

Scheme 1.1. Enzyme catalyzed transformation of linoleic acid to arachidonic acid. 4

Scheme 1.2. The radical chain mechanism of hydrocarbon autoxidation. 5

Scheme 1.3. Reactivities of saturated, monounsaturated and polyunsaturated fatty acids and their esters to oxidative stress. 6

Scheme 1.4. Products of methyl linoleate free radical oxidation. 7

Scheme 1.5. Mechanism and distribution of methyl linoleate autoxidation. 8

Scheme 1.6. Primary products of Arachidonic Acid Peroxidation. 9

Scheme 1.7. Arachidonic acid peroxidation via 5-lipoxygenase pathway and the prostaglandin pathway. 11

Scheme 1.8. The biosynthesis of prostaglandins from the sequential oxidation of arachidonic acid by cyclooxygenase enzymes and terminal prostaglandin synthases. 13

Scheme 1.9. The biosynthesis of leukotrienes from the sequential oxidation of arachidonic acid by lipoxygenase enzymes and leukotriene hydrolases or leukotriene synthases. 15

Scheme 1.10. Chemical transformation of Arachidonic acid to PGH_2 by two distinct COX catalyzed steps. 17

Scheme 1.11. LOX catalysis, forming fatty acid hydroperoxide. 18

Scheme 1.12. Active site coordination sphere of plant LOX (A) and mammalian LOX (B). 20

Scheme 1.13. The isomerization by eLOX-3 that converts fatty acid hydroperoxides to epoxy-alcohols and ketones. 27

Scheme 2.1. The total synthesis of 10,10-difluoroarachidonic acid. 42

Scheme 2.2. A general Reformatsky coupling reaction to generate a difluoromethylene group. 46

Scheme 2.3. A proposed synthesis of 11,11-difluorolinleic acid from Et-BDFA (**2.3**). 47

Scheme 2.4. The general preparation of (*Z*)-1-iodoheptene from 1-heptyne. 50

Scheme 2.5. A complex of 9-BBN in THF. Equilibrium favours the dimerized complex. 54

Scheme 2.6. A retrosynthetic design reversing the polarity of the triphenylphosphonium ylide. 66

Scheme 2.7. A central Reformatsky coupling approach, followed by two subsequent reaction pathways using either a Wittig or Bamford-Stevens reaction to generate **2.11**. 68

Scheme 2.8. The general reaction scheme for the production of **2.27**. 69

Scheme 2.9. An outline of the problems using an ionic approach to generate 11,11-difluorolinoleic acid. 77

Scheme 2.10. A radical approach to generate a bis-allylic difluoromethylene unit. 78

Scheme 2.11. Decarboxylative radical alkynylation using a modified Togni reagent. 78

Scheme 2.12. Methodology to generate desired 11, 11-difluorolinoleic acid. 80

Scheme 3.1. The proposed mechanisms of inhibition of the COX and LOX

enzymes by acetaminophen and nordihydroguaoaretic acid, respectively. 85

Scheme 3.2. Metabolism of ApAP and NDGA into electrophilic species, susceptible to nucleophilic attack by nucleophiles, such as glutathione, to form adducts. 86

Scheme 3.3. A bidentate complex of an iron atom with catechols. 88

Scheme 3.4. Suggested mechanism of inhibition of the sLOX-1 enzyme by pyridinol and pyrimidinol analogs of ApAP. 88

Scheme 3.5. Synthesis of *N*-(5-(benzyloxy)pyrimidin-2-yl)acetamide. Reagents and conditions: (a) H_5IO_6, I_2, acetic acid; (b) 2,5-hexanedione, *p*TsOH, toluene, Dean-Stark, 2 h; (c) CuI, Cs_2CO_3, BnOH, 90°C, o/n; (d) $NH_2OH{\bullet}HCl$, NEt_3, $EtOH/H_2O$, reflux, o/n; (e) $CH_3C(O)Cl$, cat. DMAP, TEA, CH_2Cl_2, rt, o/n. 93

Scheme 3.6. Suggested mechanism of inhibition of the sLOX-1 enzyme by pyridinol and pyrimidinol analogs of ApAP, through iron chelation. 97

Scheme 3.7. The mechanism of sLOX-1 and substrate inhibition modified from the work by Van der Donk.[14] 105

Scheme 3.8. Proposed oxidative decomposition of acylated 2-aminopyrimidinols during sLOX-1 inhibition studies. 110

Scheme 3.9. A synthetic approach for the introduction of an O-alkyl chain in the 5-position of the pyrimidine ring. 115

Scheme 3.10. Proposed synthetic design for the introduction of an alkyl

chain in the 5-position of the pyrimidine ring. 118

List of Figures:

Figure 1.1 Entry of fatty acid substrate (linoleic acid) into the active site of the LOX enzyme. 21

Figure 1.2 The active site cavity of Stable 5-LOX reproduced with permission from Newcomer et al. [36] 24

Figure 2.1. Aliquots removed from copper catalyzed cross coupling reaction between Et-BDFA and (*Z*)-1-iodoheptene, monitored by ^{19}F-NMR (no reference, no H-decoupling), for 24 hours. Starting material at -62ppm, desired product at -98ppm, unknown byproduct at -150ppm. 58

Figure 2.2. Aliquots removed from copper catalyzed cross coupling reaction between Et-BDFA and (*Z*)-1-iodoheptene, monitored by ^{19}F-NMR (no reference, no H-decoupling), for 24 hours. 1.0eq of (*Z*)-1-iodoheptene added at 0hr, 4hr and 6hr. Starting material at -62ppm, desired products at -98ppm. 60

Figure 3.1. A model of linoleic acid, in the active site of soybean lipoxygenase-1 reproduced by Klinman *et al*.[9] 89

Figure 3.2. A rational design for potential sLOX-1 inhibitors. A) Possible binding orientation of linoleic acid in the sLOX-1

active site. B) Proposed binding orientation of acylated 2-aminopyrimidines in sLOX-1 active site. 90

Figure 3.3. Spectrophotometric determination of pK_a for **3.1** (25mM). A) Bathochromic shift detected between pH 8 and 9 using Cary UV vis spectrophotometer determined at room temperature, in a solution of 10 mM potassium phosphate, containing 200 mM KCl, adjusted to desired pH using 1 M HCl or 1 M KOH, in the range of pH 2- 14. B) Fraction of aryloxide present as a function of pH from absorbance at λ_{max} (252nm). 95

Figure 3.4. Spectrophotometric titration for the determination of pK_a values for inhibitor **3.5** and **3.6** (25 mM) using UV vis spectrophotometer, at room temperature, in a solution of 10 mM potassium phosphate, containing 200 mM KCl, adjusted to desired pH using 1 M HCl or 1 M KOH, in the range of pH 2- 14. A) **3.5** bathochromic shift between pH 2-3 and pH 14. B) **3.6** bathochromic shift at pH 12. 96

Figure 3.5. Concentration dependence of the initial rates of the oxidation of linoleic acid at room temperature, 100 mM borate buffer, pH 9.2, 3.0 nM [sLOX-1]. Lines were obtained by fitting to the Michaelis-Menten using Origin sofware. 106

Figure 3.6. sLOX-1 inhibition studies in 100mM borate buffer (pH 9.2), at room temperature using A) ApAP and B) acylated 2-amino-5-benzoxylpyrimidines. sLOX-1 activity is expressed relative to the control where no inhibitor was added. Each data point represents the mean ± S.E.M of three values. IC_{50} (μM): **3.4** (■), 506; **3.11** (●), 468; **3.13** (▲), 114; **3.15** (▼), 551. 108

Figure 3.7. sLOX-1 inhibition studies in 100mM borate buffer (pH 9.2), at room temperature using acylated 2-amino-5-benzoxylpyrimidines. sLOX-1 activity is expressed relative to the control where no inhibitor was added. Each data point represents the mean ± S.E.M of three values. IC_{50} (μM): **3.6** (■), 371; **3.12** (●), 309; **3.14** (▲), 98; **3.16** (▼), 86. 109

Figure 3.8. Oxidative stability of compound **3.11** (25 μM) in 100 mM borate buffer (pH 9.2), at room temperature. A) Compound **3.11** stability in inert atmosphere and purged solutions. B) Compound **3.11** in the presence of molecular oxygen (open to atmosphere). 111

Figure 3.9: Oxidative stability of compound **3.6** (25 μM) in 100mM borate buffer (pH 9.2), at room temperature. A) Compound **3.6** stability in inert atmosphere and purged solutions. B)

Compound **3.6** in the presence of molecular oxygen (open to atmosphere). 112

Figure 3.10. sLOX-1 inhibition in 100mM borate buffer (pH 9.2), at room temperature using acylated 5-hexyl-2-aminopyrimidines (25 μM). sLOX-1 activity is expressed relative to the control where no inhibitor was added. Each data point represents the mean ± S.E.M of three values. IC_{50} (μM): **3.28** (■, R=CH_3), 47; **3.29** (●, R=C_3H_7), 14. 121

-1-
Introduction

1.0 Introduction

Fatty acids play many roles in biological systems. They are the building blocks of phospholipids and glycolipids, which are constituents of the cell membrane. Fatty acids are attached to many proteins and act as targeting molecules by helping to direct proteins to their place within the cell membrane. They are fuel sources for the body, as they are stored as triacylglycerides for later use. Products of fatty acid metabolism function as hormones and intracellular messengers.[1,2]

Fatty acids can be saturated, monounsaturated or polyunsaturated and vary in chain length. Saturated fatty acids and mono-saturated fatty acids are largely utilized as energy sources and also serve structural roles within cell membranes. The most common fatty acids are shown in Table 1.1.

Table 1.1. Structures of common saturated and unsaturated fatty acids.

Compound	**Structure**	**Carbon-length and Degree of Unsaturation**
Palmitic Acid	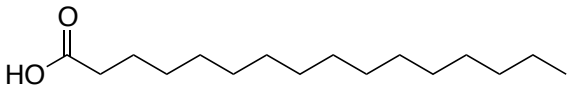	C16:0
Stearic Acid	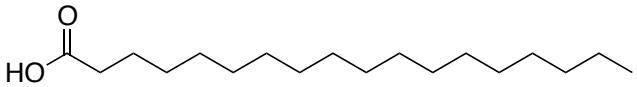	C18:0
Linoleic Acid	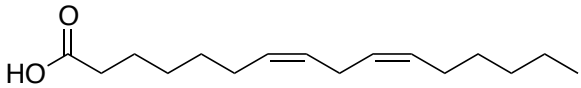	C18:2
Arachidonic Acid	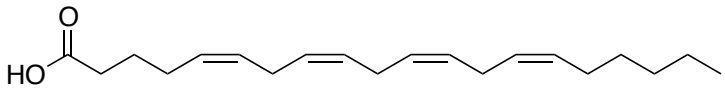	C20:4
Eicosapentaenoic Acid	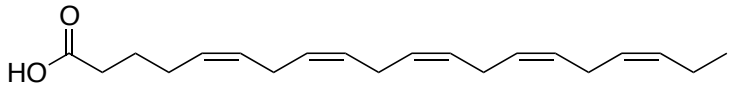	C20:5
Docosahexaenoic Acid	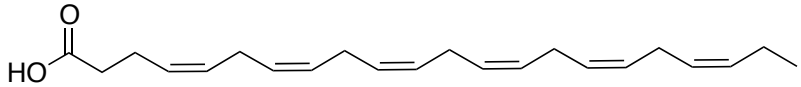	C22:6

Specific fatty acids such as linoleic acid and arachidonic acid are the starting materials for vital signaling molecules in plants and animals, respectively and are crucial for proper biological function. Humans also require, but do not have the enzymatic capacity to synthesize, linoleic acid, and therefore it must be obtained through diet; however, this is untrue of plants and other mammals. Omega-6 and omega-3 fatty acids are the two main classes of essential fatty acids.[1]

1.1 Polyunsaturated Fatty Acids

While saturated and mono-unsaturated fatty acids are used largely for structural and energy storage roles in biology, polyunsaturated lipids, being more oxidatively labile, expand on these roles. Polyunsaturated fatty acids contain more than one double bond in their backbone and can be classified into various groups based on their chemical structure. Omega-3 fatty acids are a family of polyunsaturated fatty acids that have a double bond at the third carbon atom from the end of the carbon chain. Shorter polyunsaturated lipids such as α-linolenic acid, obtained through diet, can be transformed into longer chain omega-3 fatty acids such as eicosapentaenoic acids. The omega-3 fatty acids are involved in normal metabolism and human growth.[3]

While omega-3 fatty acids have their first double bond at the third carbon from the end of the chain, omega-6 fatty acids have their first double bond positioned 6 carbons in. Linoleic acid is an 18-carbon omega-6 fatty acid that is obtained by animals through diet and following a series of enzyme mediated reactions, 20-carbon fatty acids such as arachidonic acid is generated as shown in Scheme 1.1.[3]

The arachidonic acid is esterified to the cell membrane phospholipids and is released upon enzyme activation to fulfill biological roles. Similar to omega-3 fatty acids, the omega-6 variants play a crucial role in brain function, as well as normal growth and development, and our focus herein, the promotion of inflammation.[3] Furthermore, the multiple unsaturations within polyunsaturated fatty acids make them susceptible to spontaneous oxidation.

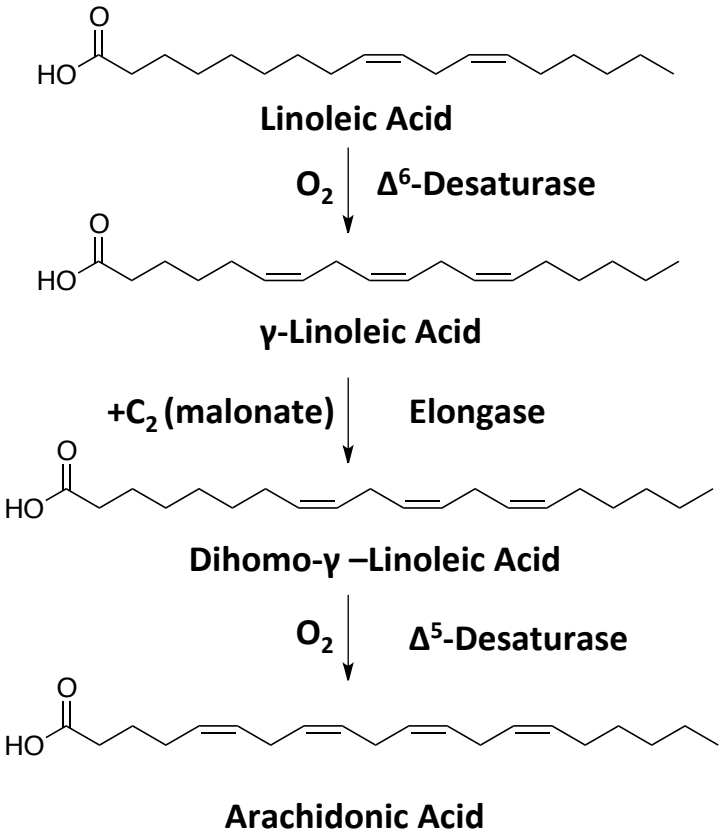

Scheme 1.1. Enzyme-catalyzed transformation of linoleic acid to arachidonic acid.

1.2 Lipid Autoxidation

The susceptibility of the multiple double bonds in polyunsaturated fatty acids to spontaneous oxidation, leads to a process known as lipid autoxidation (also referred to as lipid peroxidation). This process is a radical chain reaction that yields hydroperoxides as its primary products. This free radical chain process can be broken down into three stages: chain initiation, propagation and termination. Early work by Bolland, Bateman and colleagues defined the role of free radicals and the general accepted mechanism for hydrocarbon autoxidation is demonstrated in Scheme 1.2.[4]

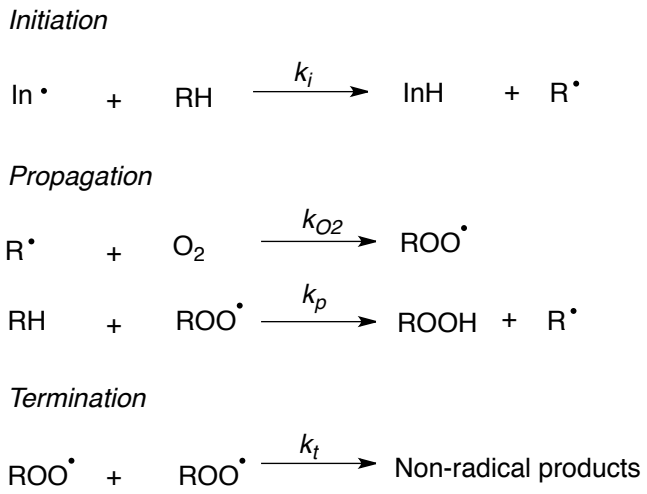

Scheme 1.2. The radical chain mechanism of hydrocarbon autoxidation.

The first step, initiation, is any chemical reaction, which yields a substrate derived alkyl radical (R•). These free radicals can be generated by the decomposition of radical initiators such as diazo compounds, peroxides or

endogenous reactive oxygen species (ROS), such as protonated superoxide (HOO•) or hydroxyl radicals (HO•). The first step is the abstraction of a hydrogen atom by the initiator (In•) to form a carbon centered radical. The carbon-centered radical (R•) can then react with molecular O_2 to form a peroxyl radical (ROO•). In the second propagation step, the peroxyl radical will abstract a H-atom from another molecule of substrate, forming a hydroperoxide (ROOH) along with another carbon centered radical (R•). The chain reaction can be terminated when two substrate-derived peroxyl radicals react, to give non-radical products (usually an alcohol, a carbonyl and O_2) by a process known as Russell termination.[5]

Polyunsaturated fatty acids and esters are particularly reactive towards auto-oxidation because they possess C-H bonds. The C-H bond strength of the bisallylic position(s) polyunsaturated lipids is especially low. The radical is stabilized by delocalization into two double bonds, as in linoleic and arachidonic acid as shown in Scheme 1.3.

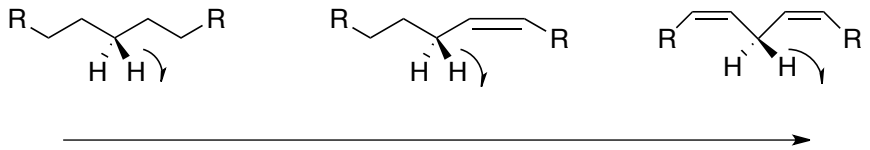

Decreasing C-H bond strength
Increasing stability of R•
Increase in rate of oxidation

Scheme 1.3. Reactivities of saturated, monounsaturated and polyunsaturated fatty acids and their esters to oxidative stress.

Extensive research by Porter *et al*, has provided a better understanding of the mechanism of oxidation of unsaturated lipids.[6,7] The products that are obtained from free radical chain oxidation of diene fatty acids or esters are primarily diene hydroperoxides as shown in Scheme 1.4. For example the polyunsaturated fatty ester methyl linoleate has a bis-allylic hydrogen located in position 11 and upon abstraction, reversible oxygen addition can occur at three different positions (C9, C11, C13).[7] The autoxidation of methyl linoleate leads to the formation of five major hydroperoxides.[7] There are two *trans*, *cis* dienes **1.2** and **1.3** that are formed as the major product in the presence of a good H-donor and two *trans*, *trans* dienes **1.5** and **1.6** that are formed in the absence of H-donors via β-fragmentation and the rearrangement of the intermediate peroxyl radicals. The fifth hydroperoxide formed is a non-conjugated hydroperoxide **1.4**.

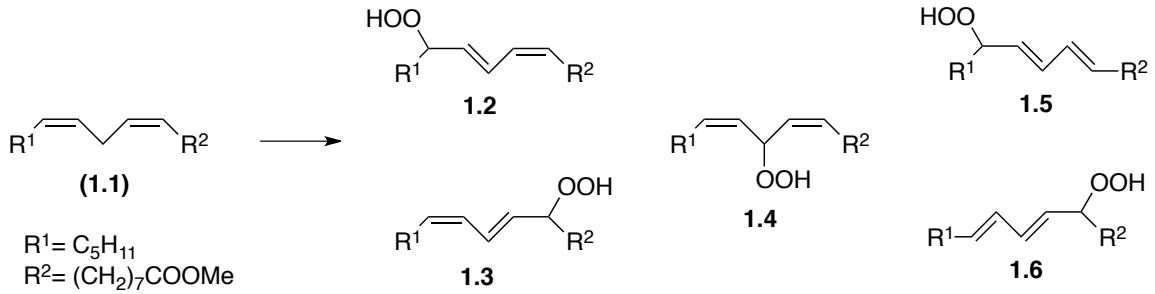

Scheme 1.4. Products of methyl linoleate free radical oxidation.

The distribution of these diene fatty acid autoxidation products is dependent on the rate constants that control the competing processes as shown in Scheme 1.5.

The relative tendency for the intermediate peroxyl radical to fragment back to the carbon-centered radical and oxygen (k_{β}) and the k_p of the substrate and the k_{inh} of a present antioxidant can trap an intermediate peroxyl radical as a hydroperoxide by donating a hydrogen atom.

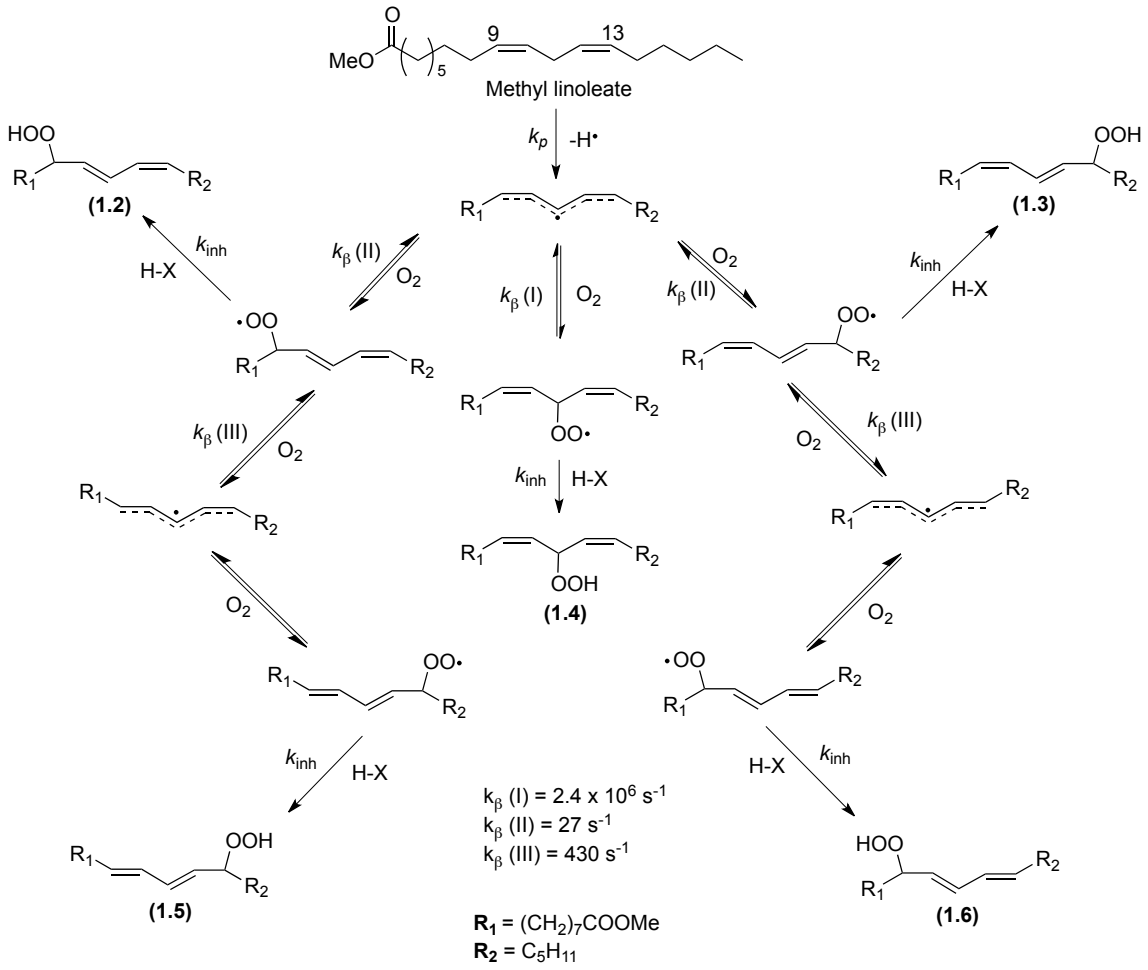

Scheme 1.5. Mechanism and distribution of methyl linoleate autoxidation.

While the above mentioned lipid autoxidation of methyl linoleate produces five major products, the autoxidation of higher polyunsaturated lipids such as arachidonic acid is much more complex as shown in Scheme 1.6. There are several unsaturations throughout the molecule and the abstraction of a bis-allylic hydrogen can occur from more than one spot on the molecule; producing several more hydroperoxides.

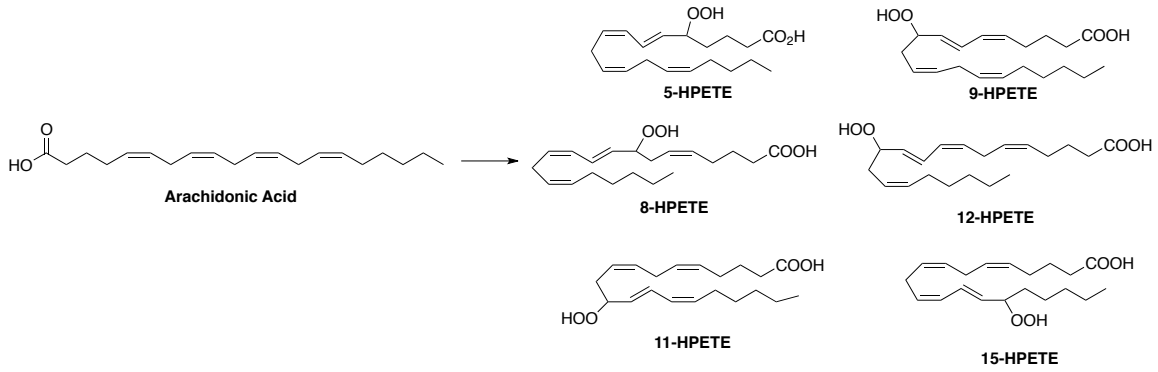

Scheme 1.6. Primary products of Arachidonic Acid Peroxidation.

The lipid hydroperoxides that are formed *in vivo* are of great pathological significance they disrupt the membrane integrity, lead to the formation of further radicals through thermolysis or reductive dissociation of the O-O bonds. Moreover they serve as precursors to cytotoxic α,β-unsaturated aldehydes such as acrolein (AC), 4-hydroxy-2-nonenal (HNE) and malondialdehyde (MDA). These compounds are excellent Michael acceptors that are capable of undergoing reactions with nucleophiles such as amines and thiols, that are present in the cells.[8-10]

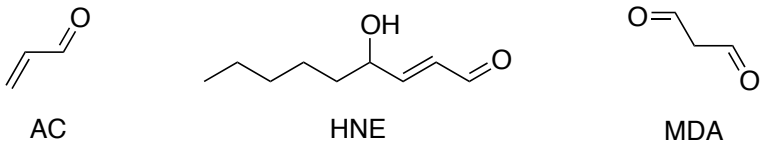

The main concern is the reaction of these aldehydes with DNA and proteins. The formation of DNA adducts, improper replication, mutations, and protein mis-folding may lead to degenerative diseases.[11]

1.3 Enzyme-Mediated Lipid Peroxidation

Lipid peroxidation has been the subject of extensive studies and can be carried out by non-enzymatic free radical-mediated reactions as described above but also by enzymatic oxidation processes. The enzymatic oxygenation of a lipid such as arachidonic acid can occur biologically through several pathways. The two pathways we focus on herein are the acyclic pathway catalyzed by the lipoxygenase enzyme (LOX), more specifically 5-LOX, or the cyclic pathway, catalyzed by the cyclooxygenase enzyme (COX), also known as prostaglandin-H synthase (PGH Synthase).

The LOX and COX enzymes are responsible for the catalysis of the first step in the transformation of arachidonic acid to a wide variety of lipid mediators, including leukotrienes and prostanoids (prostaglandins, thromboxanes and prostacyclins) respectively, as shown in Scheme 1.7.[12] These lipid mediators are responsible for mediating a wide variety of biological responses such as inflammation, immunity, pain, fever, homeostatic balance and renal function.[12,13]

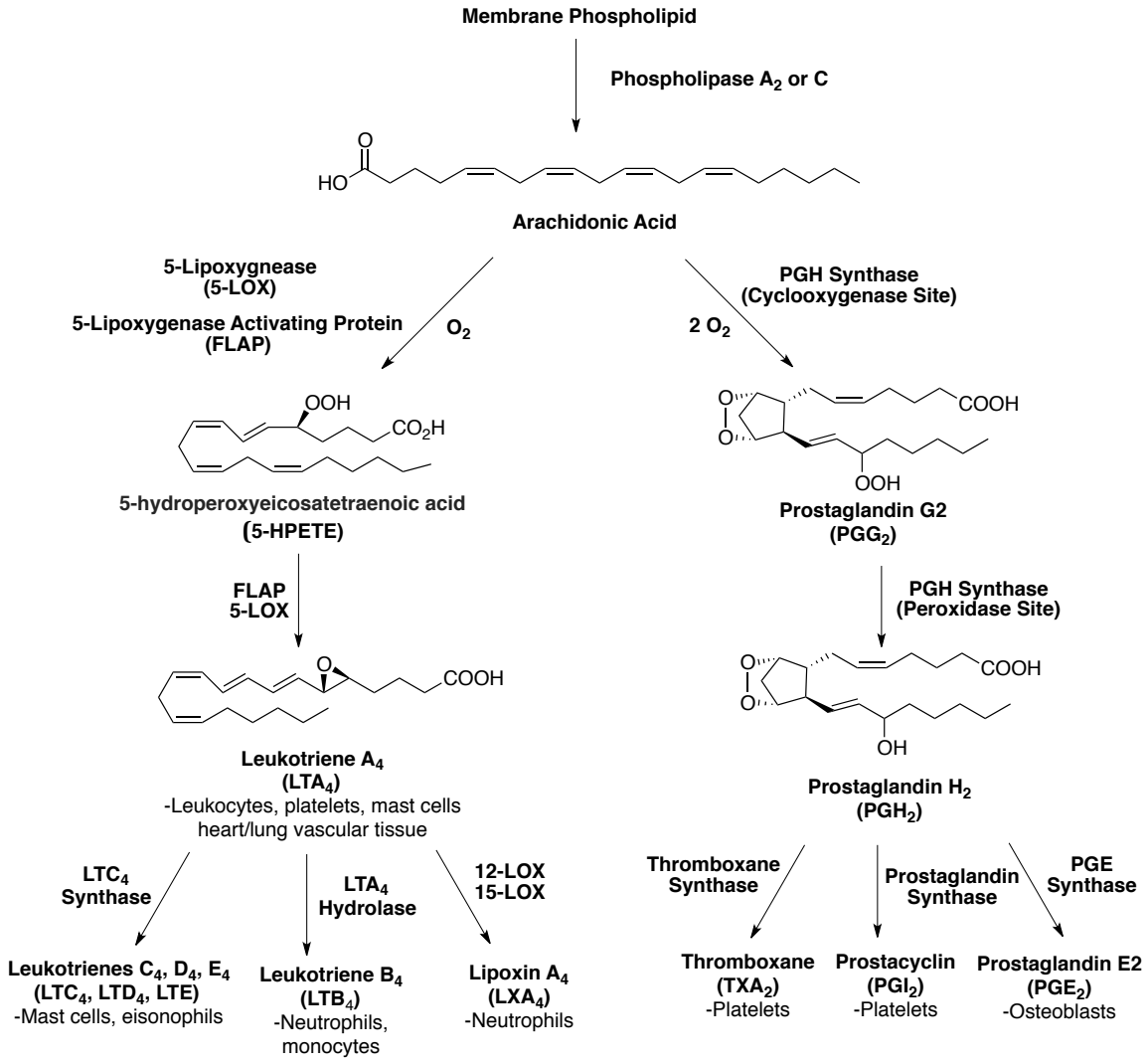

Scheme 1.7. Arachidonic acid peroxidation via 5-lipoxygenase pathway and the prostaglandin pathway.

The prostaglandins exhibit a wide range of physiological activities. For example, they mediate the contraction and relaxation of smooth muscle in the

uterus, cardiovascular system, intestinal tract and bronchial tissue making cyclooxygenase widely targeted by drugs.[14] However, due to the prevalence of prostaglandin activity in a wide variety of tissues, the chances of causing unwanted side effects are very high. Currently therapeutics have been designed to inhibit early steps in the prostaglandin biosynthetic pathway that are responsible for converting the unsaturated fatty acids into these cyclic peroxides. This will be discussed later.

Leukotrienes act primarily on transmembrane receptors and peroxisome proliferator-activated receptors (PPARs) and contribute to the pathophysiology of asthma and allergic responses.[14] The various leukotrienes are bronchoconstrictors and vasoconstrictors and induce mucous secretion.

1.4 Prostaglandins

Prostaglandin H_2 (PGH_2) is the primary prostaglandin from which all other prostaglandins are derived. PGH_2 can then be further metabolized by various cell types to generate a wide array of prostaglandin metabolites as shown in Scheme 1.8.[14]

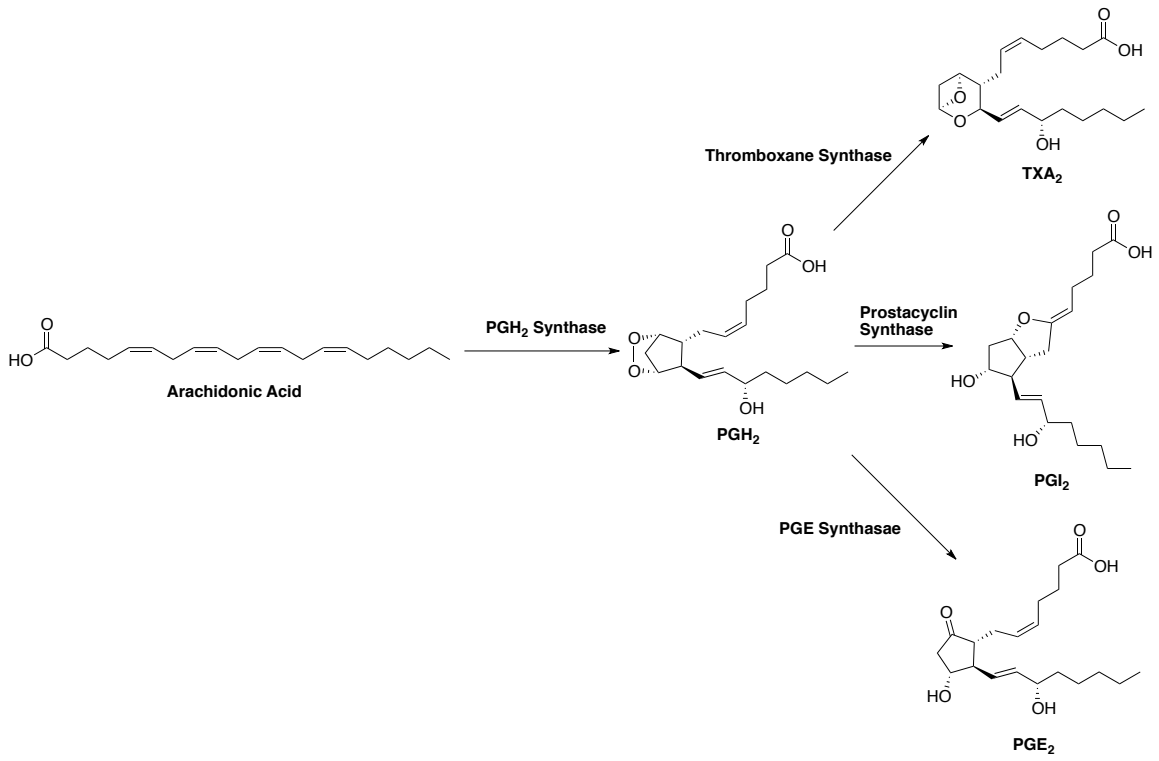

Scheme 1.8. The biosynthesis of prostaglandins from the sequential oxidation of arachidonic acid by cyclooxygenase enzymes and terminal prostaglandin synthases.

These PGH_2 derived lipid mediators are responsible for both pro- as well as anti-inflammatory responses. In the interest of space, we will only highlight three of the key downstream products here as they illustrate their structural variety: thromboxane A_2, prostaglandin I_2 and prostaglandin E_2. Thromboxane A synthase is part of the cytochrome P450 superfamily on the basis of significant sequence homology.[14] It differs in function by catalyzing the conversion of PGH_2 to thromboxane A_2, which initiates platelet aggregation. Prostacyclin synthase also

belongs to the family of cytochrome P450 isomerases.[14] This membrane protein catalyzes the conversion of PGH_2 to prostacyclin I_2, which is a potent vasodilator and inhibitor of platelet aggregation. Prostaglandin E synthase is involved in the eicosanoid and glutathione metabolism and generates prostaglandin E_2 (PGE_2) from PGH_2.[15] Prostaglandin E_2 is often important in labour (causes uterine contractions) and induces fever by acting as a triggering molecule. An imbalance of these products can contribute to the development of myocardial infarction, stroke, and atherosclerosis.[14]

PGH synthases-1 and -2, also commonly referred to as COX-1 and COX-2 are enzymes involved in prostaglandin formation and are similar in structure and catalytic activity. COX-1 is constitutively expressed, whereas COX-2 is inducible and dramatically upregulated during inflammation.[15] The pharmacological target is COX-2, which produces inflammatory prostaglandins, over COX-1, which produces the protective prostaglandins.

1.5 Leukotrienes

Leukotrienes, unlike prostaglandins, are produced almost exclusively in inflammatory cells.[12,13] Arachidonic acid is released as an immune response from the plasma or nuclear membrane, during which time calcium-dependent phospholipase A_2 ($cPLA_2$) and 5-LOX are translocated to the endoplasmic reticulum and nuclear membrane. The 5-LOX activating protein (FLAP) shuttles AA to the 5-LOX enzyme active site, where it is oxidized and transformed into leukotrienes.[16] The first step is converting the arachidonic acid to the intermediate 5-HPETE

followed by the stereospecific conversion to the highly unstable LTA_4 intermediate. LTA_4 can be metabolized by LTA_4 hydrolase to yield the potent phagocyte chemotactic agent LTB_4. LTA_4 can also be conjugated to a molecule of glutathione to give three different cysteinyl leukotrienes (LTC_4) by the enzyme LTC_4 synthase. The sequential cleavage of the glutathione moiety on LTC_4 by two enzymes yields LTD_4 and LTE_4, respectively as shown in scheme 1.9.[12]

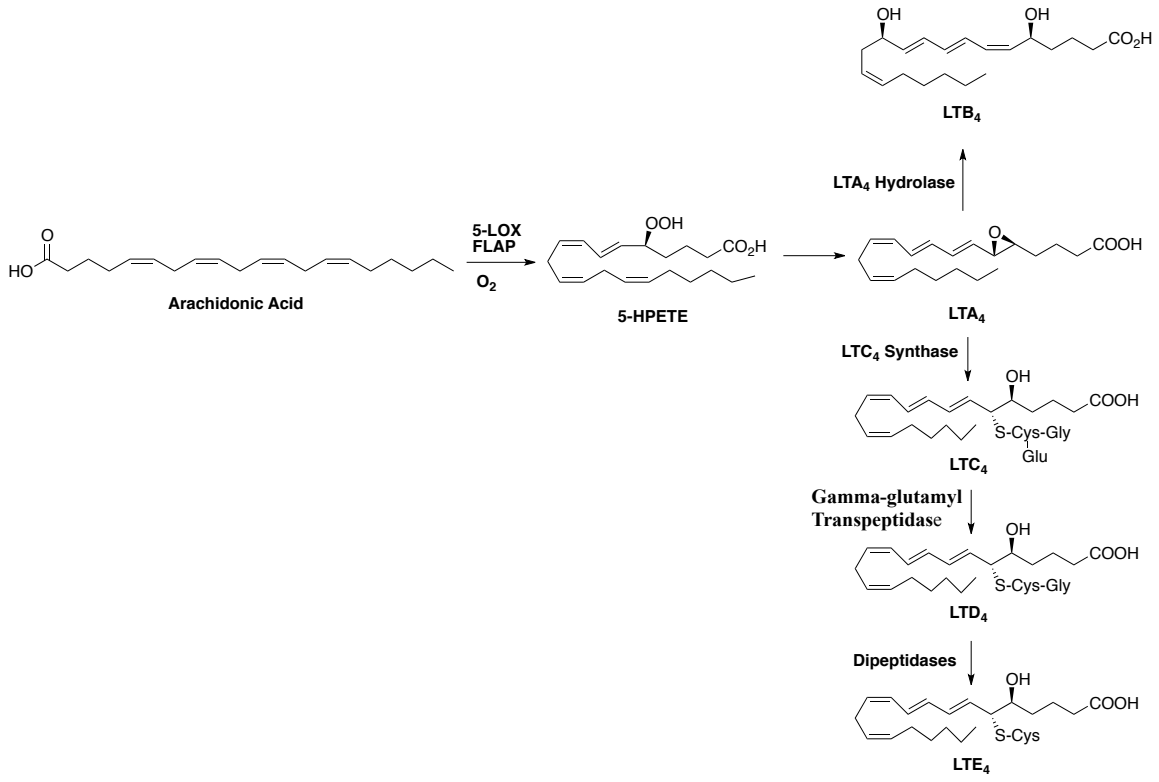

Scheme 1.9. The biosynthesis of leukotrienes from the sequential oxidation of arachidonic acid by lipoxygenase enzymes and leukotriene hydrolases or leukotriene synthases.

1.6 Cyclooxygenase: Structure and Mechanism

Prostaglandins are products of arachidonic acid oxidation catalyzed by prostaglandin endoperoxide H synthase-1 and 2. They are heme-containing proteins, active when homodimerized or heterodimerized and are located in the endoplasmic reticulum (ER) and nuclear membrane.[17-19] The reason for dimerization is unknown. Each monomer of the COX protein contains a separate peroxidase and oxygenase active site. At the endoplasmic reticulum membrane, AA is released by phospholipases A2 (PLA2s) where it can be acted upon by COX. Each monomer contains three structural domains; an epidermal growth factor domain at the N-terminus, a membrane binding domain, and a large C-terminal catalytic domain.[20]

COX catalyzes two distinct chemical transformations for the formation of PGH_2 from arachidonic acid as shown in Scheme 1.10. The first series of reactions convert arachidonic acid to prostaglandin G_2 (PGG_2). A tyrosyl radical is generated through an intramolecular oxidation by a heme cofactor. The protein-based tyrosyl radical abstracts the 13-pro-S hydrogen atom from arachidonic acid, yielding a delocalized pentadienyl radical. The radical sequentially reacts with a molecule of oxygen, undergoes two 5-exo cyclizations, and another addition of molecular oxygen, yielding the bicyclic hydroperoxide, PGG_2 after abstraction of the tyrosine H-atom, which restores the catalytic tyrosyl.[18,20] PGG_2 is reduced to the endoperoxy alcohol, PGH_2. The peroxidase reaction occurs at the heme-containing active site

located close to the surface of the protein, while the cyclooxygenase reaction occurs at the hydrophobic core of the enzyme.[17-19]

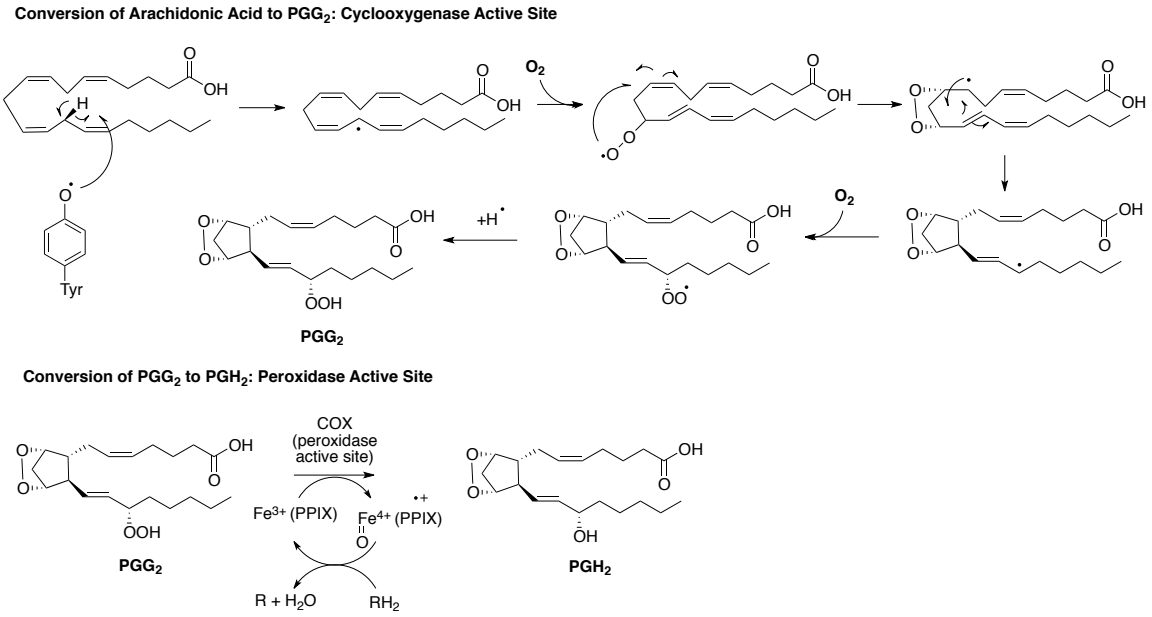

Scheme 1.10. Chemical transformation of Arachidonic acid to PGH_2 by two distinct COX catalyzed steps.

The primary structures of COX-1 and COX-2 from various species are known. There is a 60-65% sequence identity between the two isoforms within the same species and 85-90% sequence identity between the same isoforms from different species.[21,22] The crystal structures of COX-1 and COX-2 have been determined and are very similar. The main difference between the two isoforms is a 20% larger pocket for substrate access in the COX-2 enzyme.[21,22] This difference in size is due to a three amino acid difference between the two isoforms. The larger pocket enables

selective inhibition of the COX-2 isoform over the COX-1 isoform. Each monomer contains a 25-Å hydrophobic channel that begins at the membrane-binding domain and continues into the core of the globular domain. There are twenty-four residues that line the hydrophobic region of the COX active site. The only difference in this region between the two COX isoforms is an Ile in position 523 of COX-1 and Val in position 523 of COX-2.[21,22]

1.7 Lipoxygenases: Structure and Mechanism

Lipoxygenases are a family of non-heme iron containing dioxygenases, which introduce molecular oxygen into polyunsaturated fatty acids, generating fatty acid hydroperoxides as shown in Scheme 1.11.[13,20,23,24] The enzyme is activated by trace amounts of fatty acid hydroperoxides, which oxidize Fe^{2+}(inactive form) to Fe^{3+}(active form). The reaction is initiated by a stereoselective hydrogen atom abstraction at the C-3 of a 1,4-*cis,cis* pentadiene unit. The resulting radical is delocalized over the pentadienyl system. Molecular oxygen is then added regioselectively, in a antarafacial manner. The resulting peroxyl radical is then reduced by Fe^{II}-H_2O to yield the fatty acid hydroperoxide. This step is thought to proceed via proton-coupled electron transfer (PCET), which involves the tunneling of an electron to the ferric iron with simultaneous proton transfer to the hydroxide ligand.[13,20,23,24]

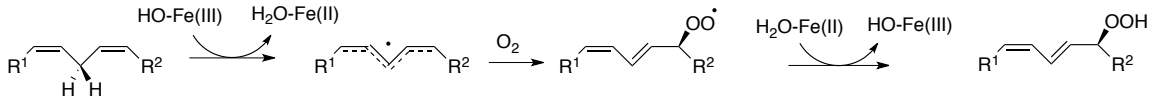

Scheme 1.11. Mechanism of LOX catalysis.

LOXs occur ubiquitously in plants and mammals and have been recently found in coral, moss, fungi and a number of bacteria.[25] Most of what is known about the LOX enzymes was attained through the extensive study of the enzyme from soybeans.[26] Plants generally have three isoforms (LOX-1, -2, -3), while mammals have six isoforms (5-LOX, 15-LOX-1, 15-LOX-2, 12S-LOX, Platelet Type 12-LOX and eLOX-3). LOXs are classified according to their regioselectivity, and sometimes their stereoselectivity (i.e. "S" or "R"). Plant LOX classification is much simpler as its substrate is linoleic acid, which has only one abstractable H-atom. Mammalian classification is much more complex as arachidonic acid has more sites for H-atom abstraction, and COX is located in various cells types.

LOXs are monomeric proteins that are roughly 95-100 kDa in size and consist of two domains. There is an α-helical catalytic domain and an N-terminal β-barrel domain that is involved in binding to the membrane.[13,20,23,24] LOX enzymes contain one iron atom, that is octahedrally coordinated to five amino acid side chains and a water hydroxide ligand as shown in Scheme 1.12.[23] In the case of the plant LOXs, three histidines, one asparagine and the carboxy group of the C-terminal isoleucine (Scheme 1.12A) are involved in coordination of the iron atom; whereas in mammals, the iron atom is coordinated to four histadine residues and the carboxy group of the C-terminal isoleucine (Scheme 1.12B).

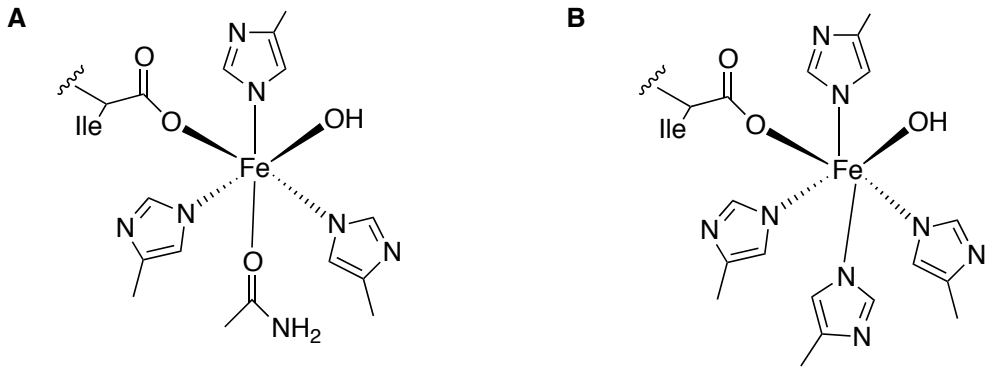

Scheme 1.12. Active site iron coordination sphere in plant LOX (A) and mammalian LOX (B).

The LOX family of enzymes can produce a wide array of products and this is related to the protein structures by changes in substrate binding. The depth and width of the substrate binding pocket is critical for substrate entry and controls the positioning of activated methylene group, with respect to catalytic iron atom, as shown in Figure 1.1A and B. Depending on the orientation of fatty acid substrate upon active site entry, different products can be formed. As shown in Figure 1.1C and D, straight or inverse orientation of the substrate is possible. Steric shielding and oxygen channeling in the LOX enzymes dictates the identity of the products generated.[14]

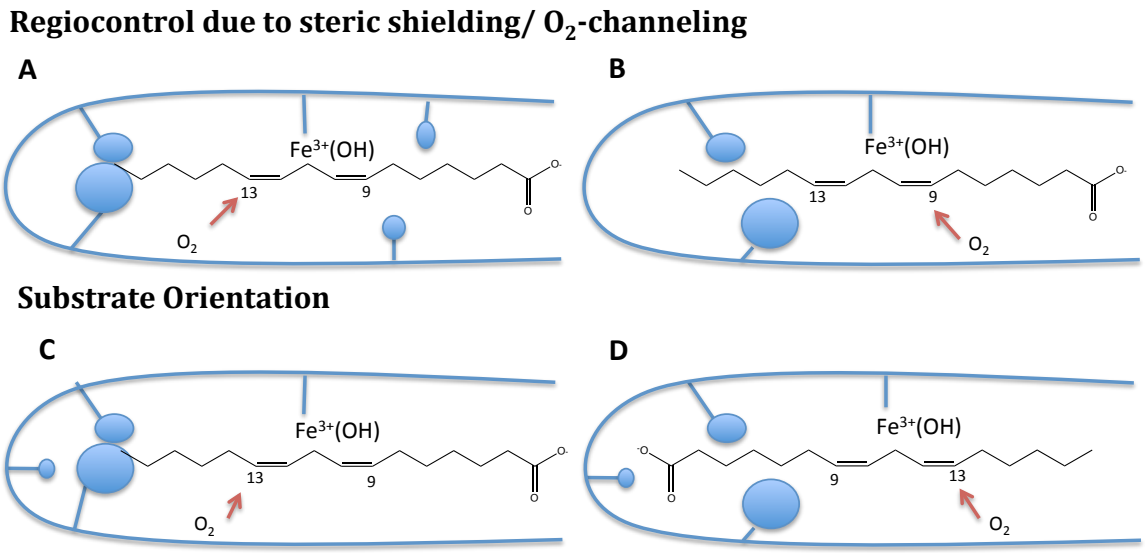

Figure 1.1. Entry of fatty acid substrate (linoleic acid) into the active site of the LOX enzyme. A) and B) represent the space related model. C) and D) represent the orientation dependent model. The red arrow indicates where molecular oxygen will attack.

1.7.1 5-Lipoxygenase

There are six known isoforms of mammalian lipoxygenases, one of which is indisputably linked to human disease.[12,13,16,20] Human 5-lipoxygenase (5-LOX) catalyzes oxygenation of AA at the 5-position to yield 5-HPETE, which is subsequently converted to leukotrienes. Aberrant products of leukotrienes as part of the immune response to allergens causes inflammation resulting in the constriction of airways, leading to asthma and bronchitis.[16,27] Many cell types constitutively express 5-LOX, including granulocytes, monocytes, mast cells,

dendritic cells and B-lymphocytes.[13] 5-LOX is a monomeric enzyme composed of 673 amino acids with a molar mass of 78 kDa.[23,28]

The cloning of the cDNA from human, rat, mouse and hamster 5-LOX demonstrated that these genes are highly conserved across species.[23] Although procedures have been reported in attempt to isolate 5-LOX, the understanding of the structure and function is still at its early stages, due to its inherent instability. 5-LOX is highly unstable in the presence of oxygen due to the non-turnover-based inactivation of the catalytic iron, making it difficult to study.[29]

After decades of crystallization attempts, Newcomer *et al*, reported the first crystal structure of an engineered human 5-LOX.[28] Based on the known crystal structures of rabbit 15-LOX and coral 8-LOX, they were able to identify a 5-LOX specific lysine rich region, which may confer instability.[30,31] In most LOXs, amino acid 655 is a conserved Leu, as is the case for 8*R*- and 15-LOX; however, 5-LOX is replaced with a Lys, which affects the orientation of the C-terminus and how the catalytic iron binds within the active site. 5-LOX does not contain common salt bridges responsible for anchoring the C-terminus, which are present in most LOXs, including 8*R*- and 15-LOX. These differences between 5-LOX and the other homologs lead to its inherent instability.[13,28]

Replacement of the Lys rich sequence with the corresponding sequence in coral 8-LOX, combined with the removal of the Ca^{2+} binding site, and assumed membrane insertion region, and the exchange of two cysteine residues for alanine, allowed for an increase in the stability of the protein and allowed for crystallization.[28] The conserved activity of the stable 5-LOX was analyzed through

the detection of intermediate 5S-HPETE and leukotriene A_4 product formation using high performance liquid chromatography (HPLC).[13,28,30,31]

The crystal structure that was obtained as shown in Figure 1.2, revealed an iron bound to His367, His372 and His550, which corresponds to other lipoxygenase structures. The 5-LOX active site revealed an elongated cavity lined with several amino acids that are distinct to this lipoxygenase. Two aromatic amino acid side chains were found to be in the center of the active site (Phe177 and Tyr181) and formed a cork like structure that is responsible for sealing off the active site, preventing substrate entry. These findings are quite interesting because they present the question as to how arachidonic acid enters into the active site and gains access to the catalytic iron. To allow substrate entry either the Phe or Tyr sidechains need to uncork, or a conformational isomerization of Trp147 on the opposite end of the active site needs to occur.[28]

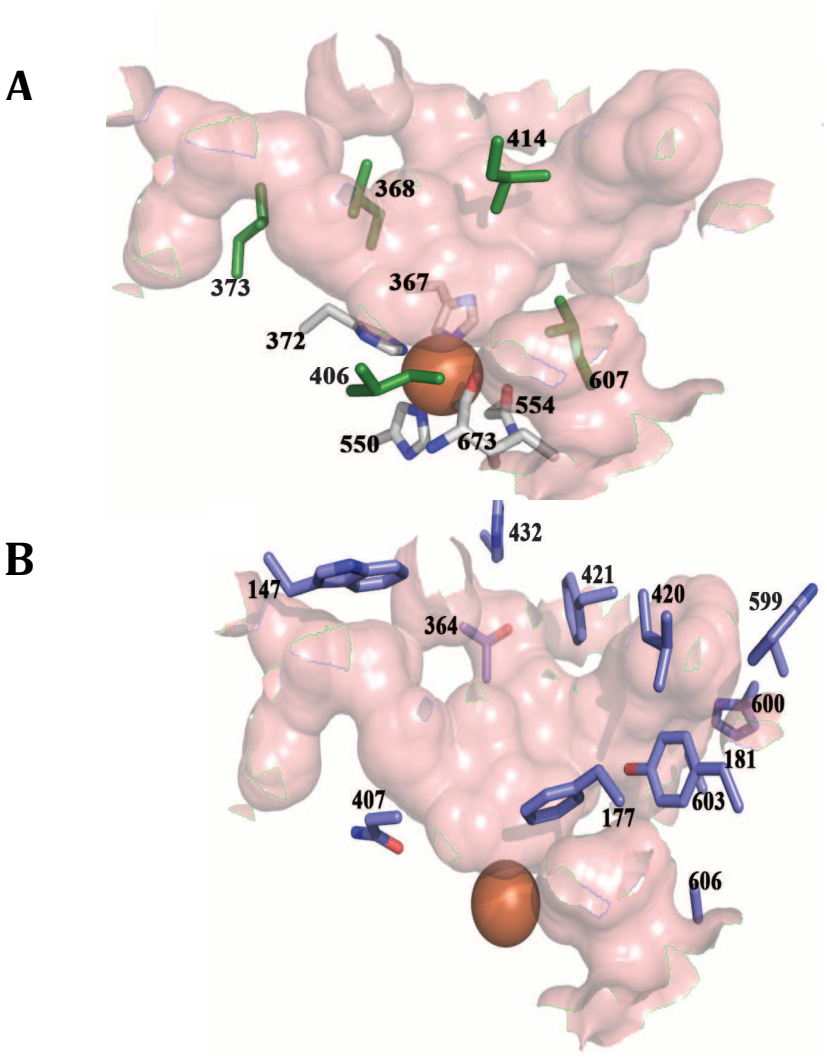

Figure 1.2. The active site cavity of Stable 5-LOX reproduced with permission from Newcomer et al.[28] A) Orientation of active site with invariant Leu and Ile side chains in green. B) 5-LOX amino acids that contribute to the active site cavity.

1.7.2. 15*S*-Lipoxygenase

While 5-LOX has been implicated in asthma, 15-LOX and its products has been linked to cardiovascular disease by promoting vascular permeability and coronary artery restriction.[31,32] There are two known isoforms of 15*S*-LOX; reticulocyte 15*S*-LOX (also called type 1), typically found in reticulocytes and eosinophils and epithelial 15*S*-LOX (also called type 2).[31,33] 15*S*-LOX-1 product formation promotes invasion of breast cancer cells and the formation of lymph node metastasis.[34]

The primary structures of the two isoforms have 40% amino acid sequence identity. The sequence contains the conserved iron-binding histidine and C-terminal isoleucine; however, a fifth iron ligand is present in 15-LOX unlike other isoforms. In the blood cell 15S-LOX-1, at amino acid 544, is a His ligand, whereas at amino acid 558 in the 15-LOX-2 is a serine ligand. It has been suggested that the difference in sequence may be cause for the preferential oxygenation at the C-15 of the substrate; however, it is unclear how this occurs.[31,33]

1.7.3. 12-Lipoxygenase

In several species 12-LOX seem to be similar to 15-LOX in structure and activity. Several studies have demonstrated that oxidized LDL, in which lipoxygenases have been linked, contributes to atherogenesis.[35-37] The isoforms refer to the cells where they were identified; platelet, leukocyte and epidermal.[35] Arachidonate 12-lipoxygenase introduces molecular oxygen at C-12 of arachidonic acid, to generate the 12-hydroperoxy derivatives (12-HETE). 12-LOX can generate derivatives with both the *R* and *S* configurations depending on the lipoxygenase isoform that is

present. Platelet-type 12*S*-lipoxygenase has also been linked to prostate cancer[38] and 12*R*-lipoxygenase is involved in skin barrier functions. [35,39]However, it should be noted that 15-LOX-1 can oxygenate AA to produce 12*S*-HPETE.

The sequence alignment shows that the five conserved histidines are present in the active site of the enzymes. The non-heme iron atom is coordinated to three of the histidine residues and the C-terminal isoleucine.[36] The active site cavity of 12-LOX is predicted to be about 6% larger than 15-LOX based on the amino acid sequence. It is speculated that the increase in size of 12-LOX active site is due to smaller side chains lining the pocket compared to those found in 15-LOX.[35,36]

1.7.4. Other Isoforms

Of the six lipoxygenases encoded in the human genome, five show activity typical of lipoxygenase enzymes; the generation of hydroperoxides via oxidation of polyunsaturated fatty acids. Epidermal lipoxygenase-3 (eLOX3) is the sixth isoform in humans, which is involved in epithelial barrier formation and does not follow typical fatty acid dioxygenase activities of other LOXs. In fact, it is incapable of oxygenating polyunsaturated fatty acids.[40] It is classified as a lipoxygenase because it has 58% sequence similarity to 12R-LOX. It catalyzes a unique hydroperoxide isomerization, that efficiently converts fatty acid hydroperoxides to epoxy-alcohols and ketones, as shown in Scheme 1.13.[40,41] Unlike 5-, 12-, and 15-LOXs, eLOX-3 does not require the non-heme iron for its hydroperoxide isomerase activity. The relationship between mode of action and its physiological role in epidermal barrier formation is still in question.

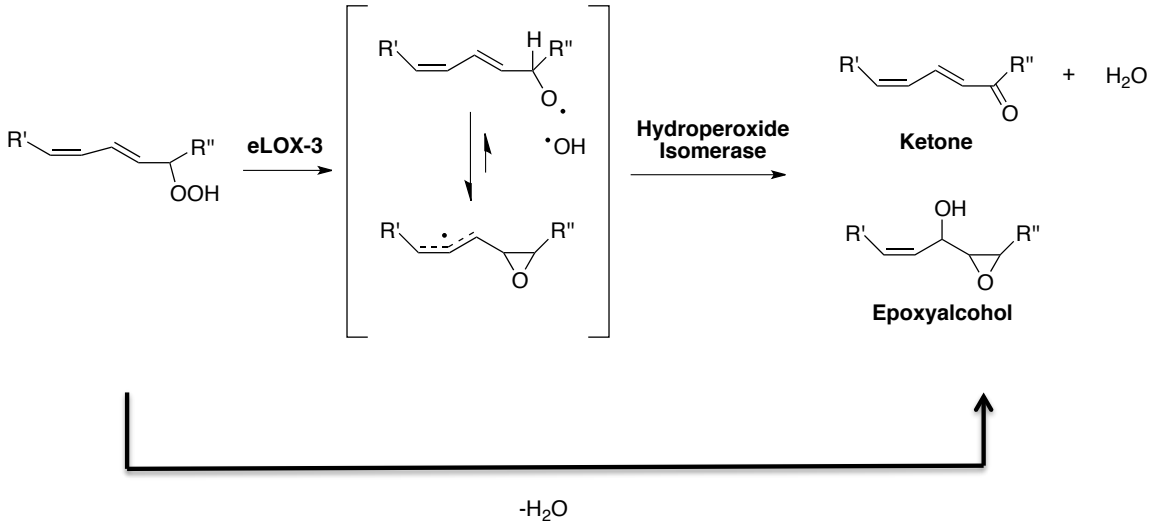

Scheme 1.13. eLOX-3 isomerization, illustrating the conversion of fatty acid hydroperoxides to epoxy-alcohols and ketones.

A large portion of the above-mentioned structure and reactivity for 5-, 12-, and 15- lipoxygenase was due to the insight of coral 8-lipoxygenase. Sequencing studies revealed C-terminal similarity to 5-LOX (41% identity). In contrast to mammalian 5-LOX, 8R-LOX was stable which made it feasible to perform crystallographic studies. This enabled structural and mechanistic exploration of the LOX enzymes.[30] Using the known crystal of 8R-LOX and its specific stabilizing features, Newcomer et al was able to solve the 3-dimensional structure of the first human 5-LOX.

1.8. Discovery of Inhibitors for COX and LOX Activity

Therapeutic targets in the arachidonic acid cascade have been of great interest for some time now. With the extensive structural and functional elucidation of the COX and LOX enzymes having been carried out, they have become the prime drug target. The extensive knowledge of COX-1, and -2 isoforms have allowed for the selective inhibition of prostaglandin formation via the design of several non-steroidal anti-inflammatory drugs. Whereas, LOX enzymes have posed a greater challenge due to difficulty in obtaining crystal structures, and a detailed understanding of how arachidonic acid binds and is regioselectively oxygenated.

1.8.1 Cyclooxygenase Inhibition by NSAIDs

Non-steroidal anti-inflammatory drugs (NSAIDs) are a class of pharmaceuticals that provide analgesic (pain-relieving) and antipyretic (fever-reducing) effects, and in much higher doses, anti-inflammatory effects. Known structure and function of COX-1 and -2 have allowed for extensive research into the interaction between NSAIDs and the enzyme active site. There are two classes of NSAIDs: the so-called classical and the so-called COX-2 selective inhibitors. The classical inhibitors are generally not isoform specific, but due to the size of the COX-2 active site they tend to bind more tightly. The NSAIDs generally compete with the substrate (AA) for binding to the active site. The most well recognized and prominent members of this group are acetylsalicylic acid (**1.7**), acetaminophen (**1.8**), ibuprofen (**1.9**) and naproxen (**1.10**).

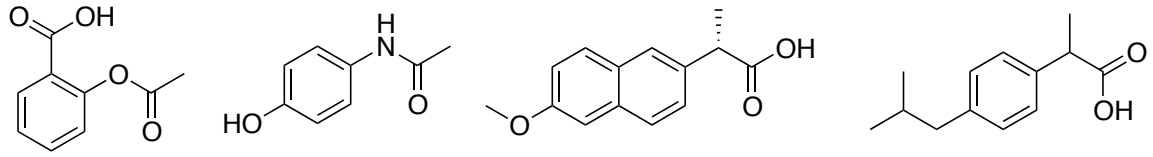

1.7 **1.8** **1.9** **1.10**

Acetylsalicylic acid (commonly known as aspirin) inhibits the COX-1 isoform more selectively than COX-2. It is an irreversible inhibitor and functions by acetylating residues in the active site of COX-1 and -2, (serine 530 and 516, respectively). These residues undergo trans-esterification rendering the enzyme inactive, due to steric hindrance of the acetyl group, which preventing normal substrate entry and fit.[42] Aspirin is often used as an analgesic and antipyretic to relieve pain and reduce fever, respectively. It is also used for its antiplatelet effect, as it inhibits the production of thromboxane, which is responsible for binding platelet molecules together. This antiplatelet ability is useful for reducing the risk of heart attack, stroke and blood clots. The non-specificity for COX isoforms leads to undesirable side effects such as gastrointestinal ulcers and stomach bleeding due to inhibition of the COX-1 enzyme, which is the predominant isoform found lining the stomach.[43]

Acetaminophen (ApAP, also commonly known as Tylenol) is a phenolic compound and is often classified as a NSAID, however it exhibits weak anti-inflammatory abilities. Studies suggest that ApAP is slightly more selective for the COX-2 isoform. ApAP is a reducing co-substrate of the peroxidase and is thought to inhibit COX activity by keeping the peroxidase in a reduced form, thereby preventing the formation of the catalytic tyrosyl radical. Although ApAP is one of the

most widely used drugs on the market, it is highly hepatotoxic and the leading cause of acute liver failure and unintentional death in the United States.[44]

Both ibuprofen and naproxen are nonselective COX inhibitors because of their ability to inhibit both COX-1 and COX-2 by reversibly binding the active site. Similar to aspirin, they both act as analgesics and antipyretics. Ibuprofen has minimal antiplatelet effect however it does act as a vasodilator and is often used for rheumatoid arthritis. Ibuprofen has a few common side effects such as nausea, gastrointestinal ulceration and bleeding again due to its non-specificity.[45] Naproxen can cause the same side effects as other NSAIDs.[46] It is often used to treat a variety of conditions that cause stiffness and may also be used against influenza; due to its ability to block the binding of the virus and ultimately preventing infection.[47]

The discovery of the COX-2 isoform and its subsequent crystallization ushered in a new era in NSAID development aimed at isoform selective inhibition.[21] Undesirable gastrointestinal side effects are minimized due to the selectivity of inhibition. Common selective COX-2 inhibitors known as coxibs are VIOXX (**1.11**), and Celebrex (**1.12**). These drugs are more bulky compared to the previous COX inhibitors, and thus fit into the larger COX-2 active site over COX-1.[21]

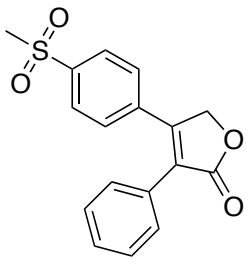

1.11

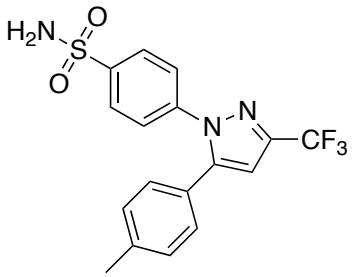

1.12

VIOXX is an anti-inflammatory drug that selectively inhibits the COX-2 enzyme and was found to lower prostaglandins responsible for inflammation, pain and fever. It was originally used to treat patients with rheumatoid arthritis; however, studies showed strong evidence for increased risks of myocardial infarction. The manufacturers (Merck) voluntarily withdrew the drug from the U.S and worldwide markets due to safety concerns related to increased risk of heart attack and stroke.[46] The two COX isoforms affect the balance of vasoactive prostanoids. TXA_2 is a vasoconstrictor and promoter of platelet aggregation and is largely COX-1 derived, whereas PGI_2, the vasodilator and inhibitor of platelet aggregation is, largely derived from COX-2 activity. Selective COX-2 inhibitors like these coxibs will shift the vascular homeostasis into a prothrombotic state causing negative atherosclerotic process such as a heart attack.[21]

Commercially available Celebrex is a selective COX-2 inhibitor used to treat osteoarthritis and rheumatoid arthritis. The polar sulfonamide side chain of the drug binds to a hydrophilic side pocket region, close to the active COX-2 binding site.[48] This drug is associated with an increased risk in cardiovascular problems. After the withdrawal of VIOXX, and similar concerns that Celebrex might carry similar risks, Pfizer voluntarily suspended advertisements and after an extended period of time resumed advertising, outlining all the risks and benefits to the general public.

1.8.2. Lipoxygenase Inhibition

Given that 5-LOX is at the beginning of the leukotriene cascade, it is an ideal candidate as a drug target. There are currently two main approaches to block leukotriene formation. The first successful efforts for the inhibition of leukotrienes target downstream receptors. Antagonists such as montelukast (Singulair) (**1.13**), zafirlukast (**1.14**), Pranlukast (**1.15**) block cysteinyl-leukotriene type-1 receptors. For example, Singular blocks the binding of leukotriene D4 on the cysteinyl leukotriene receptor in the lungs, which reduces bronchoconstriction.[49] Lukasts are generally well tolerated and have few side effects; however, not all patients are responsive to this treatment.

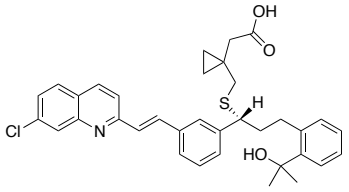

1.13

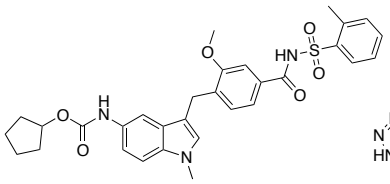

1.14

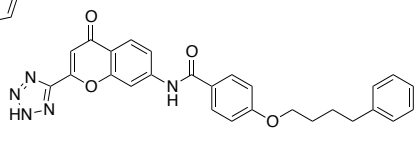

1.15

The other approach is to directly target 5-LOX. Currently drugs linked in this category lack selectivity, structure-activity relationships and enantioselectivity. Zileuton (**1.16**) is the only inhibitor specific to 5-LOX. It is believed to bind the catalytic iron located in the active site via its hydroxamic acid moiety. Zileuton is currently being marketed for its treatment of asthma; however, it has poor bioavailability and a short half-life, presumably owing to the oxidative lability of the hydroxamic acid moiety, requiring high doses.[50]

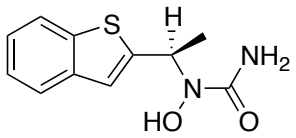

1.16

Nordihydroguaiaretic acid (NDGA) (**1.17**) is a polyphenol that is present in the leaves of the Creosote bush. For many years it was used for medicinal purposes to treat arthritis, pain and fever.[51,52] This polyphenol is present in herbal products (prepared from extracts) and was used as a dietary supplement.[51] It was later used as a food preservative because it was thought to have great antioxidant activity.[18,52] NDGA has been shown to reduce LOX from its hydroxide bound ferric (active) form to the water bound ferrous (inactive) form. NDGA is considered to be quite toxic presumably due to the redox cycling and formation of reactive oxygen species (ROS) by the oxidation of catechol to the quinone and back. It has be linked to renal and hepatotoxic side effects.[18,52] The toxicity of this compound has generated great controversy and has led to its removal as a preservative and use in supplements.

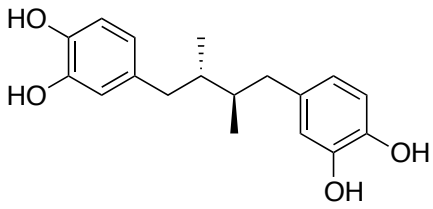

1.17

1.9 Project Proposal

Cyclooxygenase and lipoxygenase research has received a great deal of attention and made significant advancements in the past two decades; however, there are many fundamental questions surrounding the LOX enzymes. The mechanisms of regio- and stereochemical control in the oxygenation of arachidonic acid by the various isoforms is still unanswered. Structural information, particularly in the presence of bound substrate, is required to understand this, and should enable the development of isoform specific drugs, which could be beneficial, as various conditions could be treated more selectively.

Herein, we described two strategies to develop isoform-specific inhibitors of lipoxygenase. Efforts towards obtaining a substrate suitable for co-crystallization of the enzyme-substrate complex in its active conformation, along with the design and modification of inhibitors and their relative effects on LOX catalysis were investigated.

1.10. References

(1) Das, U. N. *Biotechnol. J.* **2006**, *1*, 420.

(2) Simopoulos, A. P. *Exp. Biol. Med.* **2008**, *233*, 674.

(3) Hibbeln, J. R.; Nieminen, L. R. G.; Blasbalg, T. L.; Riggs, J. A.; Lands, W. E. M. *Am. J. Clin. Nutr.* **2006**, *83*, 1483S.

(4) Bolland, J. L. *Q. Rev. Chem. Soc.* **1949**, *3*, 1.

(5) Russell, G. A. *J. Am. Chem. Soc.* **2001**, *79*, 2977.

(6) Porter, N. A. *Acc. Chem. Res.* **2001**, *19*, 262.

(7) Porter, N. A.; Weber, B. A.; Weenen, H.; Khan, J. A. *J. Am. Chem. Soc.* **1980**, *102*, 5597.

(8) Yau, T. M. *Mech. Ageing Dev.* **2002**, *11*, 137.

(9) Tanel, A.; Averill-Bates, D. A. *Free Radic. Biol. Med.* **2007**, *42*, 798.

(10) Nishikawa, A.; Sodum, R.; Chung, F. L. *Lipids.* **1992**, *27*, 54.

(11) Voet, D.; Voet, J. G. *Biochemistry*; John Wiley & Sons Incorporated, 1999.

(12) Funk, C. D. *Science.* **2001**, *294*, 1871.

(13) Haeggström, J. Z.; Funk, C. D. *Chem. Rev.* **2011**, *111*, 5866.

(14) Dewick, P. M. *Med. Nat. Prod.*; John Wiley & Sons, 2011.

(15) Harper, K. A.; Tyson-Capper, A. J. *Biochem. Soc. Trans.* **2008**, *36*, 543.

(16) Peters-Golden, M.; Brock, T. G. *PLFA.* **2003**, *69*, 99.

(17) van der Donk, W. A.; Tsai, A.-L.; Kulmacz, R. J. *Biochem.* **2002**, *41*, 15451.

(18) Nam, T.-G.; Nara, S. J.; Zagol-Ikapitte, I.; Cooper, T.; Valgimigli, L.; Oates, J. A.; Porter, N. A.; Boutaud, O.; Pratt, D. A. *Org. Biomol. Chem.* **2009**, *7*, 5103.

(19) Rouzer, C. A.; Marnett, L. J. *Chem. Rev.* **2003**, *103*, 2239.

(20) Schneider, C.; Pratt, D. A.; Porter, N. A.; Brash, A. R. *Chem. Biol.* **2007**, *14*, 473.

(21) Kurumbail, R. G.; Stevens, A. M.; Gierse, J. K.; McDonald, J. J.; Stegeman, R. A.; Pak, J. Y.; Gildehaus, D.; Miyashiro, J. M.; Penning, T. D.; Seibert, K. *Nature.* **2014**, *384*, 644.

(22) Smith, W. L.; DeWitt, D. L.; Garavito, R. M. *Annu. Rev. Biochem.* **2000**, *69*, 145.

(23) Andreou, A.; Feussner, I. *Phytochemistry.* **2009**, *70*, 1504.

(24) Glickman, M. H.; Klinman, J. P. *Biochemistry.* **1996**, *35*, 12882.

(25) Prigge, S. T.; Boyington, J. C.; Faig, M.; Doctor, K. S.; Gaffney, B. J.; Amzel, L. M. *Biochemistry.* **2003**, *79*, 629.

(26) Nelson, M. J. *Biochemistry.* **2001**, *27*, 4273.

(27) Lewis, R. A.; Austen, K. F.; Soberman, R. J. *N. Engl. J. Med.* **1990**, *323*, 645.

(28) Gilbert, N. C.; Bartlett, S. G.; Waight, M. T.; Neau, D. B.; Boeglin, W. E.; Brash, A. R.; Newcomer, M. E. *Science.* **2011**, *331*, 217.

(29) Percival, M. D.; Denis, D.; Riendeau, D.; Gresser, M. J. *Eur. J. Biochem.* **1992**, *210*, 109.

(30) Oldham, M. L.; Brash, A. R.; Newcomer, M. E. *J. Biol. Chem.* **2005**, *280*, 39545.

(31) Gillmor, S. A.; Villaseñor, A.; Fletterick, R.; Sigal, E.; Browner, M. F. *Nat. Struct. Biol.* **1997**, *4*, 1003.

(32) Steinberg, D.; Parthasarathy, S.; Carew, T. E.; Khoo, J. C.; Witztum, J. L. *N. Engl. J. Med.* **1989**, *320*, 915.

(33) Brash, A. R.; Boeglin, W. E.; Chang, M. S. *Proc. Natl. Acad. Sci. U.S.A.* **1997**, *94*, 6148.

(34) Kerjaschki, D.; Bago-Horvath, Z.; Rudas, M.; Sexl, V.; Schneckenleithner, C.; Wolbank, S.; Bartel, G.; Krieger, S.; Kalt, R.; Hantusch, B.; Keller, T.; Nagy-Bojarszky, K.; Huttary, N.; Raab, I.; Lackner, K.; Krautgasser, K.; Schachner, H.; Kaserer, K.; Rezar, S.; Madlener, S.; Vonach, C.; Davidovits, A.; Nosaka, H.; Hämmerle, M.; Viola, K.; Dolznig, H.; Schreiber, M.; Nader, A.; Mikulits, W.; Gnant, M.; Hirakawa, S.; Detmar, M.; Alitalo, K.; Nijman, S.; Offner, F.; Maier, T. J.; Steinhilber, D.; Krupitza, G. *J. Clin. Invest.* **2011**, *121*, 2000.

(35) Yoshimoto, T.; Takahashi, Y. *Prostaglandins Other Lipid Mediat.* **2002**, *68-69*, 245.

(36) Xu, S.; Mueser, T. C.; Marnett, L. J.; Funk, M. O., Jr. *Curr. Opin. Struct. Biol.* **2012**, *20*, 1490.

(37) Funk, C. D.; Cyrus, T. *Trends Cardiovasc. Med.* **2001**, *11*, 116.

(38) Nie, D.; Hillman, G. G.; Geddes, T.; Tang, K.; Pierson, C.; Grignon, D. J.; Honn, K. V. *Cancer Res.* **1998**, *58*, 4047.

(39) Hamberg, M.; Samuelsson, B. *Proc. Natl. Acad. Sci. U.S.A.* **2014**, *71*, 3400.

(40) Yu, Z.; Schneider, C.; Boeglin, W. E.; Brash, A. R. *Arch. Biochem. and Biophys.* **2006**, *455*, 188.

(41) Zheng, Y.; Brash, A. R. *J. Biol. Chem.* **2010**, *285*, 39866.

(42) Picot, D.; Loll, P. J.; Garavito, R. M. *Nature.* **1994**, *367*, 243.

(43) Sørensen, H. T.; Mellemkjær, L.; Blot, W. J.; Nielsen, G. L.; Steffensen, F. H.; McLaughlin, J. K.; Olsen, J. H. *Am. J. Gast.* **2000**, *95*, 2218.

(44) Larson, A. M.; Polson, J.; Fontana, R. J.; Davern, T. J.; Lalani, E.; Hynan, L. S.; Reisch, J. S.; Schiødt, F. V.; Ostapowicz, G.; Shakil, A. O.; Lee, W. M.; The Acute Liver Failure Study Group. *J. Hepatol.* **2005**, *42*, 1364.

(45) Rainsford, K. D. *Inflammopharmacology.* **2009**, *17*, 275.

(46) Bombardier, C.; Laine, L.; Reicin, A.; Shapiro, D.; Burgos-Vargas, R.; Davis, B.; Day, R.; Ferraz, M. B.; Hawkey, C. J.; Hochberg, M. C.; Kvien, T. K.; Schnitzer, T. J.; VIGOR Study Group. *N. Engl. J. Med.* **2000**, *343*, 1520.

(47) Duggan, K. C.; Walters, M. J.; Musee, J.; Harp, J. M.; Kiefer, J. R.; Oates, J. A.; Marnett, L. J. *J. Biol. Chem.* **2010**, *285*, 34950.

(48) Penning, T. D.; Talley, J. J.; Bertenshaw, S. R.; Carter, J. S.; Collins, P. W.; Docter, S.; Graneto, M. J.; Lee, L. F.; Malecha, J. W.; Miyashiro, J. M. *J. Med. Chem.* **1997**, *40*, 1347.

(49) Fanta, C. H. *N. Engl. J. Med.* **2009**, *360*, 1002.

(50) Lu, P.; Schrag, M. L.; Slaughter, D. E.; Raab, C. E.; Shou, M.; Rodrigues, A. D. *Drug Met. Dispos.* **2003**, *31*, 1352.

(51) Arteaga, S.; Andrade-Cetto, A.; Cárdenas, R. *J. Ethnopharmacol.* **2005**, *98*, 231.

(52) Sahu, S. C.; Ruggles, D. I.; O'Donnell, M. W. *Food and Chem. Toxicol.* **2006**, *44*, 1751.

-2-
Towards Fluorinated Substrate Analogs for Lipoxygenases

2.0 Introduction

The development of isoform-specific inhibitors for lipoxygenase would be greatly enabled by the availability of crystallographic structures of the individual enzymes with bound substrate. This would facilitate the design of inhibitors that could exploit the differences responsible for the regio- and stereoselectivity of substrate oxygenation carried out by the individual isoforms. Indeed, structures of COX-1 and COX-2 isoforms with arachidonate bound[1,2] guided the design of the blockbuster selective COX-2 inhibitors VIOXX (Merck) and Celebrex (Pfizer). The co-crystal structures were made possible by substituting the peroxidase site iron-protoporphyrin with a redox inactive cobalt-protoporphyrin to prevent enzyme turnover. No such redox cofactor swapping strategy is possible for lipoxygenase, whose non-heme iron is integral to the structure of the protein.

Therefore, in order to make a lipoxygenase-substrate complex incapable of turnover, we need to alter the structure of the substrate and not the enzyme. Unnatural lipid derivatives that fit within the active site and maintain the enzyme's active conformation, while preventing lipid oxidation, would be ideal candidates. The mechanism by which lipoxygenase catalyze arachidonic acid oxidation is initiated by the abstraction of one of the methylene hydrogen atoms on the substrate. If the methylene unit were replaced by a moiety lacking labile hydrogen atoms, this reaction can no longer take place. The similarity of the van der Waals radii of hydrogen (1.2 Å) and fluorine (1.47 Å), as well as the increased strength of a C-F bond (490 KJ/mol) compared to a C-H bond (410 KJ/mol) should allow for entry into the enzyme active site, but should prevent enzyme turnover.

In fact, there is one precedent in the literature for the design of polyunsaturated fatty acids wherein the methylene group residing between the two double bonds is replaced by a CF_2 group. Fried and coworkers carried out the synthesis of 7,7-, 10,10-, and 13,13- difluoroarachidonic acids, to examine their ability to serve as substrates for COX and sLOX-1.[3] In principle, 7,7-difluoroarachidonic acid should inhibit 5-LOX, 10,10-difluoroarachidonic acid should inhibit 12-LOXs and 13,13-difluoroarachidonic acid should inhibit 15-LOXs, based on the position of the CF_2 group.

Scheme 2.1 outlines the synthetic route to 10,10-di-fluoroarachidonic acid by Fried and coworkers. A similar approach was used to synthesize 7,7- and 13, 13-difluoroarachidonic acids.[3] The syntheses of 7,7- and 13,13-difluoroarachidonic acid were shortened by two steps; however, the overall yields were similar.

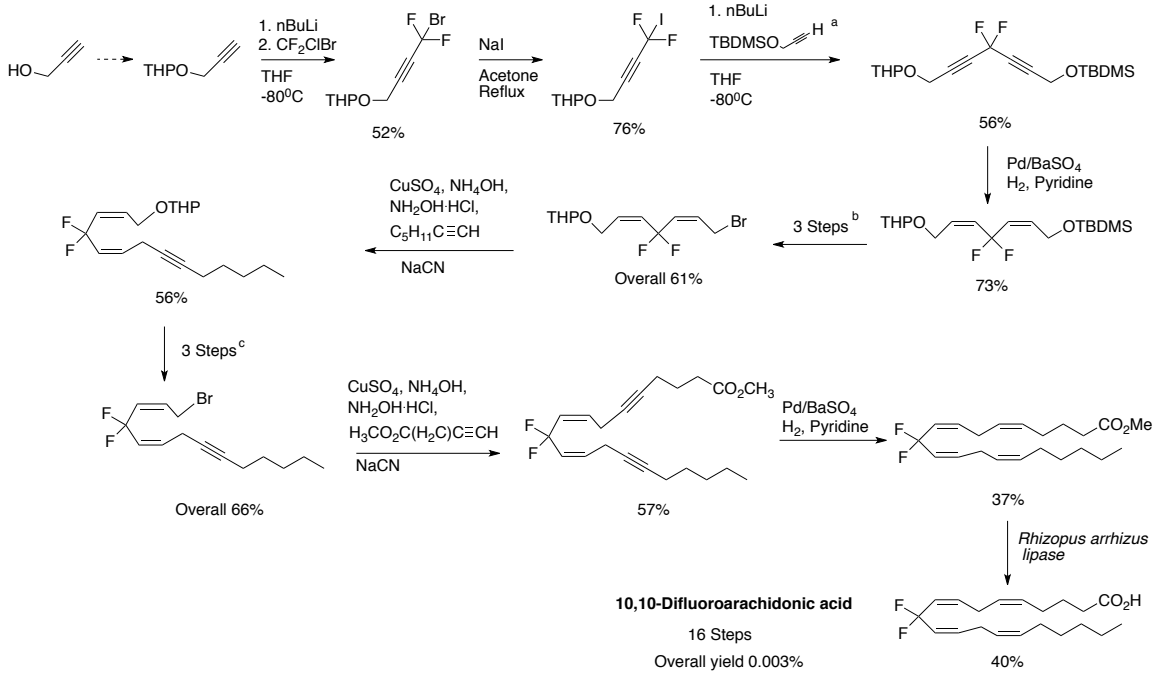

[a] Obtained from propargyl alcohol.
[b] Involved removal of TBDMS silyl protecting group, followed by mesylation and substitution with bromide.
[c] Involved removal of THP protecting group, followed by mesylation and substitution with bromide.

Scheme2.1. The total synthesis of 10,10-difluoroarachidonic acid.

Upon completion of the synthesis of these unnatural polyunsaturated acids, subsequent experiments were performed to determine their activity as substrates for COX and soybean LOX.[4] Only 10,10-difluoroarachidonic acid was assayed. Fried reports the exposure of 7,7-difluoroarachidonic acid to aqueous buffer performs the facile S_N2' substitution of fluoride by water.[3,4] We surmise that this may have also been true for 13,13-difluoroarachidonic acids. It is unclear why 10,10-difluoroarachidonic acid would be stable in aqueous solution whereas 7,7- and

13,13-difluoroarachidonic acid would not. A survey of the literature does not report any other studies using these compounds.

To determine whether 10,10-difluoroarachidonic acid was a substrate in the prostaglandin pathway it was treated with COX; derived from ram seminal vesicle microsomes (COX-1), and highly purified COX-1. The enzymatic conversion was also tested with soybean lipoxygenase. When incubated with COX-1, the resulting products were fluorinated, conjugated hydroxy acids, typical of metabolism; however, the cyclization to form prostaglandin-like products was not observed. The enzymatic oxygenation occurring in the α-position to the CF_2 group (i.e. C11) supported the general COX mechanism.[4] Both COX and sLOX catalyzed the conversion of 10,10-difluoroarachidonic acid to 10,10-difluoro-11S-HETE and 10-fluoro-8,15-diHETE as shown below.

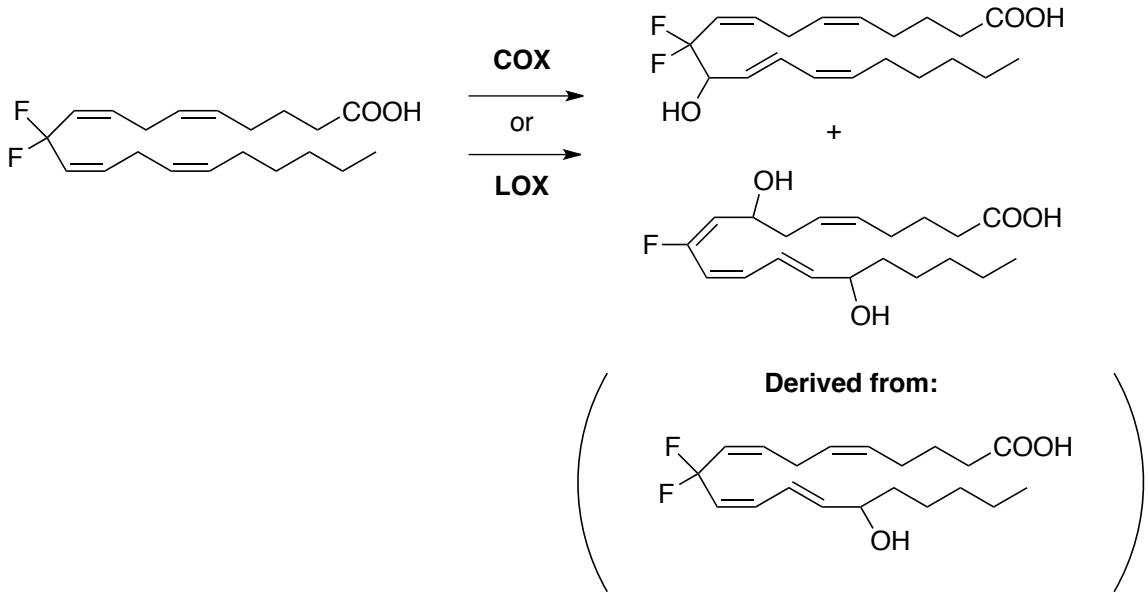

COX and LOX both abstract a methylene hydrogen from the 13-position of arachidonic acid. The formation of the above products is not surprising considering

the CF_2 group in 10,10-difluoroarachidonic acid is in neither of these specific positions. 10,10-difluoroarachidonic acid does not appear to be a good inhibitor of either of the enzymes and is also not an ideal candidate to prevent enzyme turnover.

With these results, it is likely that the 7,7- and 13,13-difluoro acids might block the pathway to leukotrienes that are generated from lipoxygenase enzymes, 5-LOX or 15-HETEs generated from 15-LOX. Knowing that 5-LOX has been unequivocally linked to a variety of human diseases, it would be ideal to examine specific inhibitors of this enzyme. The 7,7-difluoroarachidonic acid should act as an selective inhibitor for 5-LOX but not 12- or 15-LOX and would provide more insight into the mechanism of action and leukotriene cascade process. Although these compounds are reported they were never tested and have not been revisited, presumably because of the arduous nature of the syntheses, and perhaps doubts about their stability in aqueous solution.

Although Fried was able to successfully synthesize these unnatural polyunsaturated acids and confirm their activity as substrates, the designed routes were quite challenging and presented several problems. The synthesis would be difficult for us to replicate, as the haloalkane used as the source of the key geminal difluoride moiety (CF_2ClBr) is prohibited from sale or use in Canada because of its ozone depleting properties.

Our proposed approach was to use a different methodology to prepare a simpler fatty acid, such as 11,11-difluorolinoleic acid (**2.1**) and determine its activity as an inhibitor of soybean lipoxygenase L-1. This compound has not yet been synthesized. Should this compound inhibit the enzyme, it could be used in co-

crystallization attempts facilitated by the known crystallization conditions of soybean L-1.[5] Solution of a three dimensional structure of 11,11-difluoroarachidonic acid with soybean L-1 will provide the first insight into the binding mode of fatty acid substrates to lipoxygenases. This strategy could then be expanded for the synthesis of other fluorinated fatty acids as substrate analogs of the human LOXs, such as 7,7-difluoroeicosa-5(Z),8(Z)-dienoic acid (**2.2**), whose protiated analog is a known substrate for 5-LOX.[6]

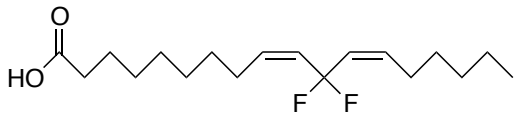

2.1

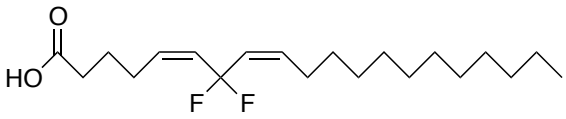

2.2

2.1 Proposed Synthesis of 11,11-Difluorolinoleic Acid

Carbon-fluorine bond formation can be quite challenging. In the past decade, there have been a number of new transformations for carbon-fluorine bond formation that have advanced the fields of enantioselective fluorination, transition metal-mediated fluorination, and applications for late stage functionalization for the synthesis of imaging agents for positron emission tomography (PET).[7] Despite this progress, general and selective carbon-fluorine bond formation is difficult, usually resulting in a vast amount of undesired products and low yields.[7] The optimal

approach to preparing our desired molecule would be to start with a difluorinated compound, as in Fried's approach, and build the lipid around it.

The most common reaction to install a difluoromethylene unit is undoubtedly via the Reformatsky reaction show in Scheme 2.2.[8,9]

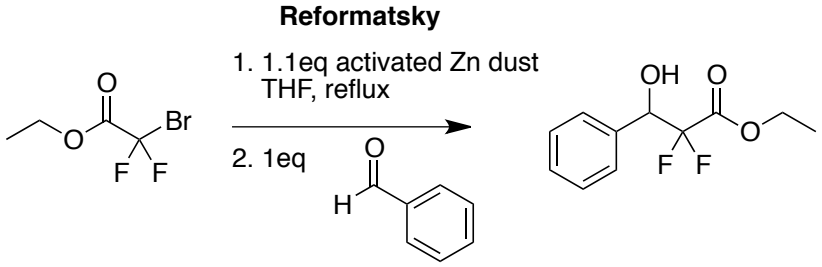

Scheme 2.2. An example of a Reformatsky coupling reaction to install a difluoromethylene group.

Regardless, literature precedence and chemical attainability focused on a synthetic strategy centered on using ethylbromodifluoroacetate (Et-BDFA, **2.3**) commonly used in Reformatsky reactions, but as shown in Scheme 2.3 to prepare 11,11-difluorolinoleic acid.

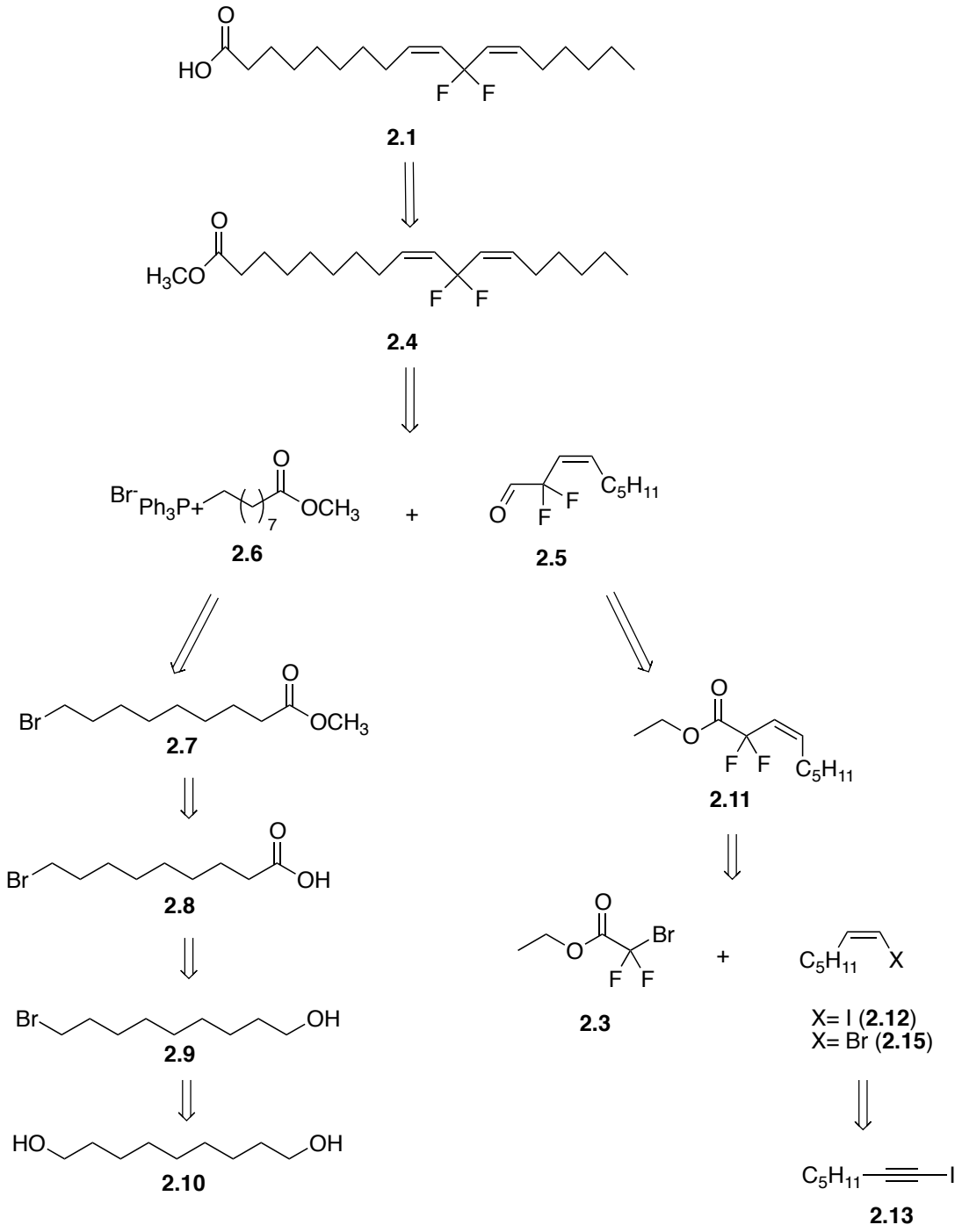

Scheme 2.3. A proposed synthesis of 11,11-difluorolinleic acid from Et-BDFA (**2.3**).

A Negishi reaction between (*Z*)-1-iodoheptene or (*Z*)-1-bromoheptene and the organozinc reagent derived from **2.3** was proposed in the preparation of the omega-6 (C10-C18) fragment. The resulting ester could then be reduced and the resultant aldehyde used in a Wittig olefination with a phosphonium salt of the C1-C9 fragment.

2.2 Synthesis of the C1-C9 Phosphonium Salt 2.6

Since literature precedent existed for the formation of the desired 8-carboxymethyl octyltriphenylphosphonium bromide salt (**2.6**)[10] of carbons 1 through 9 in our target molecule, we began with its reproduction. We carried out the bromination and Jones oxidation sequentially as reported to form 9-bromononanol (**2.9**) and then 9-bromononanoic acid (**2.8**), respectively. Similar yields to those reported were obtained.[10]

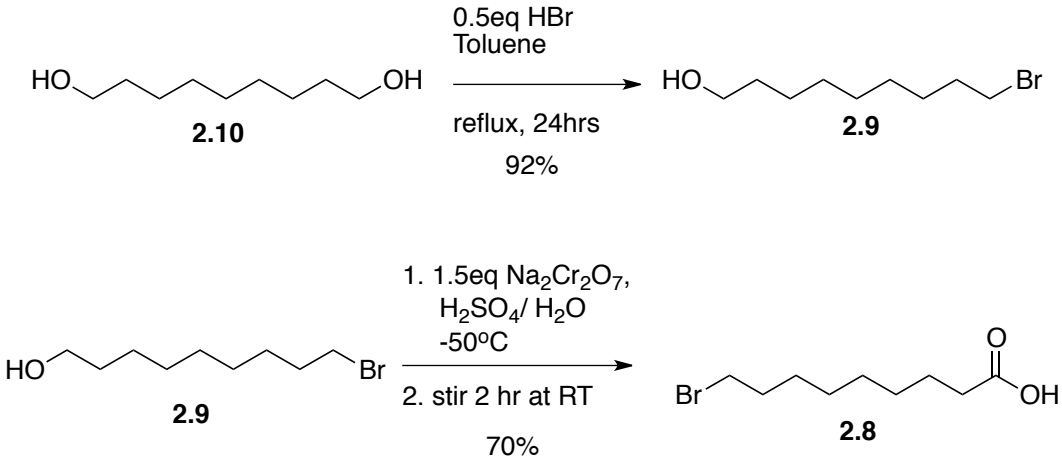

The reported esterification[10] presented some challenges. The desired product could be obtained, however the yields were very low (ranging from 10-

50%) and the mass balance was a viscous tar like substance, which made manipulation and purification very difficult.

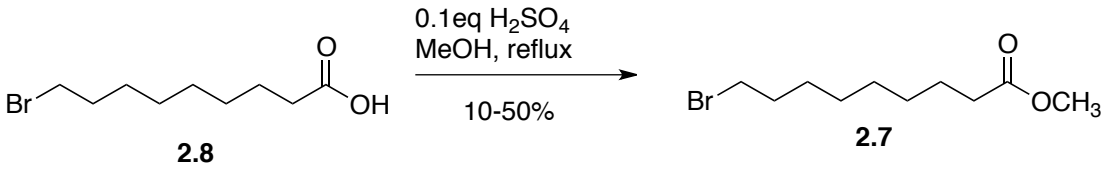

2.8 **2.7**

Alternatively, the ester could be prepared more easily via the acid chloride. Thus, the 9-bromononanoic acid was treated with oxalyl chloride and 1 drop of DMF, after which methanol was added slowly. The reaction mixture was left to stir overnight. After workup and purification the pure methyl 9-bromo nonanoate (**2.7**) was obtained in much higher yield.

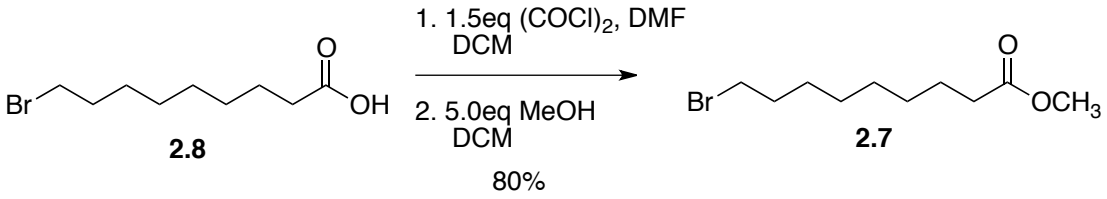

2.8 **2.7**

The final substitution step to form the 8-carboxymethyl octyltriphenylphosphonium bromide salt (**2.6**) proceeded smoothly, and following optimization of the purification, **2.6** was obtained in good yield.

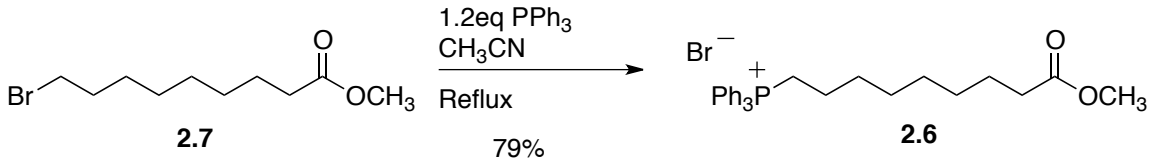

2.3 Synthesis of the C10-C18 α,α-Difluoroaldehyde 2.5

The preparation of the C10-C18 fragment first required (*Z*)-1-iodoheptene (**2.12**), which has been prepared from 1-heptyne in several literature precedents as shown in Scheme 2.4. [11] We followed the general procedure reported by Stella.[12]

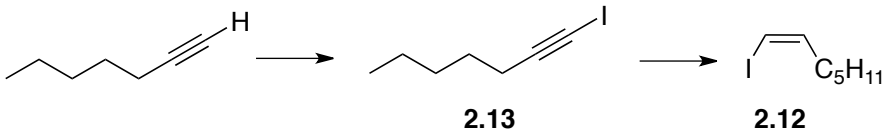

Scheme 2.4. The general preparation of (*Z*)-1-iodoheptene from 1-heptyne.

The treatment of 1-heptyne with *n*-butylithium to form the lithium acetylide reagent proceeded as expected. The temperature of the reaction was cooled further and the acetylide was treated with iodine in THF. Upon workup, the crude 1-iodoheptyne (**2.13**) was obtained. The ^{1}H-NMR spectrum of the sample showed only minor impurities and by TLC there appeared to be minimal addition products. Attempts to purify the crude material failed, with iodine being formed, presumably with concomitant polymerization of the compound. This was confirmed by a slight pink streaking on the column and the product obtained was a viscous semi-solid. Due to the good quality of the crude product, and the fact that most previous reports utilized the crude material, we decided to do the same.

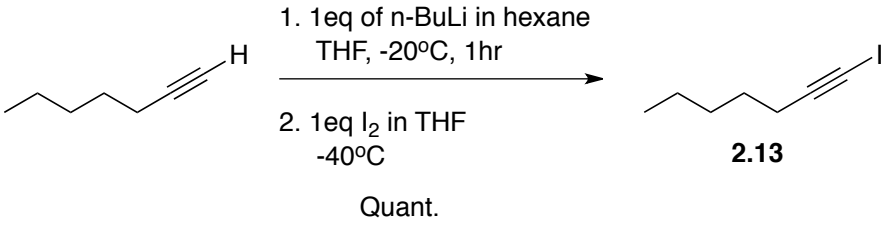

Reduction of the iodoalkyne with 9-BBN was attempted according to the literature procedure.[12] Using 9-BBN is an advantageous hydroborating reagent because it is known for its high regioselectivity.[11] In the presence of stoichiometric amounts of 9-BBN, (*Z*)-vinylboranes should form and protonolysis should provide the desired (*Z*)-alkene. Several attempts at using 9-BBN as the hydroborating agent were performed in THF, but all were unsuccessful. The two prominent spots by TLC corresponded to unreacted 1-iodoheptyne and 1-heptyne. Any products formed decomposed upon isolation attempts using flash chromatography, which was supported by 2D TLC analysis.

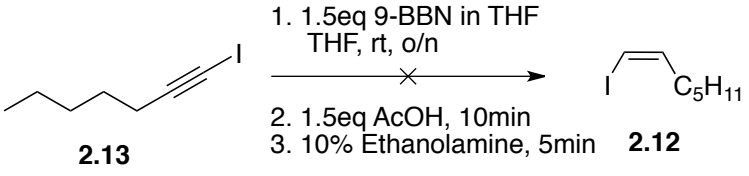

The precedence for the conversion of carbonyl compounds to vinyl iodides prompted a parallel attempt to prepare the desired compound from hexanal. In a procedure reported by Stork *et al*, (*Z*)-1-iodo-1-alkenes could be synthesized stereoselectivity via a Wittig reaction of iodomethylenetriphenylphosphorane

(**2.14**) with aldehydes.[13] In order to synthesize the desired (*Z*)-1-iodoheptene, we first prepared the iodomethyltriphenylphosphonium salt (**2.14**). The following was successfully made using a procedure by Seyferth *et al*.[14]

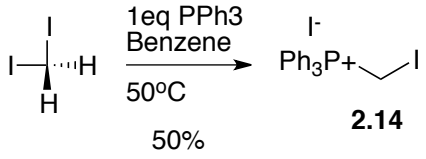

Once salt **2.14** was obtained, it was dissolved in dry THF, with an equimolar amount of sodium hexamethyldisilazane (NaHMDS), under inert atmosphere at room temperature. At this point the iodomethylenetriphenylphosphorane should be present and treatment with hexanal should generate the desired vinyl iodide. Upon examination of the products, it was disappointing to learn that the reaction was unsuccessful. There were no vinylic proton peaks present by crude ^{1}H-NMR analysis.

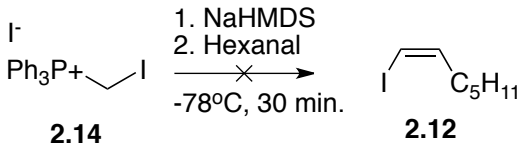

In parallel with attempts to prepare the desired vinyl iodide, the corresponding vinyl bromide was prepared.

Following experimental conditions reported by Kellersmann *et al,* the successful synthesis of *(Z)*-1-bromoheptene (**2.15**) was completed.[15]

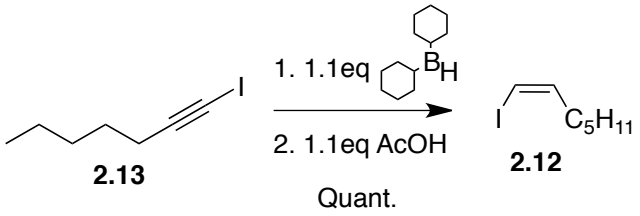

Initial attempts at the preparation of the brominated alkene were performed using a solution of 1 M catecholborane in THF. Upon analysis of the reaction by TLC, a wide array of products had formed and a fairly insoluble black semisolid was collected. It was clear that product formation had not occurred through crude ^{1}H-NMR analysis, given by the absence of the vinylic alkene protons. Due to the concern of the quality of the reactant, a new bottle of 1 M catecholborane in THF, along with a bottle of neat catecholborane (no solvent) were tested. Two parallel reactions were performed and product formation occurred only when using neat catecholborane (no solvent). It was clear that product formation was concentration dependent. In more dilute reaction conditions, the rate of our desired reaction was slower than other side reactions. However, when concentrated the rate of product formation was faster, thereby limiting the formation of the other side products.

A two dimensional TLC indicated that the (*Z*)-1-bromoheptene was not stable on silica. Reported purification methods indicate Kugelrohr distillation was the best method to purify the (*Z*)-1-bromoheptene.[15] Due to the larger scale of our reaction fractional distillation was successfully used to obtain **2.15** in similar yields.

Attempts at preparing the (*Z*)-1-iodoheptene using an analogous hydroboration, iodination sequence were unsuccessful and further search into the literature revealed a procedure that required the immediate preparation of the hydroborating reagent immediately before use. Initial attempts used commercially

available solution of 9-BBN in THF as the hydroborating reagent and the reaction was carried out in THF. The formation of 9-BBN is prepared by hydroboration of 1,5-cyclooctadiene with borane and exists as a dimer. The 9-BBN forms a complex as shown in scheme 2.5 with THF that is in equilibrium with this dimer and is said to react faster.[11] A paper by Bracher et al, reports that 9-BBN reacts much slower with alkynes and requires a 24-hour reaction period, allowing accessibility of the hydrogen.

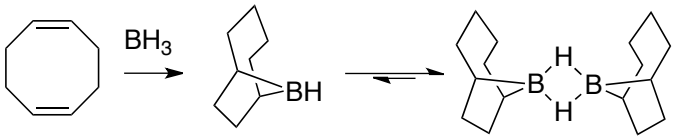

Scheme 2.5. A complex of 9-BBN in THF. Equilibrium favours the dimerized complex.

In this procedure, the use of borane-dimethylsulfide complex in ether was treated with cyclohexene. A very detailed description specified the time required for the formation of dialkylborane. The 1-iodoheptyne was added to the reaction mixture and upon completion of the general procedure; the desired (*Z*)-1-iodoheptene (**2.12**) was prepared in a shorter period of time, with minimal byproducts and in quantitative yields, compared to previous attempts. The main difference between the two approaches was the in situ preparation of the dialkylborane.

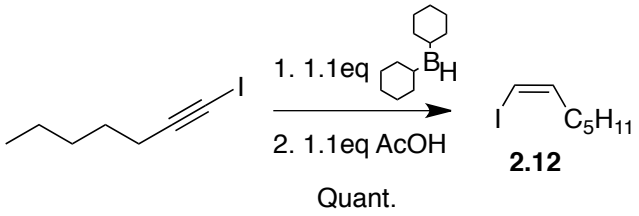

With both the vinyl bromide **2.15** and vinyl iodide **2.12** in hand, we attempted the Negishi type cross coupling of each of these with Et-BDFA, to obtain the desired compound **2.11**. Upon workup, ^{1}H-NMR analysis of the crude material, revealed no product formation.

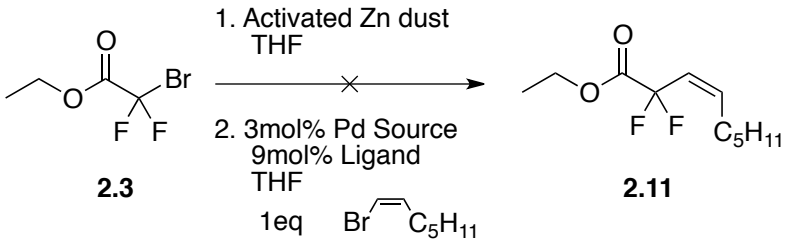

Initial concerns centered on the palladium source used, time allowed for ligand exchange, and the type of ligand being used. Table 2.1 outlines the various palladium sources and ligands used, based on a paper discussing ligand effects on alkenyl halides to acquire (*Z*) stereoselectivity.[16] After several attempts using different palladium sources, ligands and reaction times it became clear that the (Z)-1-bromoheptene was unable to be coupled through this approach. It appeared as though the Et-BDFA was reduced upon workup of the reaction.

Table 2.1. A list of palladium sources and ligands tested in a Negishi type cross coupling reactions.

Pd Source	Ligand
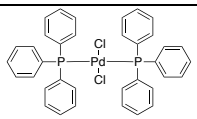 Dichlorobis(triphenylphosphine)palladium(II): $PdCl_2(PPh_3)_2$	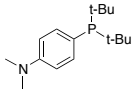 2-di-t-butylphosphine-N,N-dimethyl-aminobiphenyl
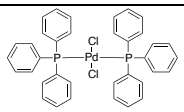 Dichlorobis(triphenylphosphine)palladium(II): $PdCl_2(PPh_3)_2$	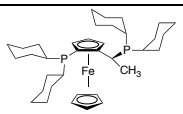 (Dicyclohexylphosphino)ferrocenylethyldicyclohexylphosphine
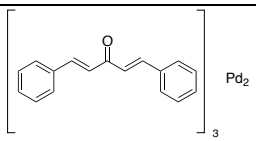 Tris(dibenzylideneacetone)dipalladium(0): $Pd_2(dba)_3$	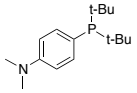 2-di-t-butylphosphine-N,N-dimethyl-aminobiphenyl
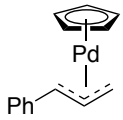 Petey: $Pd(\eta^3\text{-}1\text{-}PhC_3H_4)(\eta^5\text{-}C_5H_5)$	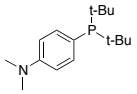 2-di-t-butylphosphine-N,N-dimethyl-aminobiphenyl
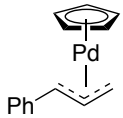 Petey: $Pd(\eta^3\text{-}1\text{-}PhC_3H_4)(\eta^5\text{-}C_5H_5)$	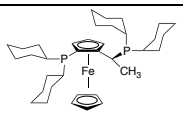 (Dicyclohexylphosphino)ferrocenylethyldicyclohexylphosphine

We surmised that formation of the organozinc reagent may be the issue with reactivity. Zinc can be activated by a series of promoters or additives.[17] A convenient titration method to test the formation of organozinc reagents, presented in a paper by Krasovskiy *et al*, was used to test our activation methods.[18] The zinc was activated best by vigorously stirring zinc dust in concentrated hydrochloric acid (to remove any zinc oxide), followed by rinsing with copious amounts of water,

methanol, and ether and dried under reduced pressure. Other attempts such as activation using iodine or ethyl-iodide did not fully activate the zinc, according to the titration results.

Now that we were confident with the preparation of the organozinc complex, one last attempt at coupling (*Z*)-1-bromoheptene was performed. However, we were disappointed to learn that once again Et-BDFA was reduced upon workup of the reaction. We were unable to successfully couple the Et-BDFA to a brominated olefin through Negishi type coupling.

2.4 A Cu-Catalyzed Cross Coupling Approach to the C10-C18 Fragment

In 1999, Sato reported a Cu-catalyzed reaction between a vinyl iodide and Et-BDFA.[19] With the failure of the Negishi approach, we elected to try the following reaction.

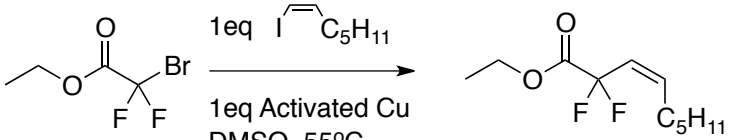

2.3 **2.11**

Copper was activated, DMSO was freshly distilled and the reaction was executed as reported. The reaction was left for the reported 24 hours and a workup was performed as mentioned. Analysis of the crude reaction mixture by ^{19}F-NMR revealed the formation of two main products: the desired product and something else. These products could not be separated by flash column chromatography on silica gel. Sato's paper did not mention the formation of any other products;

however, by ^{19}F-NMR spectrum it was clear that the undesired product was favoured.

The progress of the reaction was monitored over the 24 hour reaction period by removing aliquots, working them up and analyzing by both TLC and ^{19}F-NMR. The ^{19}F-NMR spectra are given in Figure 2.1.

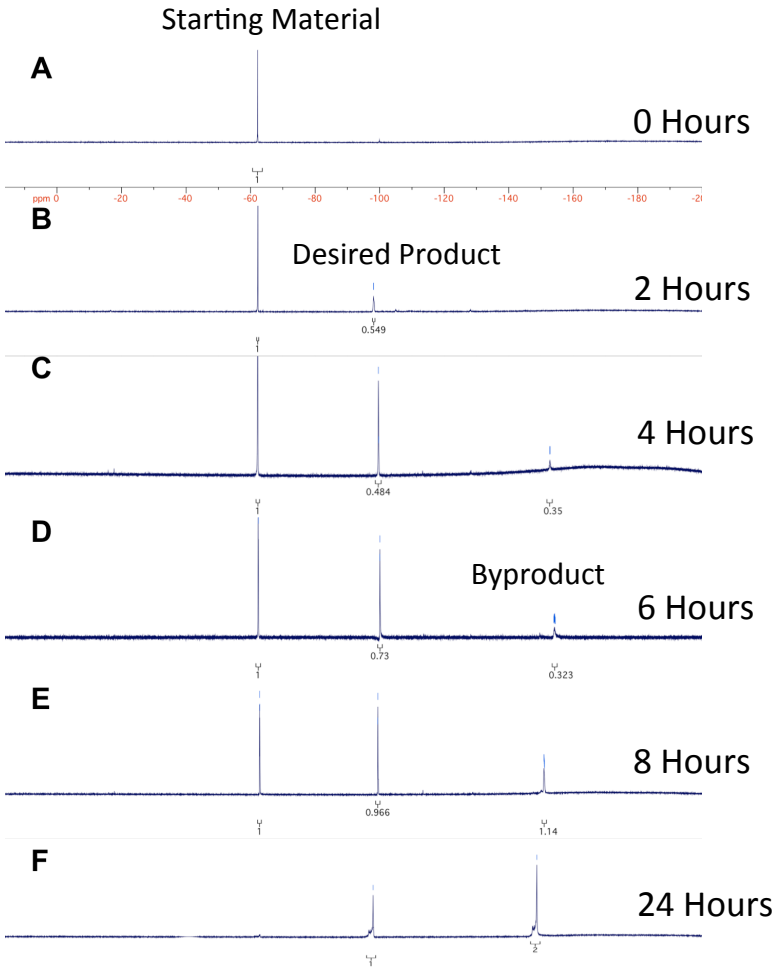

Figure 2.1. Aliquots removed from copper catalyzed cross coupling reaction between Et-BDFA and (*Z*)-1-iodoheptene, monitored by ^{19}F-NMR (no reference, no H-decoupling), for 24 hours. Starting material at -62ppm, desired product at -98ppm, unknown byproduct at -150ppm.

This was an interesting observation and correlated to earlier findings on the stability of the (*Z*)-1-iodoheptene and (*Z*)-1-bromoheptene. When left at room temperature for a long period of time the alkene begins to form a solid, believed to be the polymer. Exposing (*Z*)-1-iodoheptene to heat around 55°C (coupling temperature) resulted in an increasing rate of polymer formation. If polymer formation is occurring throughout the reaction, it becomes unavailable to couple to our fluorinated ester. With the reaction being heated to 55°C for 24 hours, it is likely that the polymer was forming, allowing the Et-BDFA starting material to perform other chemical reactions. Based on the chemical shift of the major byproduct, we propose the reduced compound **2.16** was produced, presumably from hydrolysis of the organozinc reagent upon workup.

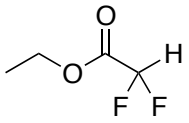

2.16

With this idea in mind, a second TLC and ^{19}F-NMR experiment was performed, wherein 1.0eq of the iodinated alkene was added at time zero, 4 hours and 6 hours (times at which byproduct was observed). The reaction was then left overnight. Upon analysis of the reaction mixture by TLC and ^{19}F-NMR (Figure 2.2) only the desired coupled product (**2.11**) was formed.

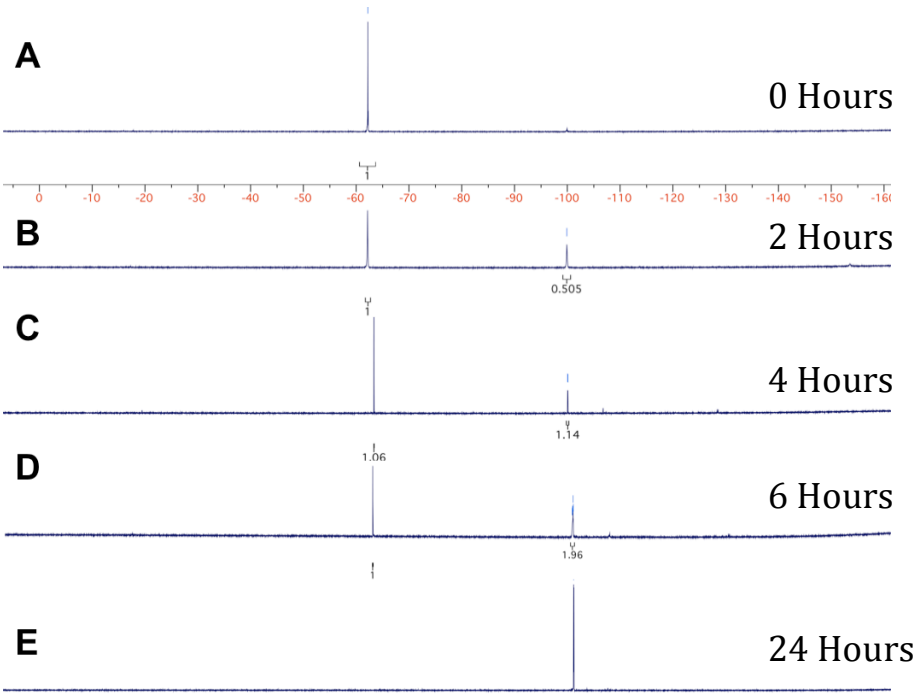

Figure 2.2. Aliquots removed from copper catalyzed cross coupling reaction between Et-BDFA and (*Z*)-1-iodoheptene, monitored by ^{19}F-NMR (no reference, no H-decoupling), for 24 hours. 1.0eq of (*Z*)-1-iodoheptene added at 0hr, 4hr and 6hr. Starting material at -62ppm, desired products at -98ppm.

This new approach of adding aliquots of (*Z*)-1-iodoheptene was repeated and compound **2.11** was purified and obtained in a reported average yield of 89%, compared to that reported (69%) by Sato and group (which could not be reproduced).[19] Attempts at coupling Et-BDFA to vinyl bromide were unsuccessful. The only product observed upon workup was that of **2.16.**

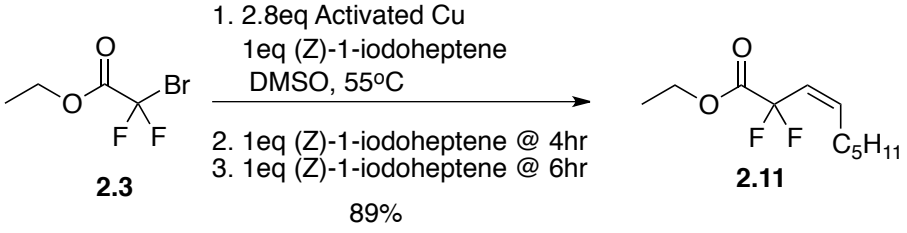

2.5 Reduction of the Ester Moiety of 2.11

With the first key step in our synthesis successfully completed, we moved on to reduce the ester moiety to acquire the desired aldehyde for the second key step (Wittig Olefination). Several attempts at reducing the ester were performed, first using DIBAL-H. Altering the reaction conditions by varying concentration of DIBAL-H, repeatedly resulted in no reaction and isolation of starting material. Increasing the reaction temperature resulted in a wide array of un-isolable products.

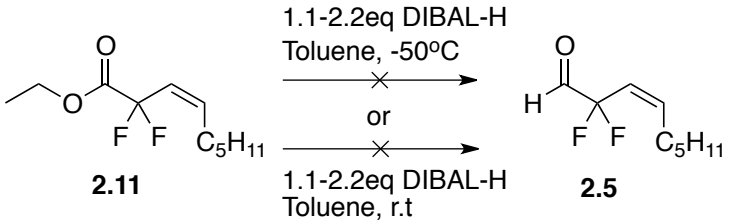

Given the difficulties in reducing the ester **2.11** with DIBAL attempts were made at reducing the ester to the corresponding alcohol, by use of $NaBH_4$; the alcohol could then be oxidized to the aldehyde later. After trying several different solvents (methanol, ethanol and isopropanol) and optimizing reagent concentration, we were successfully able to obtain (*Z*)-2,2-difluoronon-3-en-1-ol (**2.17**). Interestingly, while initial attempts in methanol and ethanol yielded no reaction, the product could be obtained in freshly distilled isopropanol, using 4.0eq of $NaBH_4$.

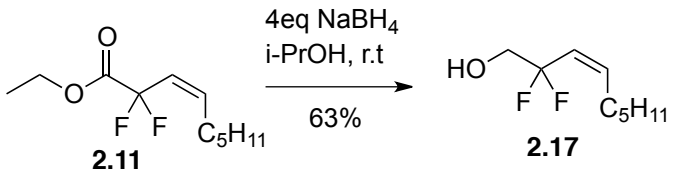

Subsequent oxidation of the alcohol to the desired aldehyde was unfortunately problematic. Initial attempts using either Swern or Dess-Martin conditions were unsuccessful and only starting material remained.

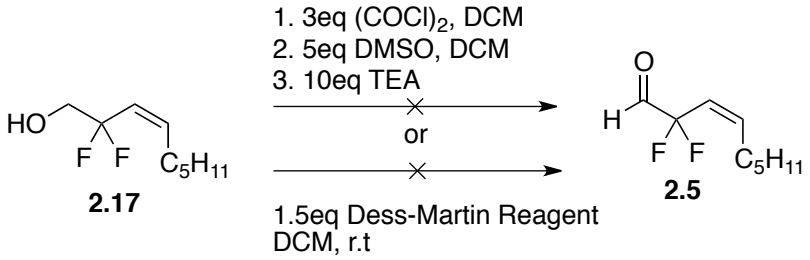

However, under PCC reaction conditions a new product spot was observed. Although difficult, the isolation of (*Z*)-2,2-difluoronon-3-ene-1,1-diol (**2.18**) was possible, implying oxidation had occurred, followed by hydration of the aldehyde to give the germinal diol. Several attempts were made to avoid exposing the aldehyde to water during the reaction and/or work-up and/or analysis. However, all attempts resulted in the same hydrated product.

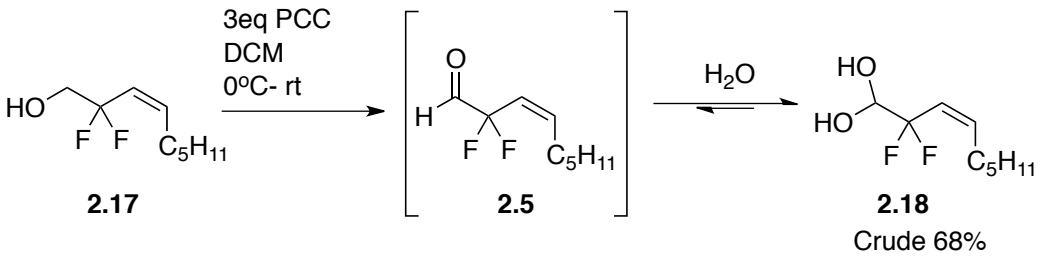

A paper by Golding *et al,* outlines the extreme and difficult measures they were forced to adopt, to acquire a similar aldehyde (CF_3CH_2CHO).[20] Discouragingly, in the end, they obtained their aldehyde in a 5.6% yield through product distillation.

Due to the inability to isolate the aldehyde directly, we decided to try forming the aldehyde in situ, using a strong base like sodium or potassium HMDS. Through a one-pot reaction our goal was to attempt a Wittig olefination with the previously made phosphonium salt (**2.6**). After workup, the hydrated hemi-acetal was isolated. Even with the aldehyde forming in situ, it is far too electrophilic that the equilibrium still favours the hydrated hemi-acetal and a Wittig olefination cannot be performed.

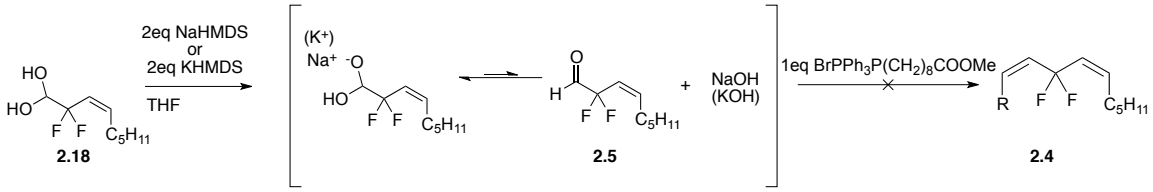

Following a paper by Tsukamoto *et al*, they show the synthesis of a di-fluorinated ethyl hemiacetal, for its use in reactions, most importantly the formation

of a double bond; producing diethyl 3,3-difluoroprop-1-ene-1,3-dicarboxylate.[21] Our assumption was that if an ethyl hemiacetal could be generated, treatment with a strong base would promote the in situ formation of the aldehyde and in the presence of our triphenylphosphonium nucleophile, the (*Z*)-alkene could be obtained. We felt the ethoxy moiety would be easier to isolate dry. The ethyl hemiacetal (**2.19**) was generated using 0.33 eq of LAH at -78°C. This material was unable to be purified because when placed on a silica column, the corresponding hydrate was formed. Tsukamoto reported similar finding and purification was done via distillation.[21] This ethyl hemiacetal was treated with KHMDS and the triphenylphosphonium salt, but once again the reaction conditions produced the hydrated aldehyde.

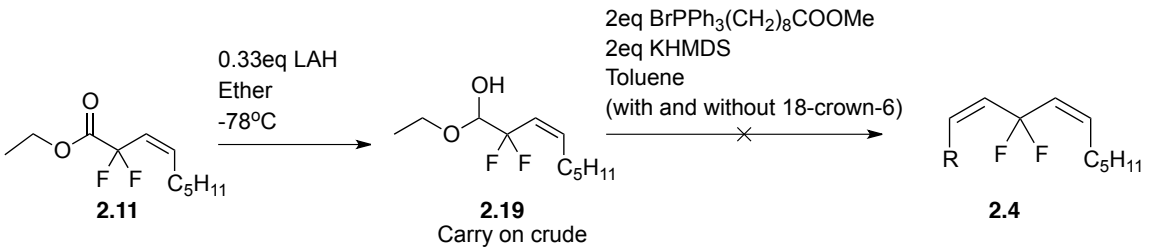

One last attempt at this reaction was performed on a tosyl hemiacetal (**2.20**). A tosyl is a better leaving group, than the previous hydroxyl and ethoxy; therefore the formation of the aldehyde, in principle, should be easier. This product again was carried on crude due to the above mentioned purification problems. The tosylated hemiacetal was treated with potassium HMDS and the triphenylphosphonium salt, and again the formation of the geminal diol was observed.

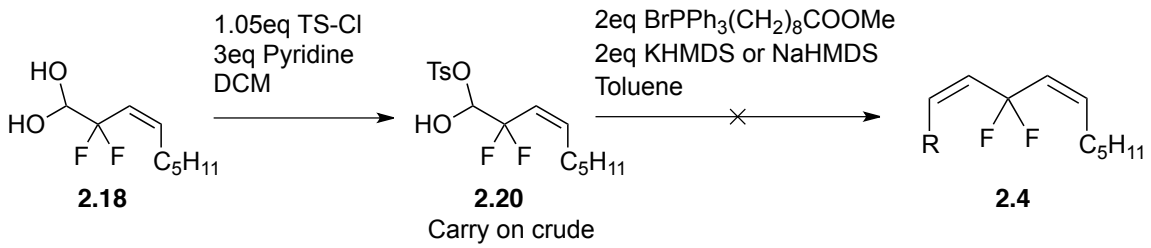

The use of a strong base is required for deprotonation and promotion of the *in situ* formation of the aldehyde; however, with trace amounts of water the strong base will generate hydroxide, which can then react with the aldehyde. The equilibrium will be driven back to the stable diol.

2.6 Polarity Reversal of the Triphenylphosphonium Ylide

Since our attempts to produce the α,α-difluorinated aldehyde, to perform a Wittig reaction with the C1-C9 triphenylphosphonium salt were unsuccessful, we wondered if the overall approach may still be successful upon changing the polarity of the Wittig olefination as shown in Scheme 2.6. In other words, use our previously synthesized (*Z*)-2,2-difluoronon-3-en-1-ol and generate its corresponding triphenylphosphonium salt, which could then be coupled to the corresponding aldehydic progenitor of the C1-C8 chain.

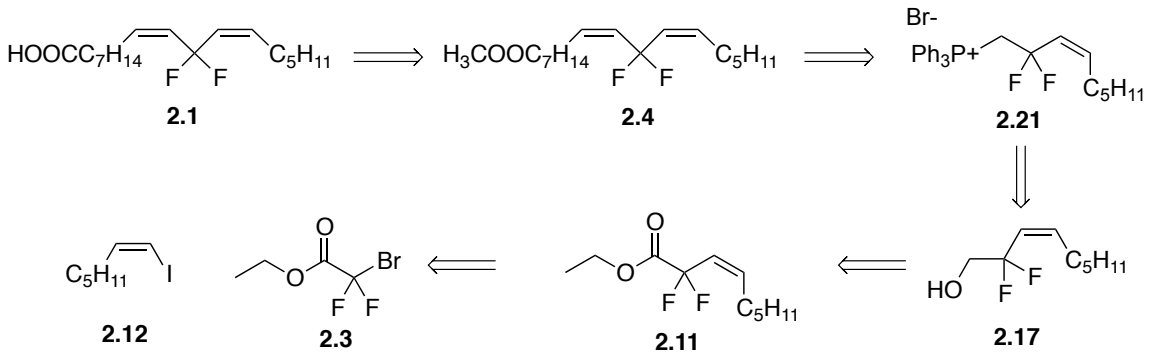

Scheme 2.6. A retrosynthetic design reversing the polarity of the triphenylphosphonium ylide.

A paper by Hanamoto *et al*, outlined the formation of several fluorinated triphenylphosphonium salts using various alkyl halides.[22] Before attempts could be made to produce the fluorinated triphenylphosphonium salts, we needed to prepare halide (**2.22**) or pseudohalides (**2.23**), (**2.24**) precursors. Parallel reactions were performed to generate the three compounds**.** However purification attempts of the alkyl halides/pseudohalides resulted in product degradation as observed by 2D TLC and therefore were carried on crude. Sadly the halides/pseudohalides decomposed back into the starting material.

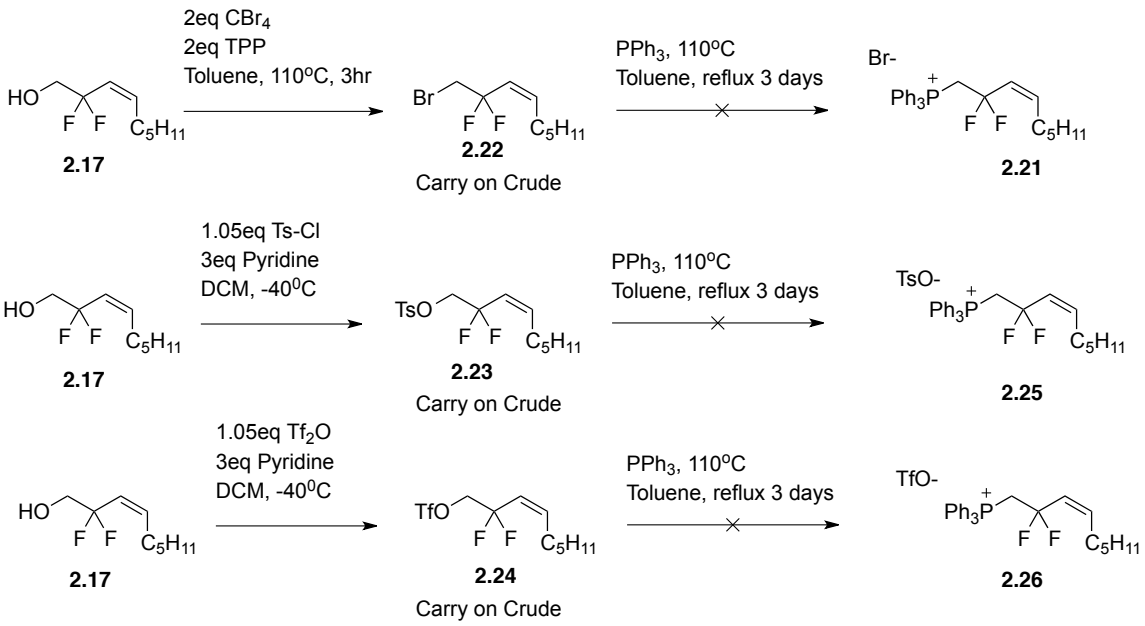

With the crude alkyl halides/pseudohalides in hand, attempts were made to prepare the corresponding phosphonium salts directly. However, all attempts were unsuccessful. The heat required for the formation of the phosphonium salt enabled other chemistry to occur. Crude analysis by ^{19}F-NMR showed an array of products being formed such as direct displacement (S_N2), S_N2' reactions and hydrolysis.

2.7 Alternative Approaches to Ester 2.11

In parallel with the Pd and Cu mediated coupling attempts described above, a Reformatsky coupling reaction using Et-BDFA was performed. Upon the success of the Reformatsky reaction, the following two synthetic approaches as shown in Scheme 2.7, were envisioned for the generation of compound **2.11**.

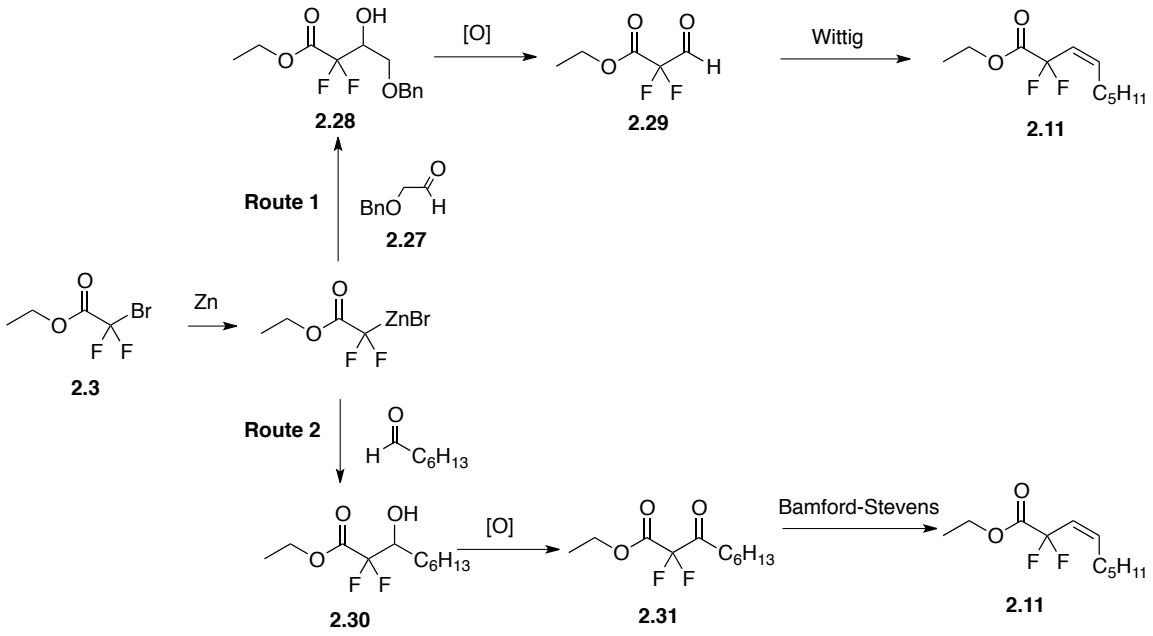

Scheme 2.7. A central Reformatsky coupling approach, followed by two subsequent reaction pathways using either a Wittig or Bamford-Stevens reaction to generate **2.11**.

In both reaction pathways a Reformatsky coupling reaction is central; however, the aldehyde used for coupling is different. In Route 1, the coupling of phenylacetylaldehyde (**2.27**), followed by oxidation and a Wittig olefination to generate **2.11** was intended. In Route 2, the coupling of heptanal, followed by oxidation and a Bamford-Stevens reaction to generate the alkene was proposed.

As mentioned previously, Reformatsky type reactions have been used to couple Et-BDFA with aldehydes, in general.[8,9] Although the reported yields are low and the products produced are not highly reactive, all other coupling attempts thus

far were unsuccessful.

To ensure a Reformatsky reaction could be performed on Et-BDFA, the work of Hallinan *et al* was replicated to obtain the target compound **2.32**. Hallinan's methods were executed to produce the successful coupling of Et-BDFA to benzaldehyde, in comparable yields.[8]

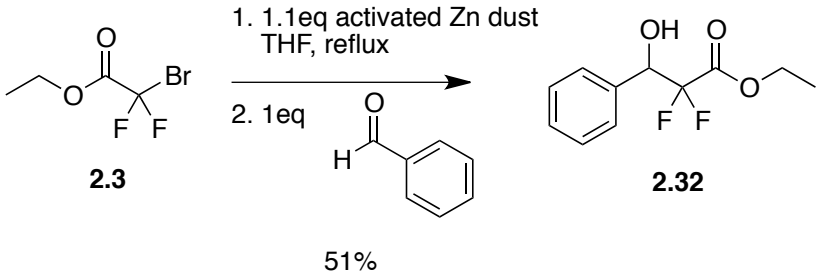

With the success of a Reformatsky coupling reaction, attempts to couple phenylacetylaldehyde (**2.27**), as outlined in Scheme 2.7, began. The production of **2.27** was pursued, following the general reaction Scheme 2.8.

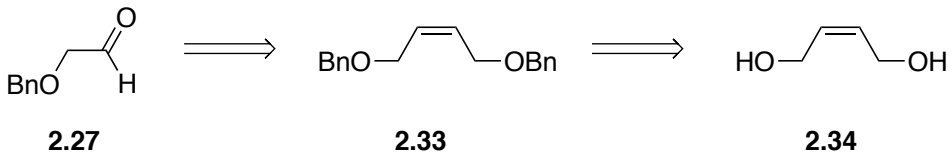

Scheme 2.8. The general reaction scheme for the production of **2.5**.

Following the procedure by Nishizonon *et al*, we obtained in quantitative yields compound **2.33**.[23] The reaction conditions were slightly modified to ensure the reaction went to completion.

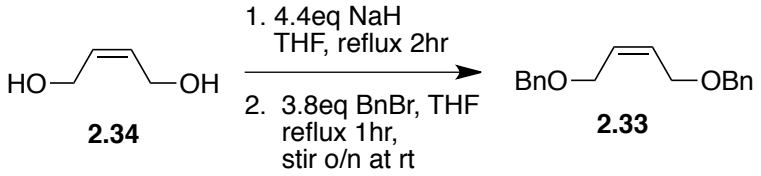

2.34 **2.33**

Quant.

Following the procedure outlined by Pollex *et al*, the preparation of 2-benzyoxyacetaldehyde (**2.27**) was attempted.[24] This procedure required that **2.33** be dissolved in a DCM/methanol mixture, at very low temperatures and exposed to a stream of ozone until the reaction turned blue. After a few hours this was observed, at which point dimethylsulfide was added and left to stir overnight. Upon workup and analysis of a crude ^{1}H-NMR, the desired product was observed, however attempts at purification were unsuccessful. Further ^{1}H-NMR analysis revealed a main impurity, which could not been removed by column purification methods, as it was a co-eluent.

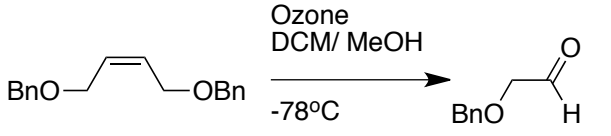

2.33 **2.27**

Crude: 112%

Due to the difficulty in obtaining pure 2-benzoxyacetaldehyde (**2.27**) a different approach reported by Garner *et al* was attempted.[25] The alkene was treated with mCPBA to form epoxide **2.34**, as reported and further treated with periodic acid; however, **2.27** was not obtained. Upon workup, analysis by TLC and ^{1}H-NMR revealed a wide array of undesired compounds.

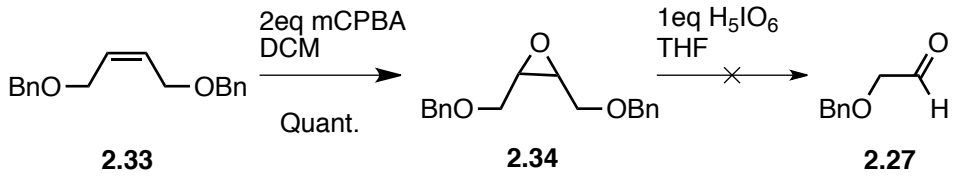

2.33 **2.34** **2.27**

In parallel with the generation of compound **2.27**, a Reformatsky reaction using an alkyl aldehyde was performed. Reaction condition reported by Fukuda *et al,* highlighted the formation of Ethyl 2,2-difluoro-3-hydroxynonanoate (**2.30**) and the oxidation of the hydroxyl compound, using Dess-Martin reagent to generate compound **2.31**. The Reformatsky reaction using activated zinc was successful.[26]

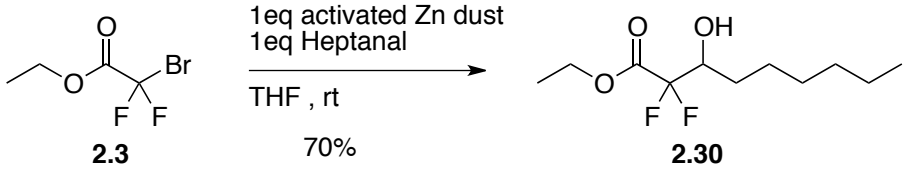

2.3 **2.30**

Due to the cost of Dess-Martin reagent and the time required to synthesize it, attempts at a more accessible oxidation were performed. A Swern oxidative procedure, as reported by Watanabe *et al,* was performed; however all attempts

were unsuccessful.[27] The amount of oxalyl chloride, and temperature at which the reaction was run, were both increased.

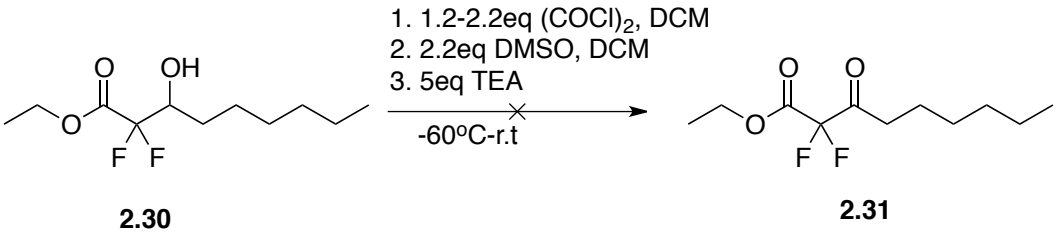

2.30 **2.31**

Since attempts using a Swern oxidation were unsuccessful, we were forced to prepare Dess-Martin reagent[28] and subject compound **2.30** to the conditions reported by Fukuda *et al*.[26] Compound **2.31** was obtained in reasonable yields.

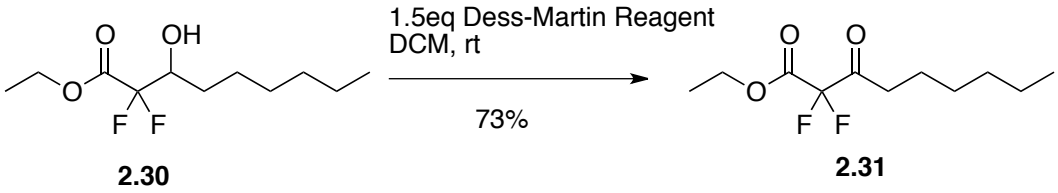

2.30 **2.31**

While the Reformatsky reaction using an aliphatic aldehyde and subsequent oxidation reactions were successful, unfortunately compound **2.27** was unattainable. Attempts at coupling crude **2.27** to Et-BDFA generated a wide array of products and all attempts to purify and identify these compounds were unsuccessful.

With ethyl 2,2-difluoro-3-oxononanoate (**2.31**) in hand, formation of a hydrazone, with the goal of performing a Bamford-Stevens reaction, for the

generation of **2.11** was sought out. First attempts were made treating compound **2.31** with p-toluenesulfonyl hydrazide, to generate the desired tosylhydrazone. However, this reaction gave a wide array of spots by TLC. ^{19}F-NMR analysis of the crude reaction mixture indicated that starting material remained, as well as the formation of several other compounds. Unfortunately, through several attempts, product isolation was unsuccessful. Sadly, analysis of the crude reaction mixture by ^{1}H- and ^{19}F-NMR, it was unclear as to what reactions were taking place.

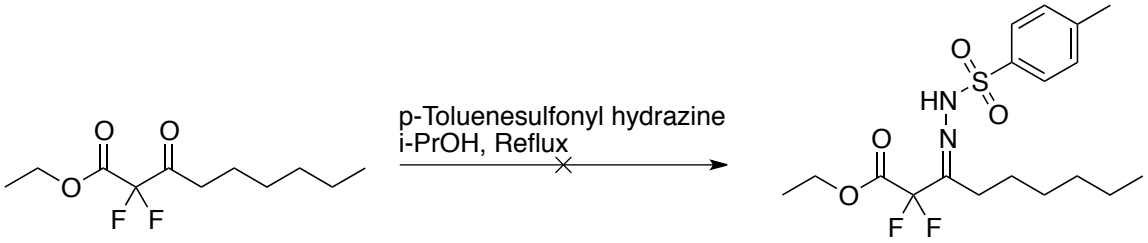

2.31 **2.35**

A paper reported by Surmont *et al*, highlighted the treatment of a similar di-fluorinated compound with hydrazine to generate a fluorinated pyrazole as shown below.[29]

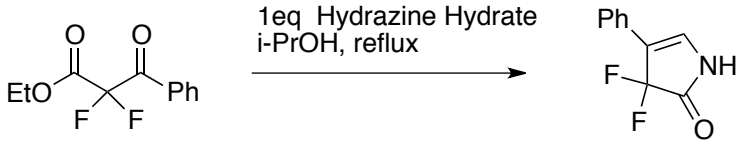

This led us to believe that a product generated in our previous attempts may be the cyclization and formation of the corresponding pyrazole. We decided to

increase the scale of the reaction to allow for easier isolation of the products. However, once again we were unable to characterize anything but starting material.

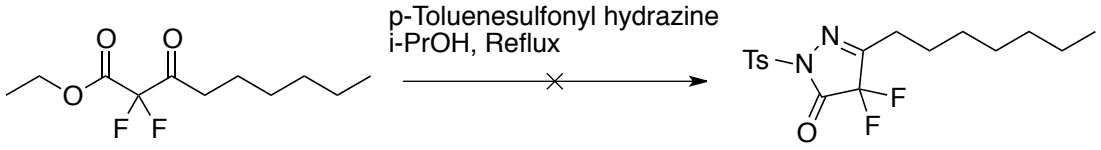

2.31 **2.36**

Treatment of compound **2.31** with hydrazine hydrate was performed in attempts to reproduce Surmont's results.[29] Unfortunately, all attempts resulted in a mixture of other unidentifiable byproducts, none of which corresponded to the previously reported pyrazole.

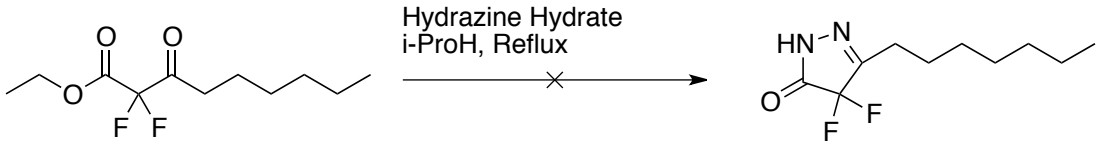

2.31 **2.37**

We wondered if a more reactive hydrazine would generate better results. A search of the literature revealed a paper by May *et al*, where a tandem rhodium-catalyzed Bamford-Stevens/thermal aliphatic Claisen rearrangement sequence was used to afford (*Z*)-alkenes. The use of N-aziridinyl imines in situ to form diazo alkanes was treated with a rhodium catalyst, to generate the desired (*Z*)-isomer.[30]

The generation of 1-amino-2-phenylaziridinium acetate (**2.41**) was performed according to an Organic Synthesis preparation.[31]

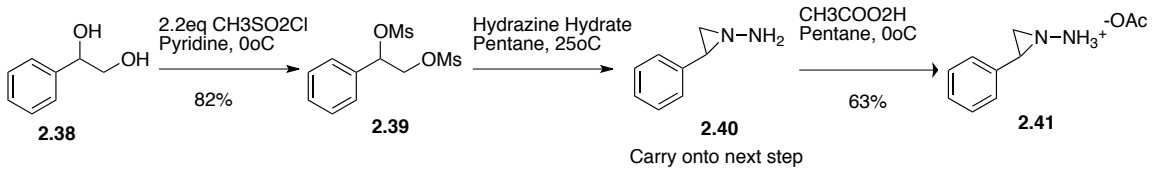

2.38 **2.39** **2.40** **2.41**

Carry onto next step

It is reported that the final recrystallization step to obtain compound **2.41** requires much attention in to prevent the formation of a yellow byproduct, which has a melting point lower than the desired product. If this yellow byproduct is observed it is inseparable. Handling of this compound cannot go above 22°C. Several recrystallization attempts were made to avoid this byproduct; however, this resulted in yields lower than reported for compound **2.41**. The stability of **2.41** was still a concern and precautions were made to prevent degradation.

Compound **2.31** was subjected to the reported reaction conditions for the formation of the hydrazone.[30] However, during reaction setup, the stability of **2.41** was problematic, as the decomposition product occurred in situ. There was no reactivity with **2.31**, as it was recovered.

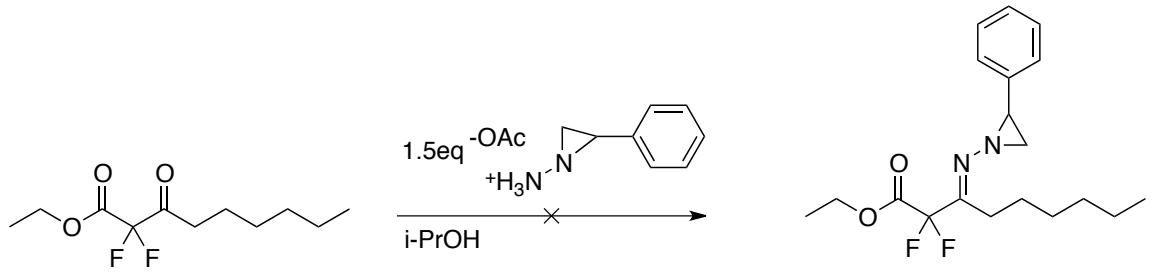

2.31 **2.42**

A survey of the literature reveals few examples of N-aziridinyl imines, implying the difficulty with which they are employed.

2.8 Conclusion & Future Work

Our efforts towards 11,11-difluorolinoleic acid (**2.1**) involved several attempts at coupling compounds to Et-BDFA through Negishi, Reformatsky and copper catalyzed reactions to ultimately generate the omega-6 chain of linoleic acid. A few key modifications to a previously reported copper catalyzed coupling reaction,[19] successfully produced one half of the desired 11,11-difluorolinoleic acid (**2.1**). The reaction conditions were optimized and the overall yield of the reaction was improved from 68% (inseparable product and undesired compound) to 89% (quantitative conversion, isolated yield).

As shown in Scheme 2.9, while the first omega-6 unsaturation was a success, the many attempts made to generate the second unsaturation through a Wittig olefination reaction were unsuccessful. The electronegativity of the difluoromethylene unit increased the electrophilicity of the α-carbon, to the point that isolation of the aldehyde was unattainable. The desired fluorinated compound could only be isolated as the hydrate and was therefore unreactive as an electrophile. In contrast the activated alkyl halide was too electrophilic and competing S_N2 (including hydrolysis) and S_N2' reactivity presented too many challenges.

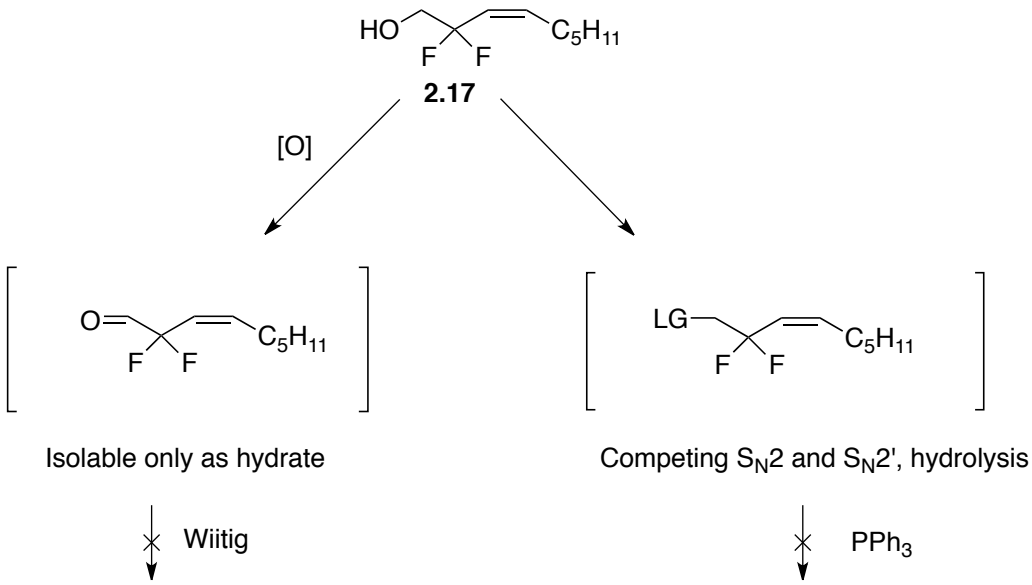

Scheme 2.9. An outline of the problems using an ionic approach to generate 11,11-difluorolinoleic acid.

Seeing as an ionic approach presented several challenges, we wondered if a radical approach, as shown in Scheme 2.10, could be a solution. Using a general radical method such as the tin hydride mediated addition/ reduction of an alkyne presents problems with regio- and stereoselectivity, as a mixture of isomers are expected to be produced.

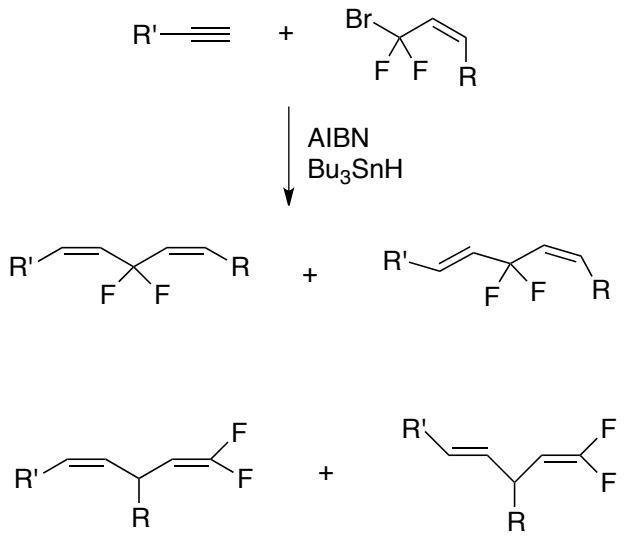

Scheme 2.10. A radical approach to generate a bis-allylic difluoromethylene unit.

Alternatively, a radical substitution, in lieu of addition, would allow us to subsequently control the stereochemistry by maintaining the alkyne, which could subsequently be hydrogenated. Li has recently described a decarboxylative radical alkynylation strategy using a modified Togni reagent as shown in Scheme 2.11 that could be useful here. [32]

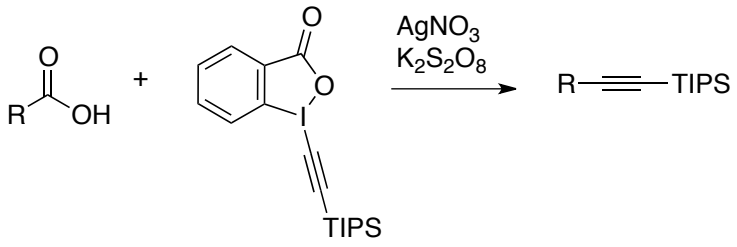

Scheme 2.11. Decarboxylative radical alkynylation using a modified Togni reagent.

While the regioselectivity of the radical addition may be a problem this would yield only two major products as opposed to four.

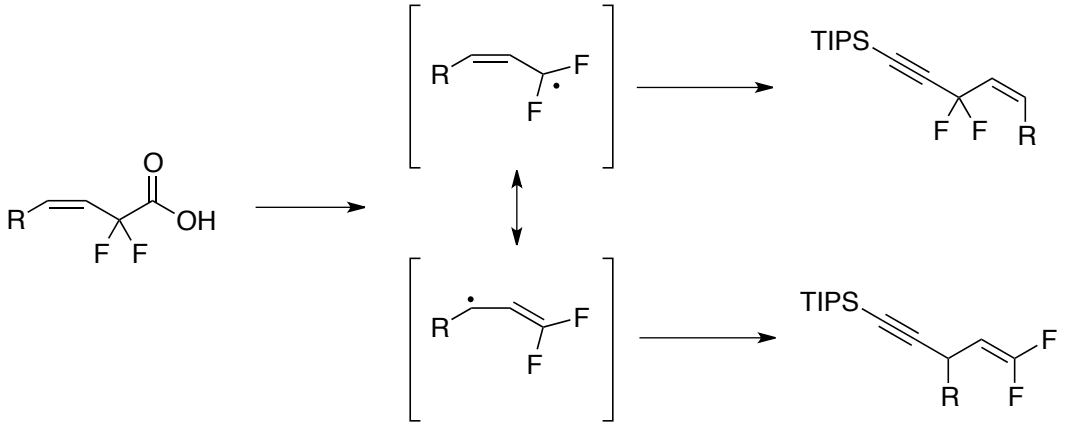

Using this methodology, the hydrolysis of compound **2.11** to the corresponding carboxylic acid, followed by treatment with the modified Togni reagent in the presence of silver nitrate and potassium persulfate may lead to the desired product. Subsequent fluorodesilyation, alkylation of the acetylide and hydrogenation would yield the desired 11, 11-difluorolinoleic acid, as shown in Scheme 2.12.

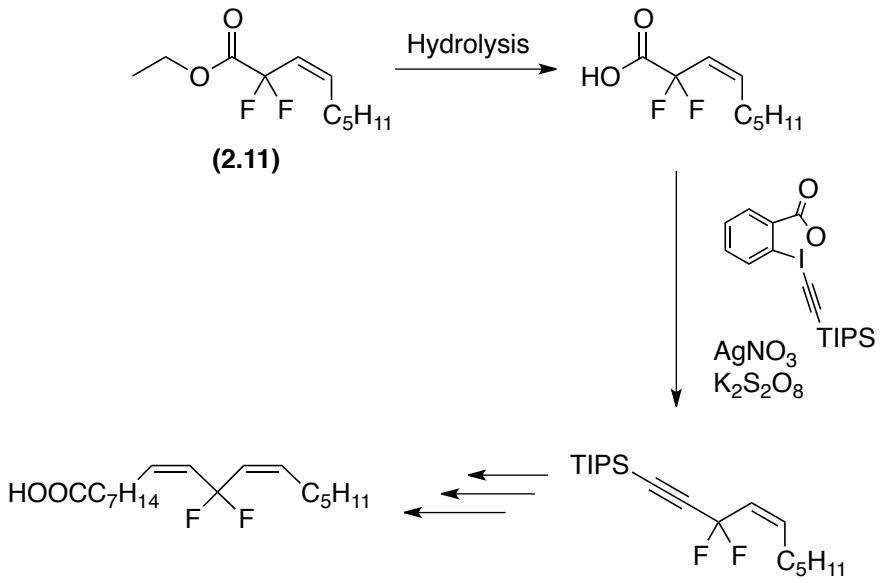

Scheme 2.12. Methodology to generate desired 11, 11-difluorolinoleic acid.

With the successful synthesis of 11,11-difluorolinoleic acid, the synthetic pathway could be applied to other fluorinated fatty acids. Their activity as inhibitors of LOXs could then be assessed and attempts at their co-crystallization made.

2.9 References

(1) Malkowski, M. G.; Ginell, S. L.; Smith, W. L.; Garavito, R. M. *Science.* **2000**, *289*, 1933.

(2) Kiefer, J. R.; Pawlitz, J. L.; Moreland, K. T.; Stegeman, R. A.; Hood, W. F.; Gierse, J. K.; Stevens, A. M.; Goodwin, D. C.; Rowlinson, S. W.; Marnett, L. J.; Stallings, W. C.; Kurumbail, R. G. *Nature.* **2000**, *405*, 97.

(3) Kwok, P. Y.; Muellner, F. W.; Chen, C. K.; Fried, J. *J. Am. Chem. Soc.* **1987**, *109*, 3684.

(4) Kwok, P. Y.; Muellner, F. W.; Fried, J. *J. Am. Chem. Soc.* **1987**, *109*, 3692.

(5) Minor, W.; Steczko, J.; Stec, B.; Otwinowski, Z.; Bolin, J. T.; Walter, R.; Axelrod, B. *Biochemistry.* **1996**, *35*, 10687.

(6) Navé, J. F.; Dulery, B.; Gaget, C.; Ducep, J. B. *Prostaglandins.* **1988**, *36*, 385.

(7) Furuya, T.; Kuttruff, C. A.; Ritter, T. *Curr. Opin. Drug Discov. Devel.* **2008**, *11*, 803.

(8) Hallinan, E.; Fried, J. *Tetrahedron Lett.* **2000**, *25*, 2301.

(9) Lang, R. W.; Schaub, B. *Tetrahedron Lett*. **2001**, *29*, 2943.

(10) Tranchepain, I.; Le Berre, F.; Duréault, A.; Le Merrer, Y.; Depezay, J. C. *Tetrahedron.* **2001**, *45*, 2057.

(11) Bracher, F.; Litz, T. *Adv. Synth. Catal.* **1996**, *338*, 386.

(12) Kyi, S.; Wongkattiya, N.; Warden, A. C.; O'Shea, M. S.; Deighton, M.; Macreadie, I.; Graichen, F. H. M. *Bioorg. Met. Chem.* **2010**, *20*, 4555.

(13) Stork, G.; Zhao, K. *Tetrahedron Lett.* **2000**, *30*, 2173.

(14) Seyferth, D.; Heeren, J. K.; Singh, G.; Grim, S. O.; Hughes, W. B. *J. Organomet. Chem.* **2000**, *5*, 267.

(15) Kellersmann, C.; Steinhart, H.; Francke, W. *Lipids.* **2006**, *41*, 777.

(16) Krasovskiy, A.; Lipshutz, B. H. *Org. Lett.* **2011**, *13*, 3818.

(17) Erdik, E. *Organozinc Reag. Organ. Synth.*; CRC Press, 1996.

(18) Krasovskiy, A.; Knochel, P. *Synthesis.* **2006**, *2006*, 0890.

(19) Sato, K.; Kawata, R.; Ama, F.; Omote, M.; Ando, A.; Kumadaki, I. *Chem. Pharm. Bull.* **2004**, *47*, 1013.

(20) Golding, B. T.; Sellars, P. J.; Watson, W. P. *J. Fluorine Chem.* **2000**, *30*, 153.

(21) Tsukamoto, T.; Kitazume, T. *J. Chem. Soc., Perkin Trans. 1* **1993**, 1177.

(22) Hanamoto, T.; Morita, N.; Shindo, K. *Eur. J. Org. Chem.* **2003**, *2003*, 4279.

(23) Nishizono, N.; Akama, Y.; Agata, M.; Sugo, M.; Yamaguchi, Y.; Oda, K. *Tetrahedron.* **2011**, *67*, 358.

(24) Pollex, A.; Millet, A.; Müller, J.; Hiersemann, M.; Abraham, L. *J. Org. Chem.* **2005**, *70*, 5579.

(25) Garner, P.; Park, J. M. *Synth. Comm.* **1987**, *17*, 189.

(26) Fukuda, H.; Kitazume, T. *J. Fluorine Chem.* **2003**, *74*, 171.

(27) Watanabe, S.; Fujita, T.; Sakamoto, M.; Takeda, H.; Kitazume, T.; Yamazaki, T. *J. Fluorine Chem.* **2004**, *82*, 1.

(28) Dess, D. B.; Martin, J. C. *J. Org. Chem.* **1983**, *48*, 4155.

(29) Surmont, R.; Verniest, G.; De Kimpe, N. *Org. Lett.* **2010**, *12*, 4648.

(30) May, J. A.; Stoltz, B. M. *J. Am. Chem. Soc.* **2002**, *124*, 12426.

(31) Müller, R. K.; Joos, R.; Felix, D.; Schreiber, J.; Wintner, C.; Eschenmoser, A. *Org. Synth.* 114.

(32) Liu, X.; Wang, Z.; Cheng, X.; Li, C. *J. Am. Chem. Soc.* **2012**, *134*, 14330.

-3-

N-Acylated 2-Aminopyrimidines as Potential Inhibitors of Lipoxygenase

3.0 Introduction

The metabolism of arachidonic acid by cyclooxygenases and lipoxygenases is mediated by peroxyl radical intermediates. As such, there has long been an interest in the potential for radical-trapping antioxidants to inhibit the formation of products derived from cyclooxygenase and lipoxygenase catalyzed oxygenation of arachidonic acid (e.g. prostaglandins and leukotrienes), respectively. Acetaminophen (ApAP, **1.8**) and nordihydroguaiaretic acid (NDGA, **1.17**) are both phenolic compounds known to inhibit COX and LOX, respectively. However, both are believed to reduce the active form of the enzyme to its inactive form, rather than reduce the peroxyl radical intermediates, as shown in Scheme 3.1.[1,2,3]

Acetaminophen Inhibition of COX Enzyme

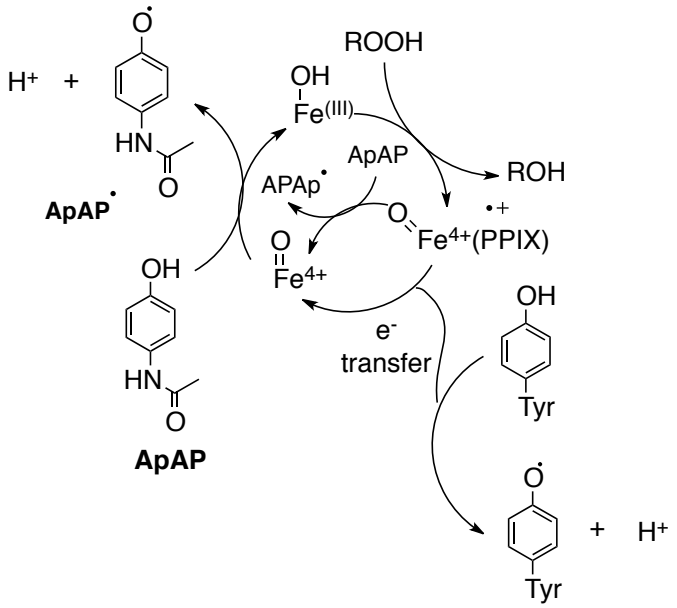

Nordihydroguaiaretic Acid Inhibition of LOX Enzyme

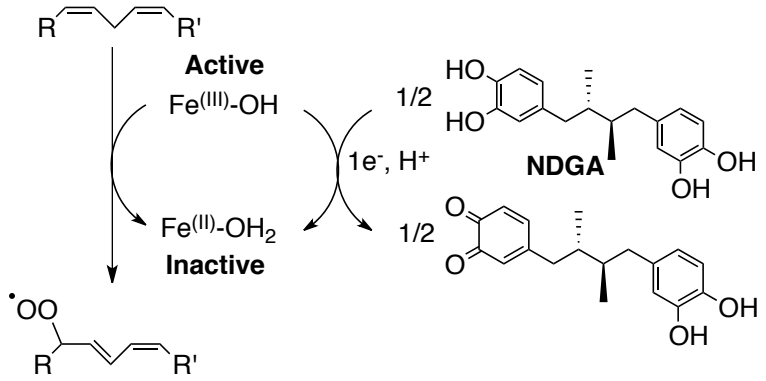

Scheme 3.1. The proposed mechanisms of inhibition of the COX and LOX enzymes by acetaminophen and nordihydroguaoaretic acid, respectively.

While ApAP and NDGA have been used clinically, they have generated much controversy due to serious concerns with their liver toxicity.[1,4] Both compounds are

rapidly metabolized by cytochrome P450s to electrophilic species that deplete glutathione, and adduct proteins and DNA, as shown in Scheme 3.2.[5]

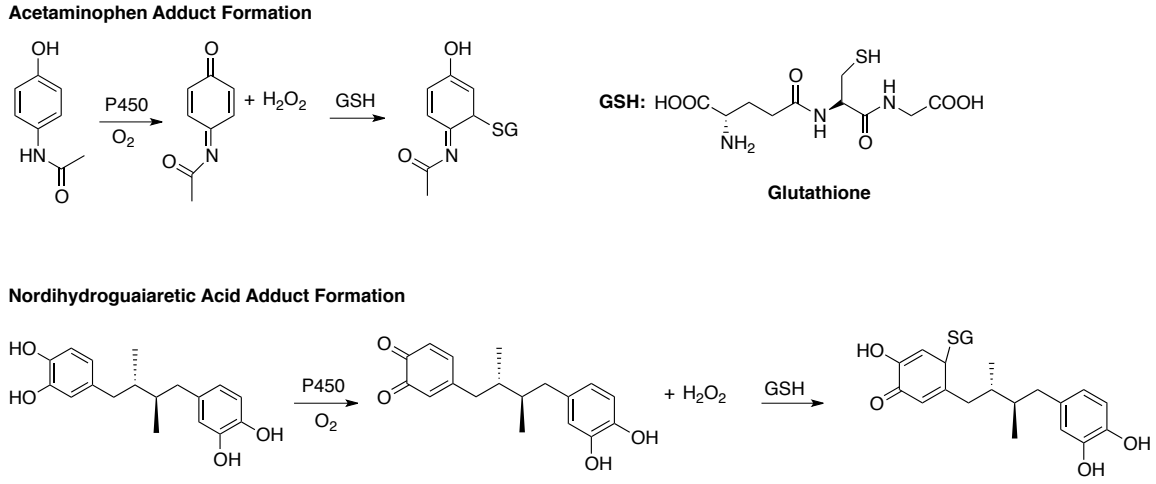

Scheme 3.2. Metabolism of ApAP and NDGA into electrophilic species, susceptible to nucleophilic attack by nucleophiles, such as glutathione, to form adducts.

Previous studies by the Pratt lab have demonstrated that the oxidative stability of electron rich phenolic compounds can be improved by the incorporation of nitrogen atoms into the aromatic ring.[6] This has enabled the design and development of the most effective phenolic like peroxyl radical trapping antioxidants, for example **3.1** and **3.2**. More recently, the Pratt lab carried out preliminary studies of the abilities of these novel phenolic-like antioxidants to serve as inhibitors of COX- and LOX- catalyzed lipid peroxidation. These studies included the pyridine and pyrimidine isosteres **3.3**, **3.4** of ApAP (**1.10**) and tested them as inhibitors of COX and LOX.[7]

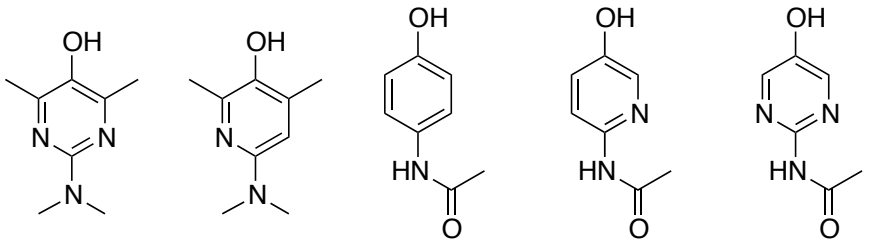

3.1 **3.2** **1.10** **3.3** **3.4**

The findings of these studies were that the incorporation of nitrogen into the phenolic ring of acetaminophen predictably deceased its antioxidant activity and its efficacy as an inhibitor of COX-1. However, the incorporation of nitrogen surprisingly increased the efficacy of ApAP analogs as an inhibitor of sLOX-1. As such, the efficacy in the inhibition of COX-1 revealed that ApAP (**1.10**) was greater than the pyridinol (**3.3**) and pyrimidinol (**3.4**), with IC_{50} values of 250 μM, 399 μM, and 761 μM, respectively. Whereas, in the inhibition of sLOX-1 the pyrimidinol (**3.4**) was more effective than the pyridinol (**3.3**) and ApAP (**1.10**) analog, with IC_{50} values of 564 μM, 1620 μM and > 2000 μM, respectively. Thus, while the trend in inhibition of COX-1 follows the simple redox chemistry of these analogs (E°= 0.32 V, 0.48 V, 1.02 V for **1.10**, **3.3**, **3.4**, respectively) the inhibition of sLOX-1 follows the trends in acidity of the OH (pK_a= 9.8, 8.3, 5.9 for **1.10**, **3.3**, **3.4**, respectively). These findings suggested that the mechanism by which these compounds inhibit sLOX is more complicated then the simple reduction of sLOX-1 from hydroxide-bound ferric (active) form to its water bound (inactive) form.

Nelson has shown that acidic catechols inhibit sLOX-1 through a bidentate complex of the iron atom within the active site, as demonstrated in Scheme 3.3.[8]

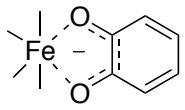

Scheme 3.3. A bidentate complex of an iron atom with catechols.

A similar rationalization can be made for the aforementioned sLOX-1 inhibition studies. Nitrogen incorporation, which increases the acidity of the pyridinol and pyrimidinol analogs relative to ApAP, may enhance complexation of the iron atom via a ring nitrogen atom and the carbonyl oxygen of the acetamide group as shown in Scheme 3.4.[7]

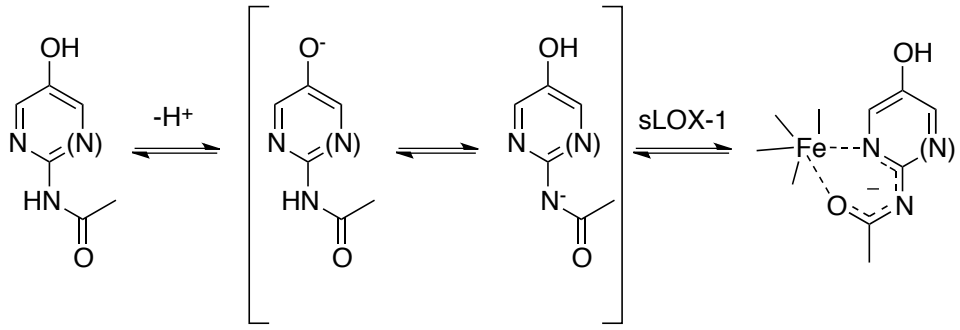

Scheme 3.4. Suggested mechanism of inhibition of the sLOX-1 enzyme by pyridinol and pyrimidinol analogs of ApAP.

Herein we begin to explore the structure-activity relationships of acylated 2-aminopyrimidines as inhibitors of sLOX-1. The mechanism above suggests that a

redox-active OH (in position 5 of the ring) is unnecessary and that it is the acidity of the acetamide hydrogen that enables iron chelation. Should this be the case, adding a more lipophilic acyl chain on the amine and/or an alkyl substituent in place of the alcohol, may increase the affinity of the inhibitor for the hydrophobic active site of sLOX-1, which is designed to bind the 18-carbon polyunsaturated lipid linoleic acid. The proximity of the reactive C-11 carbon center of LA to the active site iron is shown in Figure 3.1.[9] This model highlights the orientation at which the lipophilic chain in linoleic acid is positioned in the pocket. It should be pointed out that there is considerable debate as to the orientation of LA in the active site and the means by which the enzyme controls the regio- and stereoselectivity of substrate oxygenation.[10]

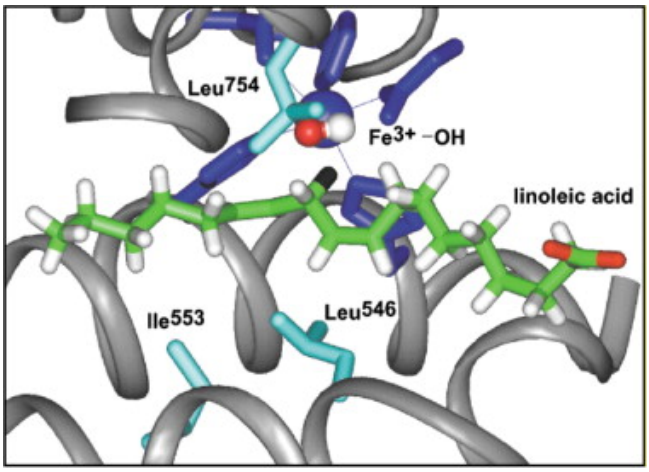

Figure 3.1. A model of linoleic acid, in the active site of soybean lipoxygenase-1 reproduced from Klinman *et al*.[9]

Based on this model, we envisioned that increasing the lipophilicity of a *N*-acylated 2-aminopyrimidines, such as **3.4,** may lead to potent inhibitors of sLOX, as shown in Figure 3.2. Soybean LOX-1 produces 3-hydroperoxy-9*Z*, 11*E*-octadecadienoic acid (13-HPODE) by oxygenating linoleic acid at C13. In order for molecular oxygen to add to the intermediate pentadienyl radical, there must be sufficient space to accommodate both linoleic acid and O_2 at once. Hence, we propose that upon chelation of the acyl chain, the pyrimidinol ring will occupy this space.

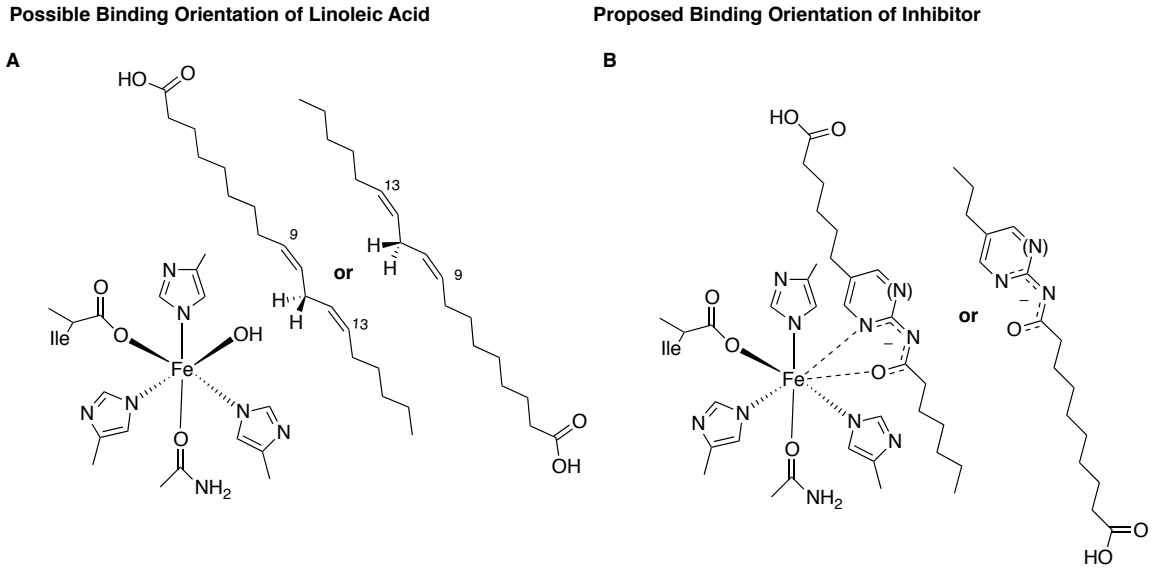

Figure 3.2. A rational design for potential sLOX-1 inhibitors. A) Possible binding orientation of linoleic acid in the sLOX-1 active site. B) Proposed binding orientation of *N*-acylated 2-aminopyrimidines in sLOX-1 active site.

To probe these ideas, a small library of acylated 2-aminopyrimidines were prepared, and their efficacy as inhibitors of soybean lipoxygenase were tested. The results are presented and discussed in the following pages.

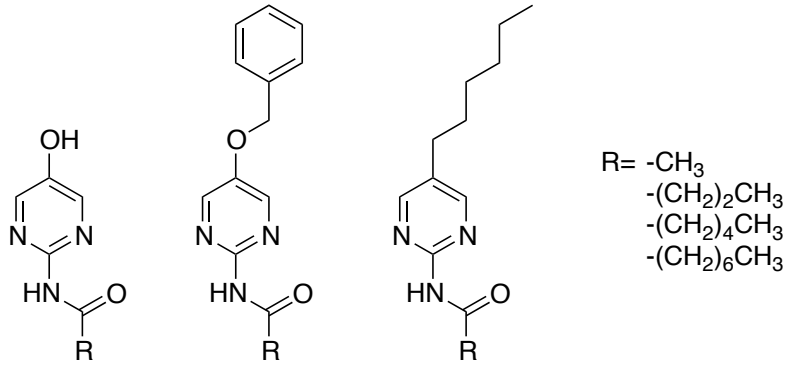

3.1 Results and Discussion

To better understand the mechanism by which compounds **3.3** and **3.4** inhibit sLOX-L1, an initial experiment to determine the acidity of the acetamide hydrogen was sought out. The previously reported pK_a measurements of **3.3** and **3.4** yielded 8.3 and 5.9, respectively. Our goal was to determine whether the trend in this acidity was due to O-H ionization or N-H ionization. In order to measure the pK_a of the acetamide hydrogen of the pyridine and pyrimidine analogs of ApAP, the moiety in the 5- position of the ring needs to be alkylated, leaving the only acidic hydrogen on the amide appended to the 2-position of the ring. The synthesis previously reported by our group, could be used to generate *N*-(5-(benzyloxy)pyridin-2-yl)acetamide (**3.5**) and *N*-(5-(benzyloxy)pyrimidin-2-yl)acetamide (**3.6**) in fact, the synthetic precursors of **3.3** and **3.4**, respectively.[7]

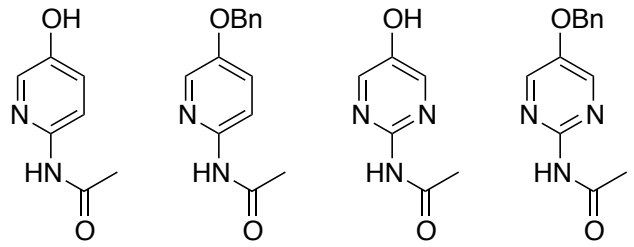

	3.3	3.5	3.4	3.6
pK_a=	8.3	?	5.9	?

3.1.1 Synthesis of O-Benzylated Pyri(mi)dine Analogs of Acetaminophen

The following synthesis reported by Nam *et al*, was followed to prepare *N*-(5-(benzyloxy)pyridin-2-yl)acetamide (**3.5**), as shown in Scheme 3.5.[7] Reagents and reaction conditions were not altered from the previously reported procedures; however, some products were difficult to purify and resulted in lower yields than those reported. Determining the optimal conditions for flash column chromatography was a challenge but ultimately *N*-(5-(benzyloxy)pyrimidin-2-yl)acetamide (**3.5**) was obtained.

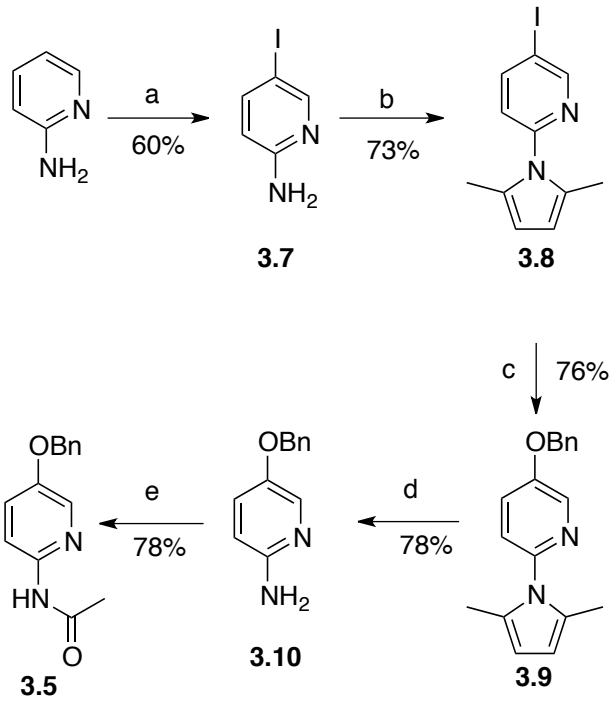

Scheme 3.5. Synthesis of *N*-(5-(benzyloxy)pyrimidin-2-yl)acetamide. Reagents and conditions: (a) H_5IO_6, I_2, acetic acid; (b) 2,5-hexanedione, *p*TsOH, toluene, Dean-Stark, 2 h; (c) CuI, Cs_2CO_3, BnOH, 90 °C, o/n; (d) $NH_2OH{\bullet}HCl$, NEt_3, $EtOH/H_2O$, reflux, o/n; (e) $CH_3C(O)Cl$, cat. DMAP, TEA, CH_2Cl_2, rt, o/n.

The pyrimidine analog was prepared using essentially the same approach by undergraduate student Ms. Nevena Cekic. Once both **3.5** and **3.6** were in hand, the pK_a measurements could be conducted to determine whether the previous pK_a trend was due to O-H bond ionization or N-H bond ionization.

3.1.2 pK_a Measurements of O-Benzylated Pyri(mi)dine Analogs of Acetaminophen

Attempts to determine the pK_a values of **3.5** and **3.6** by spectrophotometric titrations were made. The titrations were performed using a UV-Vis spectrophotometer to obtain the absorbance of the solutions ranging from pH 2-14, containing 25 μM of the test compound in ethanol. The fraction of the control compound in the aryloxide form, $f_{\text{aryloxide}}$, was computed using equation (1), where A is the absorbance at λ_{max} and was plotted as a function of pH. In order to obtain the pK_a value, equation (2) was used to fit the $f_{\text{aryloxide}}$ versus pH.

$$f_{aryloxide} = A(pH)\text{-}A(pH_{low})/A(pH_{high})\text{-}A(pH_{low}) \quad (1)$$

$$f_{aryloxide} = 10^{pH\text{-}pKa}/(1 + 10^{pH\text{-}pKa}) \quad (2)$$

Prior to carrying out experiments with **3.5** and **3.6**, we attempted to determine the pK_a of pyrimidinol **3.1**, which was previously found to be 9.0. The preliminary spectrophotometric data obtained in Figure 3.3A shows a bathochromic shift between pH 8 and 9. This indicates that the pK_a of **3.1** lies within this range. While this is consistent with previous results, upon quantitative analysis of the data (Figure 3.3B), a linear relationship is found in lieu of the expected sigmoidal curve, making it difficult to determine the exact pK_a. It is noteworthy that the isosbestic point around 245 nm is not clean, suggesting other chemistry is occurring under these conditions. Regardless, we continued on to carry out analogous experiments with **3.5** and **3.6**.

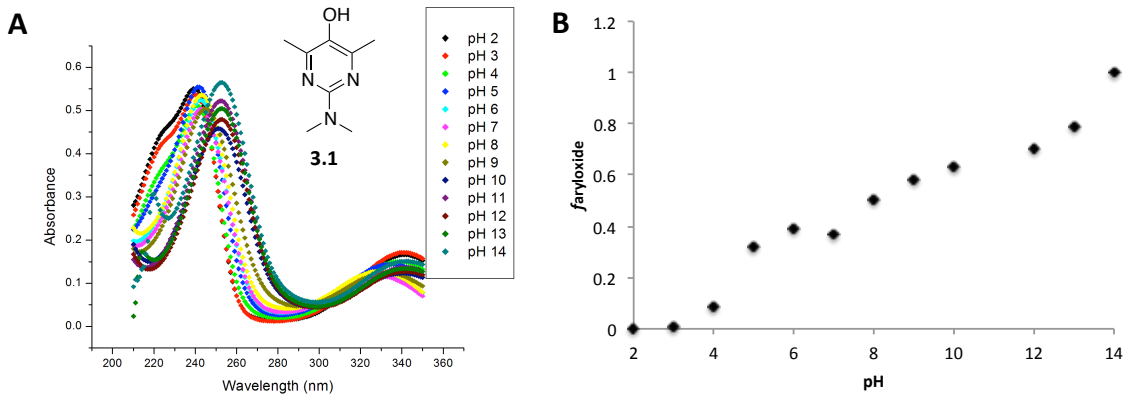

Figure 3.3. Spectrophotometric determination of pK_a for **3.1** (25 mM). A) Bathochromic shift detected between pH 8 and 9 using Cary UV vis spectrophotometer determined at room temperature, in a solution of 10 mM potassium phosphate, containing 200 mM KCl, adjusted to desired pH using 1 M HCl or 1 M KOH, in the range of pH 2- 14. B) Fraction of aryloxide present as a function of pH from absorbance at λ_{max} (252 nm).

Preliminary spectrophotometric data of compounds **3.5** and **3.6** revealed the expected increase in acidity along the pyridinol and pyrimidinol series, based on the bathochromic shifts observed in Figure 3.4. The titration results for the O-benzylated pyridine analog (**3.5**), in Figure 3.4A, reveal two major bathochromic shifts at both low and high pH. At low pH (2 and 3), a shift can be observed around 320 nm, which corresponds to the protonation of the pyridine. At pH 14, a second bathochromic shift is observed at 240 nm, indicating a pK_a higher than what is measurable using these methods. The titration results for the O-benzylated pyrimidine analog (**3.6**), in Figure 3.4B, show a bathochromic shift around pH 12,

indicating that the pK_a of **3.6** is in this vicinity. These results are consistent with the relative acidity of pyridine and pyrimidine rings; however, no further qualitative data could be obtained from the spectra.

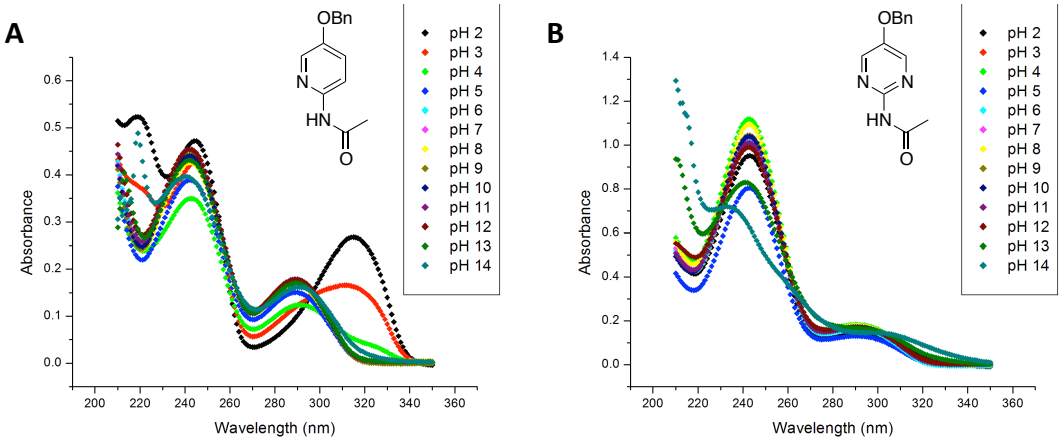

Figure 3.4. Spectrophotometric titration for the determination of pK_a values for inhibitor **3.5** and **3.6** (25 mM) using UV vis spectrophotometer, at room temperature, in a solution of 10 mM potassium phosphate, containing 200 mM KCl, adjusted to desired pH using 1 M HCl or 1 M KOH, in the range of pH 2- 14. A) **3.5** bathochromic shift between pH 2-3 and pH 14. B) **3.6** bathochromic shift at pH 12.

The qualitative results suggest that the previously reported pK_a measurements were due to O-H bond ionization and not N-H bond ionization. Since O-H ionization would not be expected to significantly increase the Lewis basicity of either the pyri(mi)dine nitrogen atom or the amide carbonyl oxygen atom as they

are not in resonance, it stands to reason that the OH/O$^-$ substituent is not strictly required for binding to sLOX, as shown in Scheme 3.6.

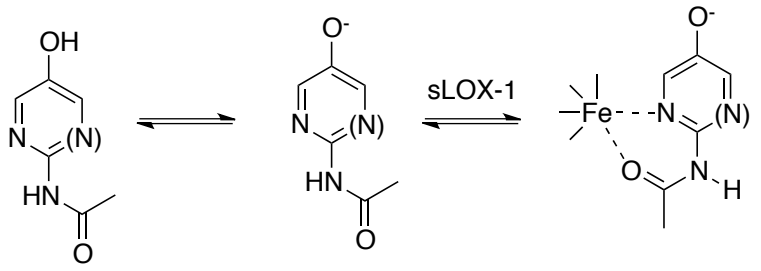

Scheme 3.6. Suggested mechanism of inhibition of the sLOX-1 enzyme by pyridinol and pyrimidinol analogs of ApAP, through iron chelation.

3.1.3 Synthesis of 5-Hydroxy *N*-Acylated 2-Aminopyrimidines

We next sought to probe the hypothesis that increasing the lipophilicity of the acyl side chain on *N*-acylated 2-aminopyrimidines would increase the binding affinity for sLOX. Using methods previously reported by the group, the synthesis of a small library of compounds began.

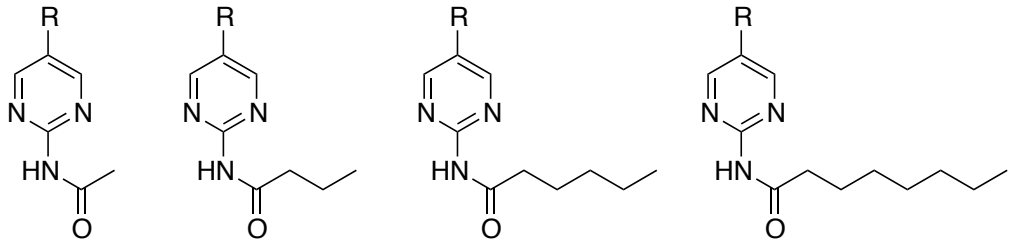

R= OH (**3.4**)
R= OBn (**3.6**)

R= OH (**3.11**)
R= OBn (**3.12**)

R= OH (**3.13**)
R= OBn (**3.14**)

R= OH (**3.15**)
R= OBn (**3.16**)

3.1.3.1 Bromination of 2-Aminopyrimidine

Previous reaction conditions, as reported by the group, were performed to prepare 5-bromo-2-aminopyrimidine.[7] Analysis of the crude reaction mixture indicated minor impurities and further purification was required. Unfortunately, through recrystallization a pure product could not be obtained and performing flash column chromatography resulted in a large loss of product.

Other experimental conditions for the production of **3.17** make use of ammonium formate, as a catalyst. A paper by Das *et* al, describes a method in which NBS, in the presence of ammonium formate was used to prepare brominated aromatic phenols or anilines, in quantitative yields, without the need for further purification.[11] The reaction of NBS with NH_4HCO_2 is known to produce HBr, which can polarize the N-Br bond of NBS and facilitate bromination of the anilines.[12]

This method was used to produce **3.17**, in quantitative amounts, without the need for further purification, and in a fraction of the time.[11]

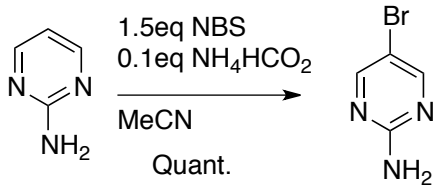

3.17

3.1.3.2 Introduction of a 2,4-Dimethylpyrrole Protecting Group

A copper catalyzed benzyloxylation is not effective when a free amine is present at the 2-position of the pyrimidine ring in compound **3.17** and the amine group must

first be protected as the 2,4-dimethylpyrrole.[7] Other protecting groups were not useful, as they were easily removed in subsequent reaction steps. Attempts to reproduce the procedure reported by Nam *et al* were quite challenging.[7] Unless repeated on the same scale described or smaller (<2.0 g), it was difficult to obtain any product and the yield was very low. The main concern with this reaction was the solubility of 2-amino-5-bromopyrimidine (**3.17**). After several attempts, we were able to increase the product yield by diluting the reaction with large amounts of toluene (0.1 M) and rather than using a Dean Stark apparatus, a reflux was performed for longer periods of time. Minor amounts of starting material were still unreacted; however, the product yield was increased and this was the only impurity to remove by flash column chromatography.

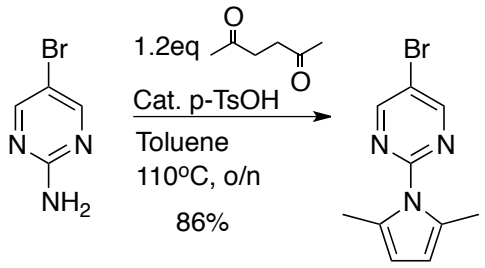

3.17 **3.18**

3.1.3.3 Copper-Catalyzed C-O Coupling

Upon protection of the free amine to form **3.18**, a copper-catalyzed coupling reaction to generate a C-O bond was performed. By subjecting **3.18** to the same reaction conditions previously reported, we were successfully able to obtain the desired compound **3.19**.[7] Potassium carbonate was also used in place of the more

expensive cesium carbonate, and L-proline was also tested in replace of 1,10-phenathroline. Both conditions produced the desired product in similar yields. The purification conditions were slightly altered, as the excess benzyl alcohol was difficult to remove. A gradient mobile phase was required to best **3.19**.

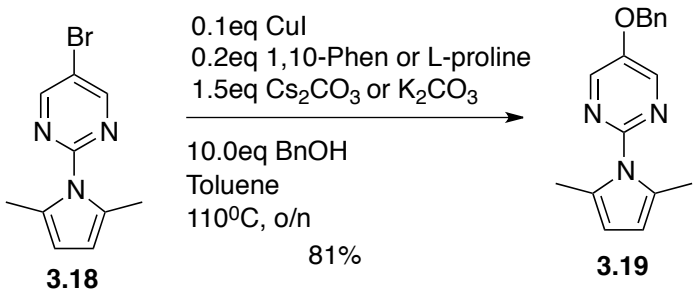

3.1.3.4 Removal of 2,4-Dimethylpyrrole Protecting Group

Previous reaction conditions reported by the group were used for the removal of the 2,4-dimethylpyrrole protecting group to produce **3.20**.[7] However, a longer reaction time was required for complete consumption of the starting material. An unfavorably large excess of hydroxylamine hydrochloride was required to remove the protecting group. Following acid/ base workup a crude material was obtained and rather than purifying using flash column chromatography as reported, the free amine was recrystallized from an ethyl acetate/ethanol mixture.

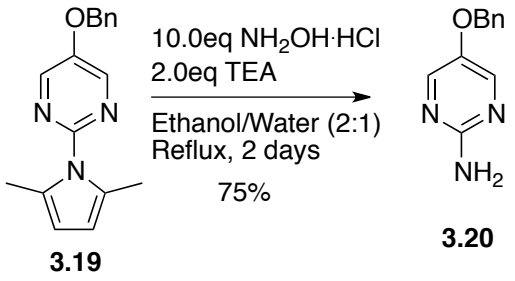

3.1.3.5 *N*-Acylation of 2-Aminopyrimidines

Upon production of the free amine **3.20**, we attempted acylation with increasing chain lengths, using the previously reported reaction conditions.[7] However, upon analysis it was revealed that the conditions produced the diacylated compound. Using 2.0 equivalents of both triethylamine and the acylating reagent, in the presence of catalytic DMAP, it is reasonable to expect the formation of the di-acylated compound.

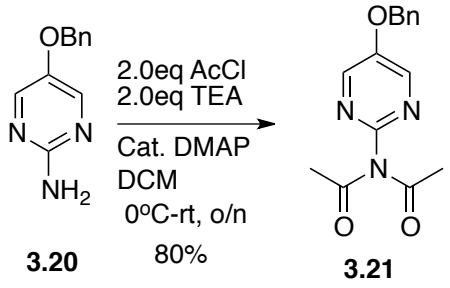

The base and acyl chloride were reduced to 1.0 equivalent each and the reaction was monitored by TLC. After leaving the reaction overnight, analysis of the products indicated a rough 50:50 mix of starting material and di-acylated product. The acidity of the amide proton is greater than those of the amine found in solution

and therefore the deprotonation of the amide proton was favourable, thereby promoting formation of the diacylated compound.

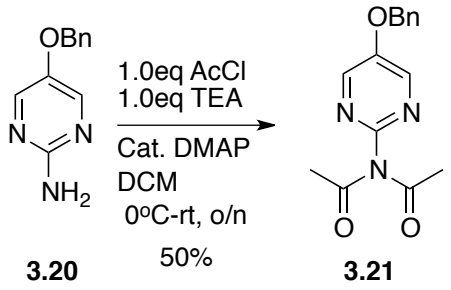

3.20 **3.21**

These observations implied that the use of a weaker base was required to prevent diacylation. We also thought it would be best to try the reaction without the catalyst (DMAP). First reaction attempts were performed using 1.0 equivalent of each of pyridine and acetyl chloride, without the presence of DMAP. Product formation was not observed after several hours by TLC. DMAP was added to the reaction flask and within a couple of hours product formation could be seen. The R_f of the product being formed did not correlate to the diacylated compound, which was promising. Optimal reaction conditions revealed that the use of 1.5 equivalents of pyridine, as base and 1.4 equivalents of acetyl chloride, gave the desired mono-acylated product **3.6** in reasonably high yields. The product could also be easily purified through recrystallization from ethyl acetate. Once the reaction conditions were optimized, attempts for acylating the free amine using more lipophilic chains were performed successfully.

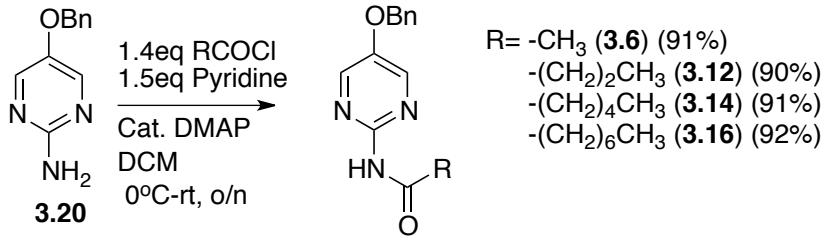

The corresponding acyl-chlorides; butanoyl-, hexanoyl-, and octanoyl-chloride were used and acyl chains of four, six and eight carbons in length were introduced as in **3.12**, **3.14**, **3.16**, respectively.

3.1.3.6 Hydrogenation of the *N*-Acetylated 2-Aminopyrimidines

Standard reaction conditions as previously reported for the hydrogenolysis of the *O*-benzyl ether were repeated, and we obtained **3.4**, **3.11**, **3.13** and **3.15** from **3.6**, **3.12**, **3.14** and **3.16**, respectively.[7]

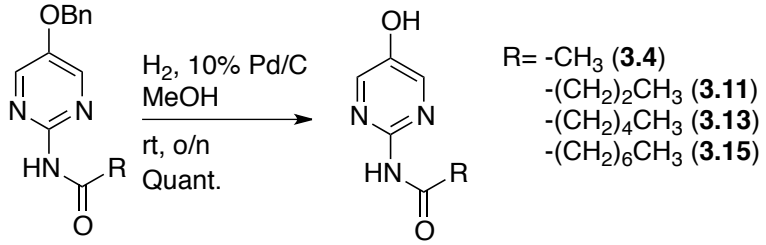

However, it was found that the O-benzyl starting material had to be extremely pure in order for the subsequent reaction to occur. If the starting material had the slightest impurities, a rather large amount of the palladium catalyst (>30%) was required. The purity of the compound also had an impact on its

solubility; the more pure the starting material, the more solvent required to solubilize it. Once the reaction was complete, these compounds were very difficult to handle due to decomposition. If stored below room temperature and under inert atmosphere the compounds remained stable.

3.1.4 The sLOX-1 Catalyzed Oxidation of Linoleic Acid to give 13-HPODE

The efficacy with which the acylated 2-aminopyrimidines inhibited soybean lipoxygenase-1 (sLOX-1) catalyzed oxygenation of linoleic acid was assayed at pH 9.2, by determining the effect on the initial rates of 13-HPODE formation by UV-Vis at 234 nm.

3.1.4.1 Kinetics of sLOX-1 Catalyzed Oxidation of Linoleic Acid

Soybean lipoxygenase kinetics are known to show substrate inhibition,[13] which arises due to the binding of substrate to the ferrous (inactive) form of the enzyme, as demonstrated in Scheme 3.7.

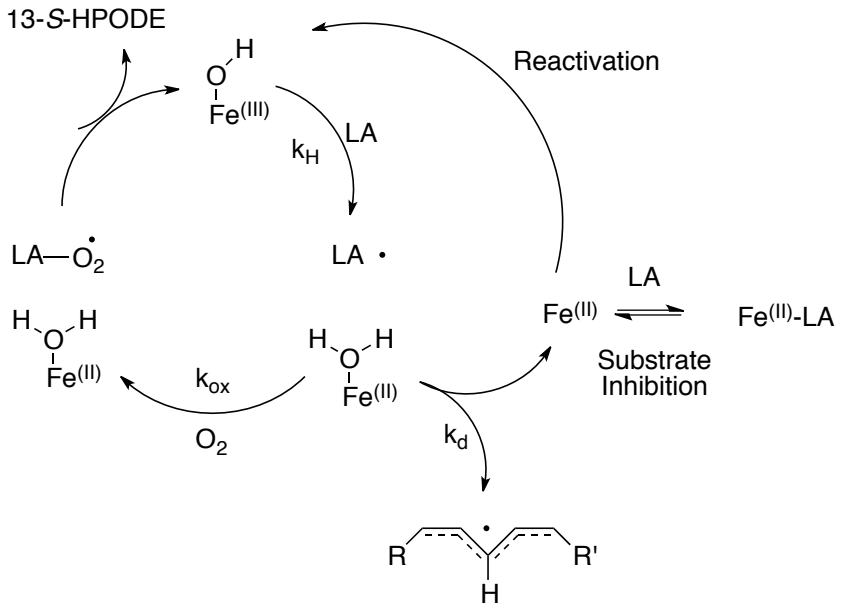

Scheme 3.7. The mechanism of sLOX-1 and substrate inhibition modified from the work by Van der Donk.[14]

Under our experimental conditions, a Michaelis-Menten plot revealed substrate inhibition above 50 μM, hence we decided on a substrate concentration of 20 μM (ca. ½ V_{max}) to assay the effects of our inhibitors on sLOX activity, as shown in Figure 3.5. The K_M in our experiment is lower than those reported in the literature (~62 μM).[13]

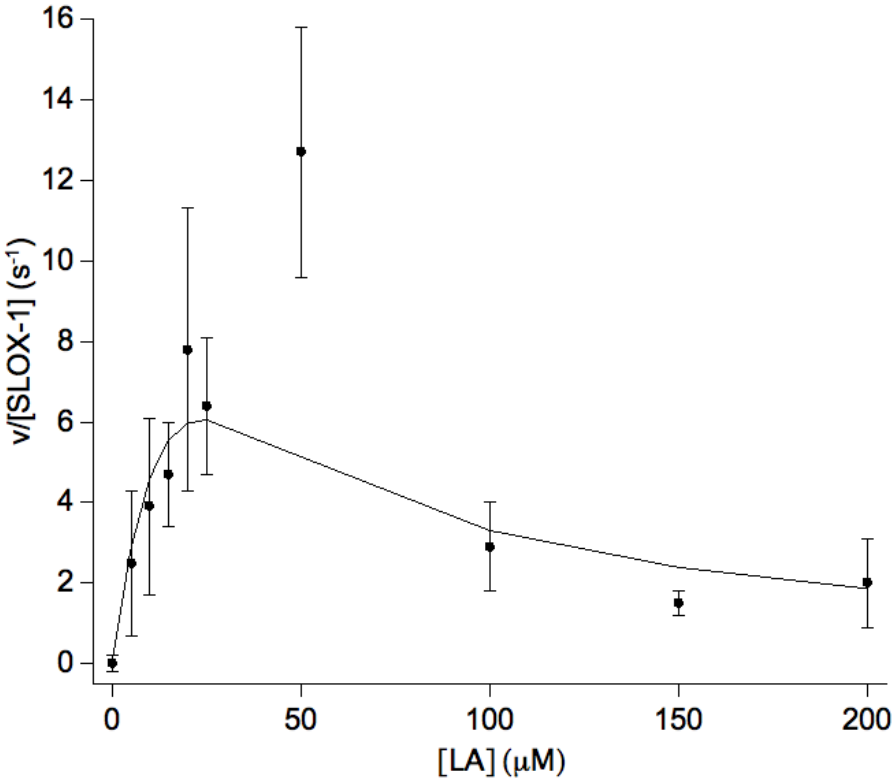

Figure 3.5. Concentration dependence of the initial rates of the oxidation of linoleic acid at room temperature, 100 mM borate buffer, pH 9.2, 3.0 nM [sLOX-1]. Solid line was obtained by using the equation for substrate inhibition (LA): $v = k_{cat}[E][LA]/(K_a + [LA] + ([LA]^2/K_i))$. Values for oxidation of LA were k_{cat}= 22 s^{-1}, $K_{M,\,LA}$=32 μM and $K_{i,\,LA}$= 19 μM.

3.1.4.2 Inhibition of sLOX-1 with *N*-Acylated 2-Aminopyrimidinols

Inhibitors **3.4**, **3.11**, **3.13**, **3.15** samples were prepared and characterized immediately before use in the assay. Consistent with earlier work, it was determined that ApAP does not significantly inhibit sLOX-1, up to 2 nM as shown in Figure 3.6A. Compound **3.4** was previously reported to inhibit sLOX-1 activity and have an IC_{50} value of 564 μM.[7] As shown in Fig.3.6B, a similar result was obtained

(IC_{50}: 506 μM). The order of efficacy in the inhibition of sLOX-1 is **3.13** > **3.11** > **3.4**. Compound **3.15** was the least effective inhibitor in the series. However, it must be pointed out that the values obtained do not differ greatly from one another and are more or less within the experimental error. It was also observed that over the course of the experiment, the inhibitor stock solutions began to change colour. They went from a translucent, colourless solution to a translucent, yellow or slightly brown solution. Based on the appearance of the resulting inhibitor stock solutions, it is speculated that the IC_{50} value for **3.13** was slightly lower than all other compounds because it had not degraded as quickly. Compound **3.15** had to highest IC_{50} value in the series, which is consistent with the noticeable colour change and the appearance of a precipitate in the stock solution.

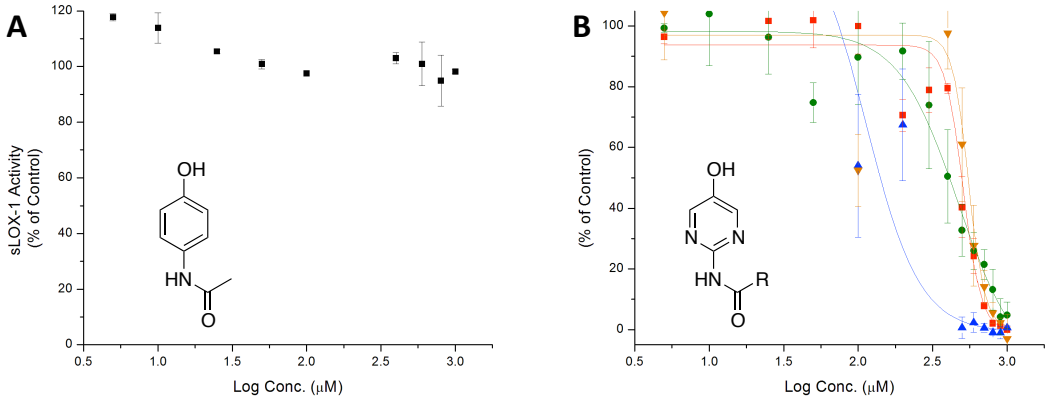

Figure 3.6. sLOX-1 inhibition studies in 100 mM borate buffer (pH 9.2), at room temperature using A) ApAP and B) acylated 2-amino-5-benzoxylpyrimidines. sLOX-1 activity is expressed relative to the control where no inhibitor was added. Each data point represents the mean ± S.E.M of three values. IC_{50} (μM): **3.4** (■), 506; **3.11** (●), 468; **3.13** (▲), 114; **3.15** (▼), 551. Solid lines were obtained by fitting to a sigmoidal function using Microcal Origin software.

3.1.4.3 Inhibition of sLOX-1 with *N*-Acylated 2-Amino-5-Benzoxylpyrimidines

With compounds **3.6**, **3.12**, **3.14**, **3.16** in hand, their efficacy as sLOX-1 inhibitors were assayed using the above-mentioned conditions as shown in Figure 3.7. The results indicate that as the acetamide chain length increases the efficacy of the inhibitor also improves. It was determined that **3.16** >**3.14** >**3.12** >**3.6**. While the potency is not particularly impressive, the observed trend in increasing lipophilicity in the 2-position is interesting and is consistent with our hypothesis. As the acetamide chain length increases and becomes more similar to the linear

hydrocarbon of the enzyme substrate, the ability to inhibit enzyme activity is improved.

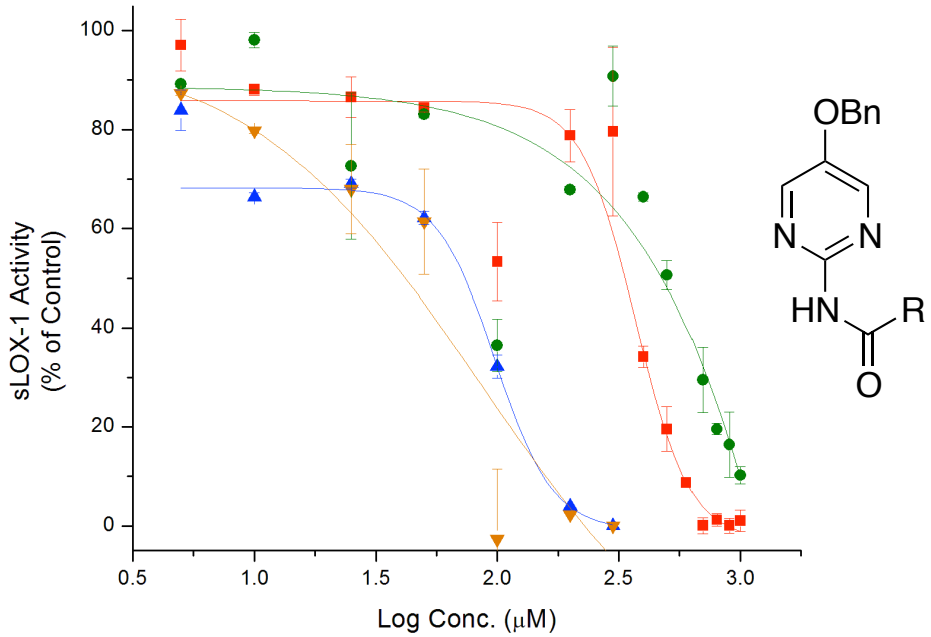

Figure 3.7. sLOX-1 inhibition studies in 100 mM borate buffer (pH 9.2), at room temperature using acylated 2-amino-5-benzoxylpyrimidines. sLOX-1 activity is expressed relative to the control where no inhibitor was added. Each data point represents the mean ± S.E.M of three values. IC_{50} (μM): **3.6** (■), 371; **3.12** (●), 309; **3.14** (▲), 98; **3.16** (▼), 86. Solid lines were obtained by fitting to a sigmoidal function using Microcal Origin software.

The fact that IC_{50} for the O-benzyl compounds were much more promising and demonstrated an obvious trend compared to the acylated 2-aminopyrimidinols,

led us to question the stability of the inhibitors **3.4**, **3.11**, **3.13** and **3.15**. With these compounds there were no noticeable improvement with an increase in chain length. This observation prompts the question of whether we were measuring the IC_{50} values of our inhibitors or a similar degradation product of these compounds? This observation, along with the colour change throughout the course of one trial prompted us to test the stability of the *N*-acylated 2-aminopyrimidinols under the reaction conditions.

3.1.4.4 Stability Studies of Lipophilic *N*-Acylated 2-Aminopyrimidinols

The electron deficiency of the pyrimidine greatly acidifies the phenol-like O-H in compounds **3.4**, **3.11**, **3.13**, and **3.15**. (in fact, the pK_a of the parent compound is 5.9). Since the buffer solution in which the sLOX-1 assays are carried out are at a pH of 9.2, we surmised that they were undergoing a reaction with molecular oxygen as shown in Scheme 3.8.

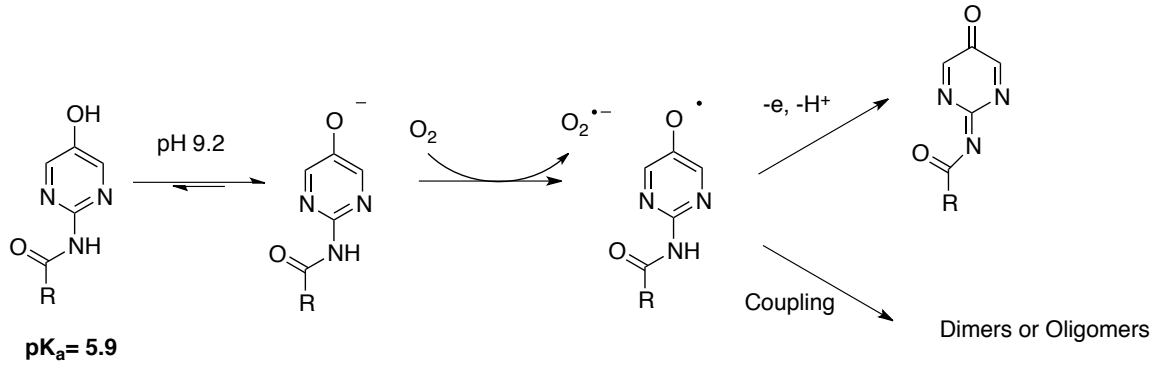

Scheme 3.8. Proposed oxidative decomposition of acylated 2-aminopyrimidinols during sLOX-1 inhibition studies.

To determine if this proposed reaction was occurring during the time required to complete an enzyme assay, an experiment in the absence and presence of molecular oxygen was performed as shown in Figure 3.8.

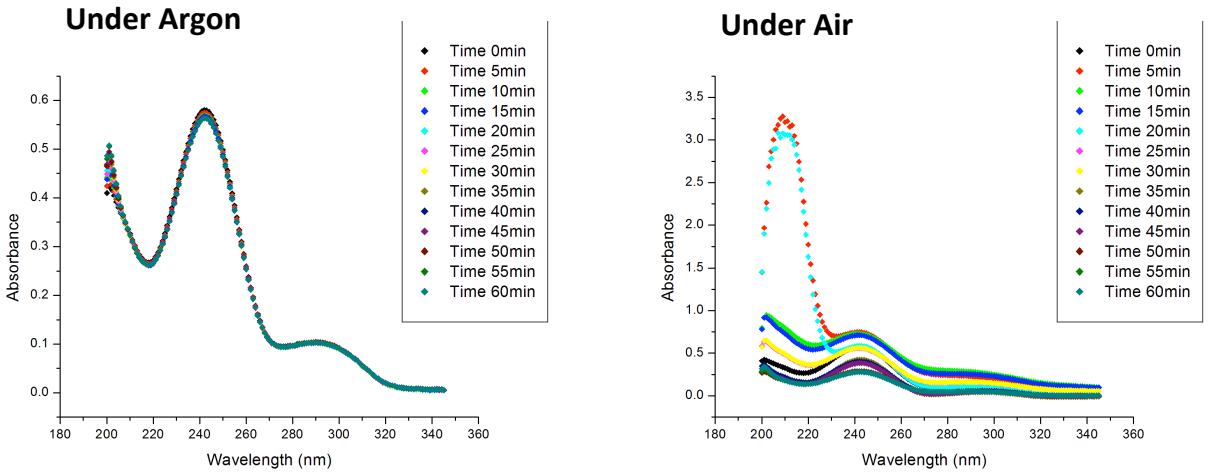

Figure 3.8. Oxidative stability of compound **3.11** (25 µM) in 100 mM borate buffer (pH 9.2), at room temperature. A) Compound **3.11** stability in inert atmosphere and purged solutions. B) Compound **3.11** in the presence of molecular oxygen (open to atmosphere).

In Fig. 3.8A the basic borate buffer was purged with argon and 25 µM of compound **3.11** was injected, under inert atmosphere. The sample was monitored over a range of 200-350 nm every 5 minutes, for 1 hour. In Fig 3.8B, non-purged basic borate buffer, exposed to the atmosphere was used and 25 µM of compound **3.11** was injected. From the above figure, it is clear that when left exposed to the atmosphere, the absorbance spectra changes over time. The maximum absorption at 234 nm begins to decrease as time elapses and the compound begins to

decompose. Over the period of 1 hour, the sample exposed to atmospheric conditions had changed colour and a visible precipitate began to crash out of solution. This would affect the concentration of inhibitor in the sLOX-1 inhibitions studies. This may explain why the compounds all have similar IC_{50} values and are not particularly effective inhibitors.

To confirm that the oxidative properties of the O-H bond was the reason for instability of the compounds, the precursor molecule of the *N*-acylated 2-aminopyrimidinols was tested using the same methods. With an O-benzyl group in the 5-position these concerns would be avoided. In principle, under basic conditions the only abstractable proton was the acetamide proton but our foregoing pK_a studies indicate that the pK_a of this proton is >12. Compound **3.6** was tested for its stability in the buffer as shown in Figure 3.9.

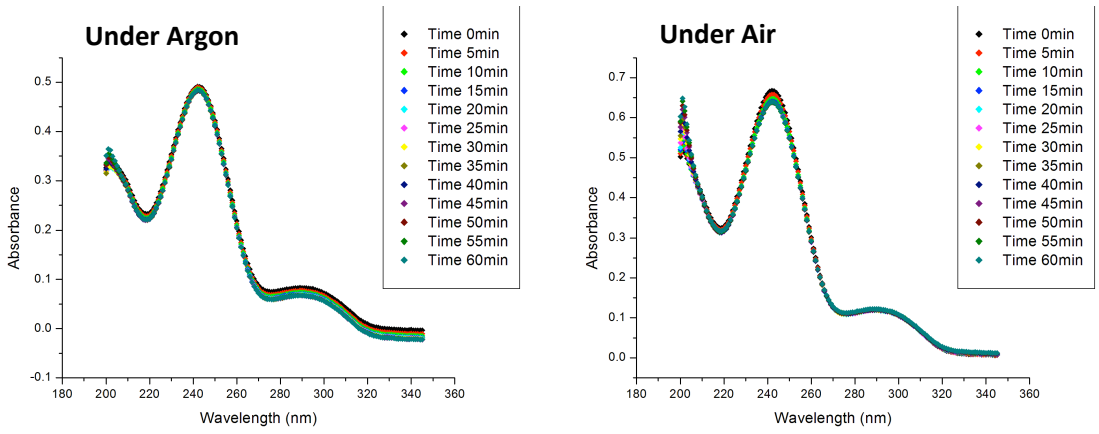

Figure 3.9. Oxidative stability of compound **3.6** (25 μM) in 100 mM borate buffer (pH 9.2), at room temperature. A) Compound **3.6** stability in inert atmosphere and purged solutions. B) Compound **3.6** in the presence of molecular oxygen (open to atmosphere).

As shown in Figure 3.9, in the absence of the acidic hydrogen atom in the 5-position, the stability of the compound is no longer a concern. The maximum absorption at 234 nm is consistent over a period of 1 hour in the atmospheric and inert reaction conditions. These finding correlate to the bench stability of the compounds. The O-benzyl compounds remain stable for months at room temperature and open to air. However, the hydroxyl compounds are not stable at room temperature and decompose rapidly. A visible colour change and precipitation in basic solution is observed.

3.1.5. Synthesis of 5-Alkyloxy *N*-Acylated 2-Aminopyrimidines

Since it can be anticipated that the O-benzyl substituent is not ideal for binding, given that the enzyme substrate is a linear hydrocarbon and the aromatic ring is a rather bulky and planar moiety, we sought to replace this with a linear aliphatic chain.

3.1.5.1 General Reaction Conditions to Introduce an Alkyl Chain in Position 5

Several attempts were made to introduce an alkoxy group of varying chain lengths onto compounds **3.4**, **3.11**, **3.13** and **3.15** in hopes to increase their stability and improve the binding ability of these inhibitors for the sLOX-1 active site. Compounds **3.4**, **3.11**, **3.13** and **3.15** were each added to a separate flask and dissolved in DMF. To each solution 1.0 eq of potassium carbonate was added and the desired alkyl iodides (methyl- and hexyl -iodide) were added dropwise. However, analysis of the reaction by TLC showed only baseline product. Upon workup of the reaction it appeared that

the decomposition products of compounds **3.4**, **3.11**, **3.13** and **3.15** were formed. The stability of the free alcohol was making it difficult to obtain varying alkoxy chain lengths in the 5-position of the ring.

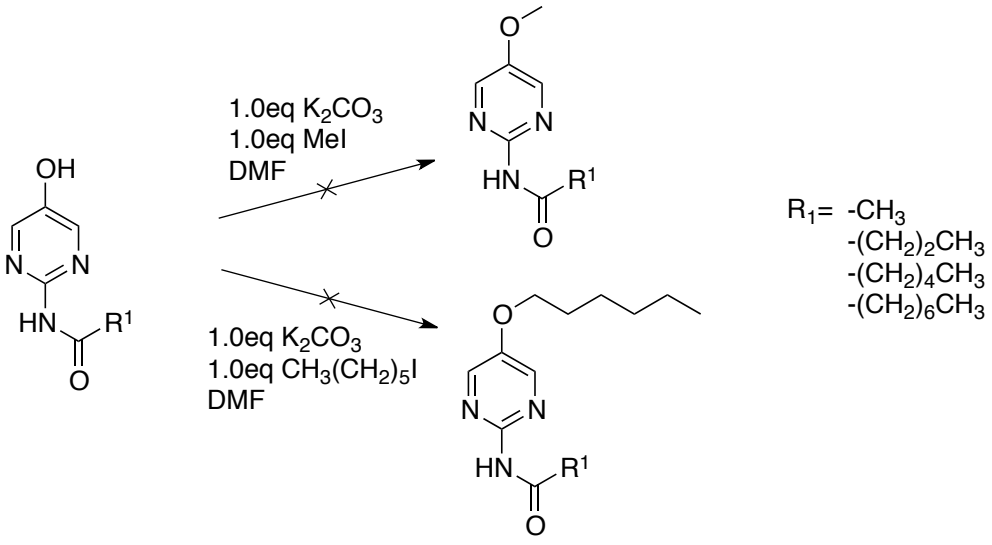

3.1.5.2 New Synthetic Approach to Introduce Alkyl Groups

With the high oxidative potential of the acylated 2-aminopyrimidinols and the difficulties encountered while introducing different alkoxy chain lengths after hydrogenolysis, we elected to introduce the desired alkoxy functionality by copper catalyzed nucleophilic aromatic substitution, as we did for the O-benzyl derivatives shown in Scheme 3.9.

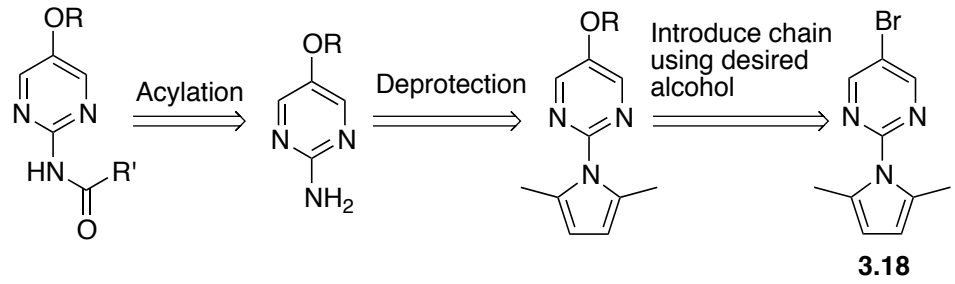

Scheme 3.9. A synthetic approach for the introduction of an O-alkyl chain in the 5-position of the pyrimidine ring.

The introduction of these linear O-alkyl groups in replacement of the O-benzyl group would eliminate the need for hydrogenolysis and avoid the rapidly oxidizable acylated 2-aminopyrimidinols. Using the above mentioned reaction conditions for copper catalyzed C-O coupling using benzyl alcohol the desired linear chain alcohols would be substituted. The following compounds were prepared **3.22**, **3.23**, **3.24**, and **3.25**.

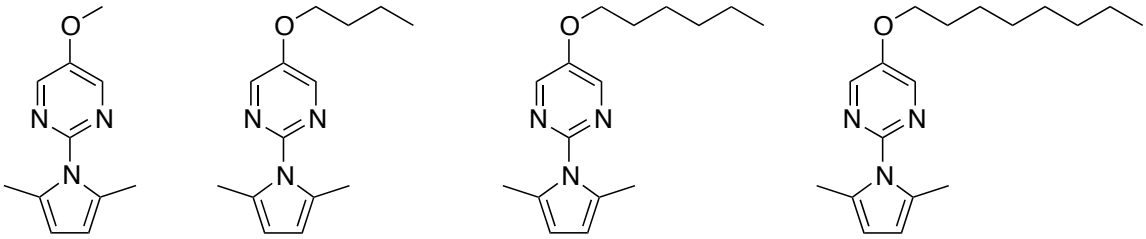

3.1.5.3 Deprotection of the 2,4-Dimethylpyrrole Group on the Alkoxy Compounds

Deprotection of the 2,4-dimethylpyrrole groups on compounds **3.22**, **3.23**, **3.24**, and **3.25** were subjected to the previously mentioned reaction conditions. Excess hydroxylamine hydrochloride and triethylamine, in a 2:1 mixture of ethanol and water were stirred at reflux for several days; however, only starting material remained. The addition of excess reagents still did not force the reaction to go to completion. With the addition of a long aliphatic chain in the 5-position, over the bulky aromatic of the O-benzyl group, concerns with solubility arose. Emulsions were observed throughout the ethanol solution.

The solvent was changed from ethanol to butanol in repeated attempts to remove the 2,4-dimethylpyrole protecting group from compounds **3.22**, **3.23**, **3.24**, and **3.25**. The moderate miscibility of n-butanol in water was thought to aid in the solubility of our compounds. Nevertheless, after several days of prolonged heating, only starting material remained.

Previous attempts by the group claim that other protecting groups had been investigated in the original design of the synthesis; however, all would hydrolyze in subsequent steps. The use of this doubly protected amine is ideal because it is non-ionizable, stable to strong bases and stable to strong reducing agents. Although these are assets for subsequent steps in the reaction, it also makes it very difficult to remove. Recently a paper by Walia *et al*, discuss the difficulties involved with conventional removal procedures and report a new method.[15] They report using microwave-assisted protection of primary amines as 2,5-dimethylpyrroles and their

subsequent deprotection. The general procedure for the deprotection using a microwave was followed as reported. The solvent was not altered, as we expected the use of microwaves would assist in the compounds solubility.

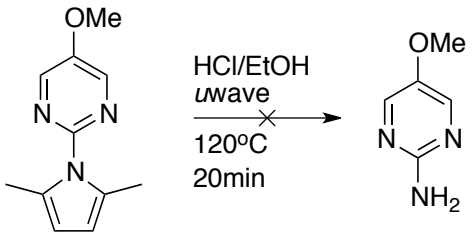

3.22

The protected amine was dissolved in ethanol and concentrated HCl was added dropwise. The reaction flask was heated in a microwave irradiator for 20 minutes, at 120 °C. TLC analysis of the reaction mixture showed a wide array of products but the starting material was consumed. However, the desired protect was not obtained as determined through ^{1}H-NMR analysis. Another microwave experiment in which the time was lowered to 5 minutes, at 120 °C was tested. Again, all starting material was consumed but the desired product was not obtained. ^{1}H-NMR analysis indicated that the pyrimidine ring was destroyed under these conditions, as pyrimidine peaks were no longer present in the spectrum.

3.1.6. Synthesis of 5-Alkyl *N*-Acylated 2-Aminopyrimidines

Given the problems associated with accessing the foregoing substrates and because we questioned whether an electron donating group at the 5-position was even desirable for inhibition, we sought to prepare analogs with a linear aliphatic chain in

the 5-position. This would also greatly simplify the synthetic efforts, as shown in Scheme 3.10.

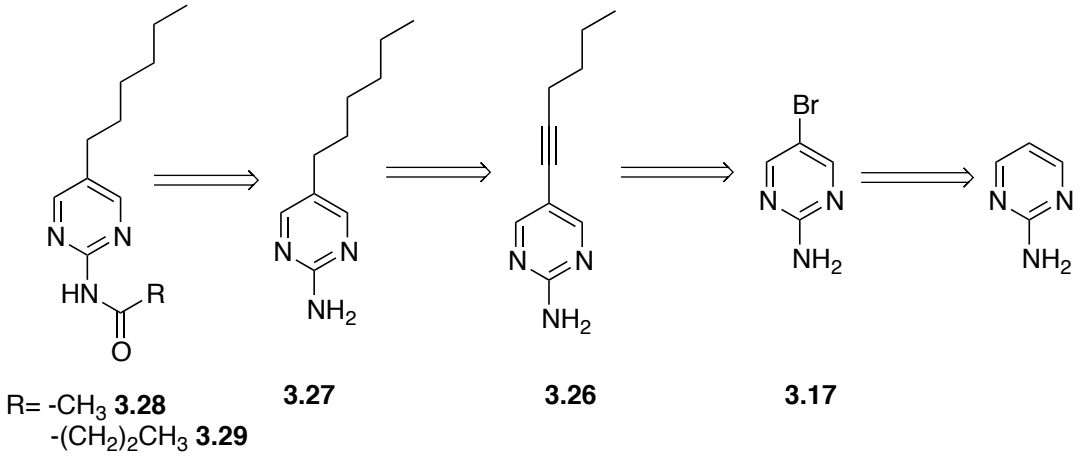

Scheme 3.10. Proposed synthetic design for the introduction of an alkyl chain in the 5-position of the pyrimidine ring.

3.1.6.1 Sonagashira Cross Coupling to Produce 5-Alkynyl 2-Aminopyrimidines

With easy access to 5-bromo-2-aminopyrimidine, it was envisioned that a Sonagashira cross coupling would be ideal for the introduction of the alkyl substituent at the 5-position of the pyrimidyl halide. Known reaction conditions by Robins *et al*, were successfully attempted.[16] The best catalyst to fully promote the consumption of starting material was tetrakis(triphenylphosphine)palladium(0). Other palladium sources ($Pd_2(dba)_3$, and $PdCl_2(PPh_3)_2$) could be used, however, higher catalyst loading and an excess of alkyne was needed to force the reaction to completion. The starting material and product are very difficult to separate by

column, and recrystallization attempts results in a loss of desired product. The use of tetrakis(triphenylphosphine)palladium(0), however, resulted in a relatively clean product conversion, and recrystallization with hot methanol resulted in the pure compound.

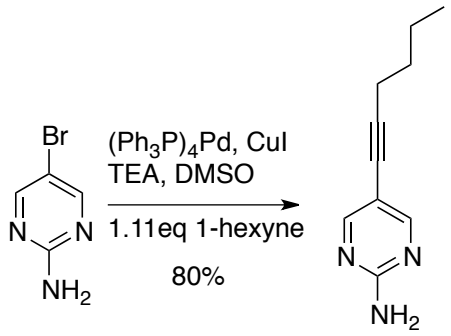

3.17 **3.26**

3.1.6.2 Hydrogenation of 5-Alkynyl 2-Aminopyrimidines

Hydrogenation of 5-alkynyl 2-aminopyrimidines to reduce the triple bond was attempted, following known reaction procedures.[16] However, compound **3.26** was more soluble in ethanol, and an increase in pressure and temperature, from that reported, was required for the reaction to commence. Hydrogenation at 1200 psi, over 10% Pd/C for 2 days at 50°C was required for complete conversion to the desired compound **3.27**.

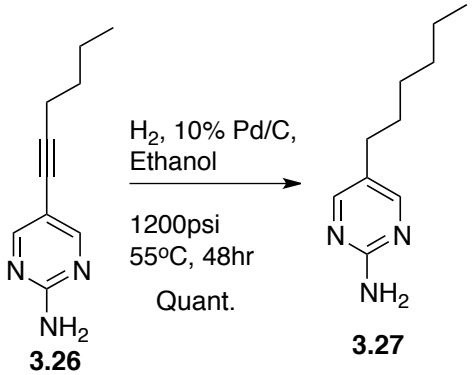

3.26 **3.27**

3.1.6.3 Acylation of 5-Alkyl-2-Aminopyrimidines

Compound **3.27** was acylated following the optimized reaction conditions mentioned earlier. Two derivatives were synthesized.

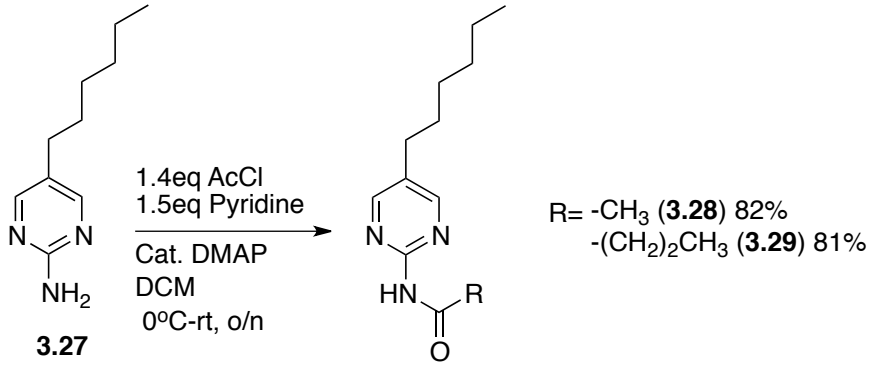

3.1.7 Inhibition of sLOX-1 with *N*-Acylated 5-Hexyl-2-Aminopyrimidines

These alkylated compounds were tested for their efficacy as inhibitors of sLOX-1, as described before, and the results are shown in Figure 3.10. As predicted, the absence of the bulky benzyl group increased the efficacy of the inhibitors. The trend with increasing acetamide chain length is consistent with earlier results as the C4 chain has greater affinity for the active site of sLOX-1 than the C2 chain. Unfortunately, due to time constraints, the rest of the series were not explored (R=C_5H_{11}, C_7H_{15}), but based on our earlier results, we anticipate that the longer chain lengths will demonstrate a similar trend in inhibitory effects, as the O-benzyl compounds. The inhibitory activity absence of the O-H group in the 5-position supports the theory that the mechanism follows iron chelation with the acetamide oxygen and ring nitrogen.

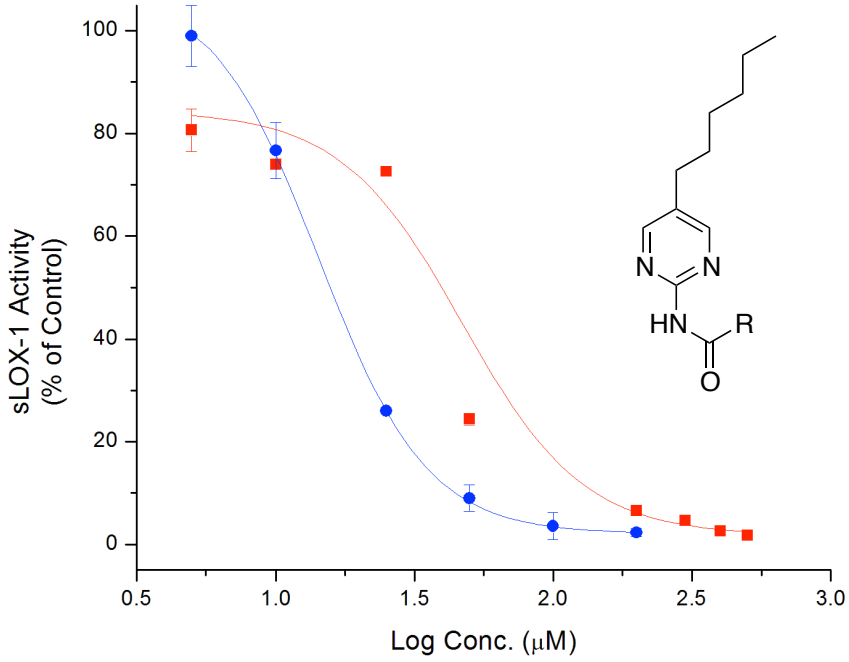

Figure 3.10. sLOX-1 inhibition in 100 mM borate buffer (pH 9.2), at room temperature using acylated 5-hexyl-2-aminopyrimidines (25 μM). sLOX-1 activity is expressed relative to the control where no inhibitor was added. Each data point represents the mean ± S.E.M of three values. IC_{50} (μM): **3.28** (■, R=CH_3), 47; **3.29** (●, R=C_3H_7), 14. Solid lines were obtained by fitting to a sigmoidal function using Microcal Origin software.

The IC_{50} values of compounds **3.28** and **3.29** were the lowest of the *N*-acyl 2-aminopyrimidines to date, with IC_{50} values of 47 μM and 14 μM, respectively. It appears as though the long chain functionality in the 5 position of the ring induces a better fit in the active site versus the large bulky O-benzyl substituent as predicted.

3.2 Conclusions

The following chart summarizes the IC_{50} values obtained from the sLOX-1 assays reported herein.

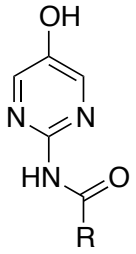

Compound	IC_{50} (μM)
3.4 (-CH_3)	506
3.11 (-$(CH_2)_2CH_3$)	468
3.13 (-$(CH_2)_4CH_3$)	114
3.15 (-$(CH_2)_6CH_3$)	552

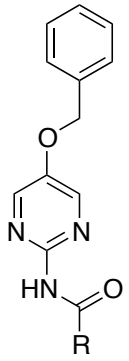

Compound	IC_{50} (μM)
3.6 (-CH_3)	371
3.12 (-$(CH_2)_2CH_3$)	309
3.14 (-$(CH_2)_4CH_3$)	98
3.16 (-$(CH_2)_6CH_3$)	86

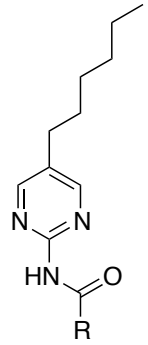

Compound	IC_{50} (μM)
3.28 (-CH_3)	47
3.29 (-$(CH_2)_2CH_3$)	14

As mentioned previously, NDGA is a natural product extensively studied for its inhibition of soybean lipoxygenase. The putative mechanism of action is the reduction of the active site ferric iron atom to the inactive ferrous form.[3] Alongside NDGA, Holm*an et al* have investigated a number of NDGA derivatives, some of which are shown below along with their IC_{50} values for soybean lipoxygenase.[17]

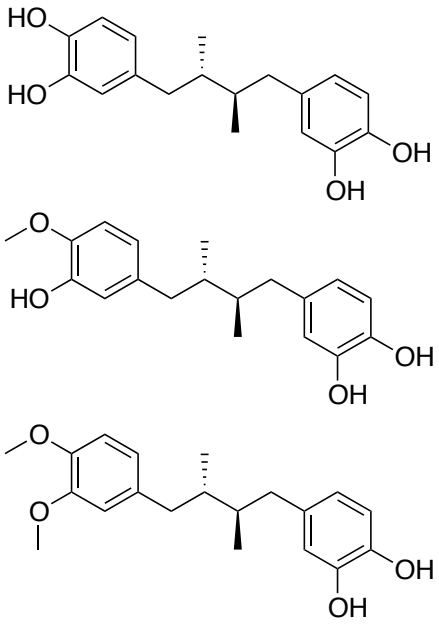

IC_{50}= 0.18 µM ± 0.02

IC_{50}= 0.17 µM ± 0.009

IC_{50}= 3.1 µM ± 0.3

Although the potencies of our analogs were not outstanding compared to the reported NDGA derivatives, with our lowest IC_{50} being 14 µM, the inhibitory trend is promising and suggests that with further optimization of the sidechains, potentially useful inhibitors, *without a redox active site* could be obtained. The absence of a redox active site is highly favourable as these inhibitors are unlikely to be hepatotoxic, as are NDGA and acetaminophen.

The IC_{50} values are markedly better with the increasing lipophilicity of the acetamide group in 2-position of the molecule and the introduction of an aliphatic substituent in 5-position. These findings help to support the proposed mechanism in Scheme 3.4, whereby iron chelation with the acyl oxygen and one of the ring nitrogens occurs, and the mechanism is not dependent on the presence or acidity of the phenolic O-H. It is speculated that the pK_a of the acetamide hydrogen will be

<<12, now that the electron donating OH (O^-)/OR moiety has been replaced with an alkyl group, and this may enhance binding.

Although the inhibitors and their corresponding IC_{50} values follow the above-mentioned trends, this does not confirm the direct affinity for the enzyme active site. There are two applications of kinetic measurements that distinguish between different types of inhibition, such as competitive and non-competitive inhibition. These measurements provide quantitative information on the effectiveness of various inhibitors, and how enzymatic activities are regulated. To determine if these inhibitors act competitively or non-competitively, a double-reciprocal plot of the rates of catalysis (1/v), at different concentrations of substrate (1/[S]), using different concentration of inhibitor, serve to distinguish the two types of inhibition. In competitive inhibition all series intersect at the same point; $1/V_{max}$ (y-intercept). In non-competitive inhibition the same plot is measured; however, the all series intersect at the same point; $-1/K_M$ (X-intercept). The slopes of both plots and the intercepts are linear function of $1/K_i$, where K_i is the dissociation constant. These experiments must be carried out to confirm our expectation that the N-acylated 2-aminopyrimidines do indeed compete with linoleic acid for the active site of soybean lipoxygenase.

The results also support the model by which the increasing chain length mimics the natural linoleic acid substrate and fills the active site of the enzyme, as demonstrated above in Figure 3.2. In Klinman's model (Figure 3.1) it is suggested that the carboxylic acid moiety at the end of linoleate aids in substrate binding. The anionic carboxylate formed may be important in salt bridge formation with a

cationic ammonium from one of the ionizable side chains of the amino acid residues (i.e. Arg, Lys, or His), positioned in the active site.[9]

With this in mind and the results reported herein, the following targets could be potentially useful isoform-specific inhibitors of mammalian LOXs, which utilize the 20-carbon arachidonic acid as the substrate.

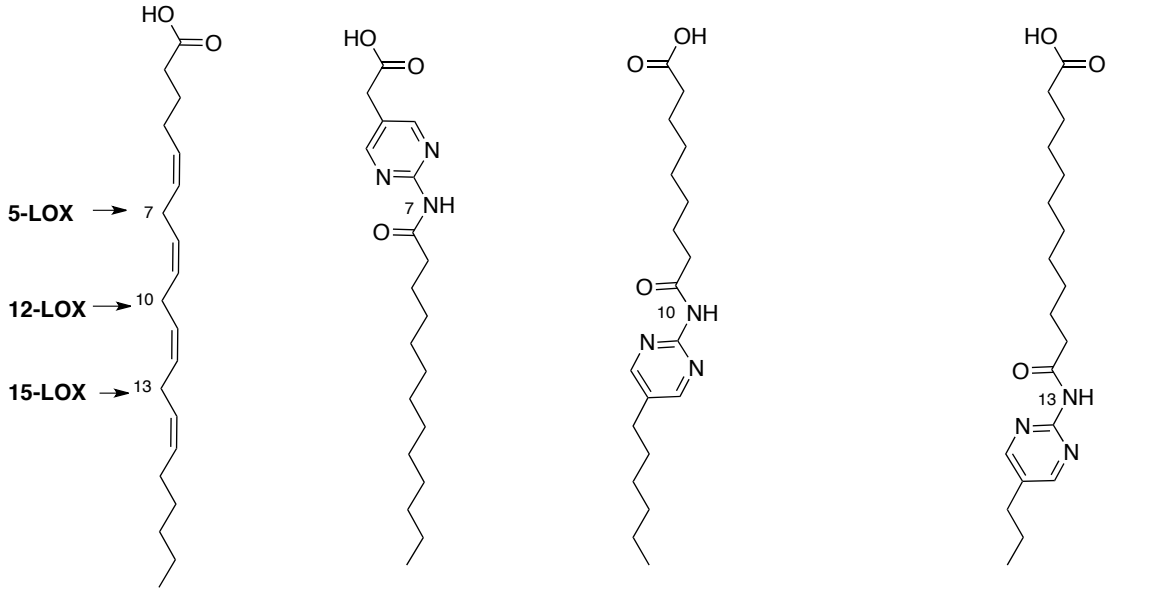

As mentioned previously, each human isoform of lipoxygenase abstracts a specific methylene hydrogen from arachidonic acid (5-LOX: 7-position, 12-LOX: 10-position, and 15-LOX: 13-position). The variation in chain lengths in the 2 and 5 positions of the pyrimidine ring may allow entry into the active site for one isoform but may not be favourable for another. The ring occupies the space where molecular oxygen can react. The introduction of a carboxylic acid at the end of the

hydrocarbon chain in position 5 may also help with the specificity and salt bridges that form.

3.3 References

(1) Larson, A. M.; Polson, J.; Fontana, R. J.; Davern, T. J.; Lalani, E.; Hynan, L. S.; Reisch, J. S.; Schiødt, F. V.; Ostapowicz, G.; Shakil, A. O.; Lee, W. M.; The Acute Liver Failure Study Group. *Hepatology.* **2005**, *42*, 1364.

(2) Hinz, B.; Cheremina, O.; Brune, K. *FASEB J.* **2007**, *22*, 383.

(3) Whitman, S.; Gezginci, M.; Timmermann, B. N.; Holman, T. R. *J. Med. Chem.* **2002**, *45*, 2659.

(4) Sahu, S. C.; Ruggles, D. I.; O'Donnell, M. W. *Food Chem. Toxicol.* **2006**, *44*, 1751.

(5) James, L. P.; Mayeux, P. R.; Hinson, J. A. *Drug Metab. Dispos.* **2003**, *31*, 1499.

(6) Pratt, D. A.; DiLabio, G. A.; Brigati, G.; Pedulli, G. F.; Valgimigli, L. *J. Am. Chem. Soc.* **2001**, *123*, 4625.

(7) Nam, T.-G.; Nara, S. J.; Zagol-Ikapitte, I.; Cooper, T.; Valgimigli, L.; Oates, J. A.; Porter, N. A.; Boutaud, O.; Pratt, D. A. *Org. Biomol. Chem.* **2009**, *7*, 5103.

(8) Nelson, M. J. *Biochemistry.* **1988**, *27*, 4273.

(9) Meyer, M. P.; Tomchick, D. R.; Klinman, J. P. *Proc. Natl. Acad. Sci. U.S.A.* **2008**, *105*, 1146.

(10) Schneider, C.; Pratt, D. A.; Porter, N. A.; Brash, A. R. *Chem. Biol.* **2007**, *14*, 473.

(11) Das, B.; Venkateswarlu, K.; Majhi, A.; Siddaiah, V.; Reddy, K. R. *J. Mol. Catal. A: Chem.* **2007**, *267*, 30.

(12) Tanemura, K.; Suzuki, T.; Nishida, Y.; Satsumabayashi, K.; Horaguchi, T. *Chem. Commun.* **2004**, 470.

(13) Berry, H.; Debat, H.; Larreta-Garde, V. *FEBS Lett.* **1997**, *408*, 324.

(14) Peng, S.; van der Donk, W. A. *J. Am. Chem. Soc.* **2003**, *125*, 8988.

(15) Walia, A.; Kang, S.; Silverman, R. B. *J. Org. Chem.* **2013**, *78*, 10931.

(16) Robins, M. J.; Nowak, I.; Rajwanshi, V. K.; Miranda, K.; Cannon, J. F.; Peterson, M. A.; Andrei, G.; Snoeck, R.; De Clercq, E.; Balzarini, J. *J. Med. Chem.* **2007**, *50*, 3897.

(17) Wecksler, A. T.; Garcia, N. K.; Holman, T. R. *Bioorg. Med. Chem.* **2009**, *17*, 6534.

-4-
Experimental Methods

4.1 General

Starting materials, reagents and solvents were purchased from commercial sources and used as received unless otherwise indicated. ^{1}H-NMR, ^{13}C-NMR and ^{19}F-NMR spectra were collected on a BRUKER Advance 300, BRUKER Advance II 300 and BRUKER Advance 400 spectrometers. High-resolution mass spectra were obtained by electron ionization on a Kratos Concept Tandem mass spectrometer. All pKa measurements and enzyme assays were obtained using a Cary 50 spectrophotometer. Plots were generated using Microcal Origin software.

4.2 Preparation of Compounds Described in Chapter 2

9-Bromononanol. **(2.9)** To a flask was added 1,9-nonanediol (16 g, 0.1 mol, 1.0 eq) in toluene (200 mL, 0.5 M), under inert atmosphere. HBr (12.5 mL, 1.5 eq) was slowly added to the reaction flask. The reaction was equipped with a Dean-Stark apparatus and reflux condenser and left overnight. The reaction flask was cooled to room temperature and the reaction was quenched by slow addition of water. The mixture was extracted with ethyl acetate (×3), which was then washed with sodium bicarbonate and brine. The combined organic layers were dried using magnesium sulfate, filtered and concentrated under reduced pressure. The residue was purified by flash column chromatography on silica gel with 2:1 hexane: ethyl acetate (R_f=0.4) to yield 20.7 g of a white solid (93% yield). ^{1}H-NMR [300 MHz; $CDCl_3$]: δ (ppm) 1.29-1.37 (m, 8H), 1.41-1.43 (m, 2H), 1.50 (bs, 1H), 1.52-1.60 (m, 2H), 1.81-1.87 (m, 2H),

3.42 (t, *J*=6.6 Hz, 2H), 3.62 (t, *J*=6.6 Hz, 2H). Analytical data were in accordance with those reported in the literature.[1]

9-Bromononanoic acid. **(2.8)** To chromium trioxide (10.0 g, 0.1 mol, 1.4 eq) in water (15 mL, 7.0 M), at 0 °C was added concentrated sulfuric acid (8.6 mL), followed by water (28.5 mL; to a final concentration of 2.3 M) dropwise. To the mixture was added 9-bromononanol (16.2 g, 0.07 mol, 1.0 eq) in acetone dropwise, at −5 °C. The reaction was warmed to 0 °C and left to stir for 2 hours. The reaction was then warmed to room temperature and left to stir for an additional 2 hours. Ether was added to the reaction mixture and the mixture was extracted several times (×3), which was then washed with brine. The combined organic layers were dried using magnesium sulfate, filtered and concentrated under reduced pressure. The residue was purified by flash column chromatography on silica gel with 30% ethyl acetate in hexanes (R_f= 0.3) and 11.4 g of white, needlelike crystals were obtained (70% yield). ^{1}H-NMR [300 MHz; $CDCl_3$]: δ (ppm) 1.20-2.10 (m, 12H), 2.35 (t, *J*= 6.7 Hz, 2H), 3.41 (t, *J*= 6.6 Hz, 2H). Analytical data were in accordance with those reported in the literature.[2]

Methyl-9-bromononanoate**. (2.7)** To 9-bromononanoic acid (0.25 g, 1.0 mmol, 1.0 eq) in dichloromethane (5.0 mL, 0.2 M), at 0 °C was added oxalyl chloride (0.19 g, 1.5 mmol, 1.5 eq) dropwise, followed by 1 drop of DMF. Once the bubbling subsided, methanol (0.2 mL, 5.0 eq) was added dropwise over several minutes. The

solution was left to stir for several hours until all starting material was consumed, as monitored by TLC. Water was slowly added to quench the reaction mixture. Ether was added to the reaction flask and the mixture was extracted several times (×3), which was then washed with brine. The combined organic extracts were dried using $MgSO_4$, filtered and concentrated under reduced pressure. The residue was purified by flash column chromatography on silica gel with 5% ethyl acetate in hexanes (R_f= 0.23) to yield 0.20g of a colourless oil (80% yield). ^{1}H-NMR [300 MHz; $CDCl_3$]: δ (ppm) 1.20-2.10 (m, 12 H), 2.33 (t, *J*= 6.8 Hz, 2H), 3.41 (t, *J*= 6.6 Hz, 2H), 3.65 (s, 3H). Analytical data were in accordance with those reported in the literature.[2]

***8-Carboxymethyl octyltriphenylphosphonium bromide*. (2.6)** To triphenylphosphine (0.18 g, 0.70 mmol, 1.5 eq) was added methyl 9-bromononanoate (0.12 g, 0.47 mmol, 1.0 eq) in acetonitrile (3.8 mL, 0.1 M). The solution was heated to reflux and left to stir until all starting material was consumed. The solvent was removed under high pressure and the resulting brown, oily residue was purified by flash column chromatography on silica gel. The excess triphenylphosphine was eluted in 50% diethylether and pentane and then the mobile phase was exchanged for 7% methanol in dichloromethane to yield 0.19 g of a viscous, yellow oil (79% yield). ^{1}H-NMR [300 MHz; $CDCl_3$]: δ (ppm) 0.98-1.79 (m, 12H), 2.20 (t, *J*=6.8 Hz, 2H), 3.60 (s, 3H), 3.69 (m, 2H), 7.31-7.50 (m, 15H). Analytical data were in accordance with those reported in the literature.[2]

***1-Iodoheptyne*. (2.13)** A double necked, round bottom flask was sealed with a new septum, flame dried in vacuo, flushed with argon and equipped with an argon balloon. The septa were para-filmed for extra precaution. A 2.5 M solution of *n*-butyl lithium in hexane (5.4 mL, 13.5 mmol, 1.3 eq), was added slowly to a solution of heptyne (1.0 g, 10.4 mmol, 1.0 eq) in dry THF (dried using Na; 38.5 mL, 0.2 M) at −20 °C and allowed to stir for 1 hour. The reaction mixture was then cooled to −40 °C. In a separate flask, vacuumed and argon filled, was added iodine (3.4 g, 13.5 mmol, 1.3 eq) that had been dissolved in minimal amounts of dry THF. The iodine solution was then added dropwise to the heptyne mixture and allowed to stir overnight. It was left to slowly warm to room temperature and wrapped in tin foil. The reaction mixture was then quenched with aqueous ammonium chloride solution. The mixture was extracted with ethyl acetate (×3), which was then washed with saturated sodium thiosulfate solution and saturated brine. The combined organic layers were dried using magnesium sulfate, filtered and concentrated under reduced pressure. Bleach was added to the rotavap trap while solvent was removed under pressure (Note: strong pungent smells may be released). The 1-iodoheptyne was used without any further purification. Reaction produces quantitative amounts of desired product. Material can be stored at −20 °C under argon and protected from light for several months. ^{1}H-NMR [300 MHz; $CDCl_3$]: δ (ppm) 0.89 (t, *J*= 6.5 Hz, 3H), 1.29-1.34 (m, 4H), 1.35-1.38 (m, 2H), 2.32-2.37 (t, *J*= 6.0 Hz, 2H). Analytical data were in accordance with those reported in the literature.[3]

***Iodomethyltriphenylphosphonium iodide*. (2.14)** To a flask, equipped with a reflux condenser was added methylene iodide (0.05 g, 0.17 mmol, 1.0 eq), in dry benzene (0.5 ml), under inert atmosphere. To this was added triphenylphospine (0.04 g, 0.17 mmol, 1.0 eq). The reaction flask was protected from light and heated to 50 °C. After 15 minutes the solution became cloudy and the formation of small needlelike crystals were observed. The reflux was left overnight. The solution was cooled to room temperature. The solid were rinsed with benzene, followed by ether and any remaining solvent was removed under vacuo to yield 0.44 g of a white solid (50% yield). ^{1}H-NMR [400 MHz; $CDCl_3$]: δ (ppm) 3.33-3.72 (m, 2H), 7.81-8.16 (m, 15H). Analytical data were in accordance with those reported in the literature.[4]

***(Z)-1-Bromoheptene*. (2.15)** To a flame dried and argon filled flask was added 1-heptyne (5.1 g, 53 mmol, 1.0 eq) and neat catecholborane (6.3 g, 53 mmol, 1.0 eq) slowly. The mixture was heated for 2 hours, at 70 °C and then cooled to room temperature. After the addition of dry dichloromethane, to a concentration of 3.54 M, the solution was cooled to −20 °C; and bromine (6.0 ml, 2.0 eq), dissolved in dry dichloromethane (15 ml) was added dropwise. Upon completion 2 N NaOH solution (60 mL) was carefully added at −75 °C. The resulting solution was warmed to room temperature and left to stir for 1 hour. The solution was extracted with dichloromethane (×3), which was then washed with brine. The combined organic layers were dried using magnesium sulfate, filtered and concentrated under

reduced pressure. The product was purified by fractional distillation to yield 6.7 g of a translucent, colourless oil (71% yield). ^{1}H-NMR [300 MHz; $CDCl_3$]: δ (ppm) 0.89 (t, *J*= 6.9 Hz, 3H), 1.22-1.46 (m, 6H), 2.16-2.23 (m, 2H), 6.06-6.15 (m, 2H). Analytical data were in accordance with those reported in the literature. [5]

***(Z)-1-Iodo-heptene*. (2.12)** To a flame-dried, two-necked round-bottomed flask under inert atmosphere, equipped with a magnetic stir bar and fitted with para-filmed rubber septa was added borane dimethyl sulfide complex (0.95 g, 12.3 mmol, 1.06 eq) and dry ether (11 mL, 1.0 M). The resulting solution was stirred and placed in an ice-bath for 10 minutes. Cyclohexene (2.1 g, 25 mmol, 2.11 eq) was added dropwise over 10 minutes via a plastic syringe. A white precipitate should appear within the final minutes of addition. After 15-20 minutes, the ice bath was removed and stirring was continued for 1 hour; at which point a large amount of white precipitate had formed. The reaction flask was again placed in an ice bath and, after 10 minutes, treated with 1-iodoheptyne (2.5 g, 11.2 mmol, 1.0 eq). The 1-iodoheptyne was added dropwise over 10 minutes, via a plastic syringe. The solution was stirred for 30-40 minutes, the ice bath was removed, and stirring was continued for 1.5 hours. The flask was once again placed in the ice bath, and the mixture was allowed to stir for 15 minutes, while glacial acetic acid (5.6 mL, 6.5 eq) was added slowly via a syringe. The ice bath was removed and the mixture was stirred for 2 hours. Finally, the mixture was diluted with ether (11 mL) and deionized water. The resulting biphasic mixture was transferred to separatory funnel and the aqueous phase was discarded (very pungent smell-use of bleach

necessary). The organic phase was washed with water (×3), and dried over magnesium sulfate, filtered and solvent was removed under pressure. A clear to slightly yellow oil, containing small amounts of a white precipitate was obtained. This suspension was applied to a silica gel plug and eluted with pentane. Fractions containing the product were concentrated by rotary evaporation and the desired product was obtained in quantitative yields. ^{1}H-NMR [300 MHz; $CDCl_3$]: δ (ppm) 0.90 (t, *J*= 6.5 Hz, 3H), 1.30-1.33 (m, 4H), 1.40-1.43 (m, 2H), 2.11-2.14 (m, 2H), 6.11-6.16 (m, 2H). Analytical data were in accordance with those reported in the literature. [6]

Preparation of Activated Zinc

To an Erlenmeyer flask, equipped with a stir bar was added zinc dust. Concentrated HCl acid was added to flask and the contents were left to stir for approximately 30 minutes or until majority of bubbling had subsided. The contents of the flask were filtered through suction filtration. The zinc was thoroughly rinsed with copious amounts of distilled water, followed by methanol, acetone and ether. The resulting zinc dust was then placed under reduced pressure and allowed to dry as needed. The zinc should appear as a fine, grey powder when dry. Activated zinc was stored under inert atmosphere until use.

Preparation of Activated Copper

An Erlenmeyer flask, equipped with a stir bar, was added copper (II) sulfate

pentahydrate and a minimal amount of deionized water. The stir bar speed was set to high. Activated zinc (1.0 eq) was added to the flask and left to stir for 30 minutes. A reddish/brown precipitate began to crash out. The precipitate was filtered and rinsed with copious amounts of water, followed by methanol, acetone and ether. The activated copper was then dried in vacuo and used immediately.

***(Z)-Ethyl 2,2-difluoronon-3-enoate*. (2.11)** To a flame dried schlenk flask, under argon atmosphere, ethyl bromodifluoroactetate (0.18 g, 0.88 mmol, 1.0 eq) was added dropwise to a suspension of activated copper in freshly distilled DMSO (4.4 mL, 0.2 M). (Z)-1-iodoheptene (0.2 g, 0.88 mmol, 1.0 eq) was added dropwise to the mixture. The reaction mixture was heated to 55 °C and allowed to stir for 4 hours, at which point an additional equivalent of (Z)-1-iodoheptene (0.2 g, 0.88 mmol, 1.0 eq) in distilled DMSO (0.5 mL, 0.5 M) was added. At 6 hours, one final equivalent of (Z)-1-iodoheptene (0.2 g, 0.88 mmol, 1.0 eq), in distilled DMSO (0.5 mL, 0.5 M) was added to the reaction mixture and left to stir overnight. The mixture was poured into a mixture of ice and saturated ammonium chloride, and extracted with ether (×3). The ether layer was then washed with saturated ammonium chloride and sodium chloride. The combined organic layers were dried over magnesium sulfate and filtered and concentrated under reduced pressure. The residue was purified by flash column chromatography on silica gel with 20% ether in hexanes (R_f=0.4) to yield 0.17 g of a translucent and colourless oil (89% yield). ^{1}H-NMR [300 MHz; $CDCl_3$]: δ (ppm) 0.88 (t, J = 6.8 Hz, 3H), 1.26-1.41 (m, 10H), 2.26 (dd, J = 5.1, 2.3 Hz, 2H), 4.31 (q, J = 7.1 Hz, 2H), 5.55-5.64 (m, 1H), 5.88-5.94 (m, 1H); ^{13}C NMR [75 MHz;

$CDCl_3$] δ (ppm) 13.9, 13.9, 22.4, 28.4, 28.8, 31.3, 62.9, 112.9, 120.8, 142.4, 164.3; ^{19}F NMR [282 MHz; $CDCl_3$] δ (ppm) -98.8 (d, *J*=15 Hz).

***(Z)-2,2-Difluoronon-3-en-1-ol*. (2.17)** To a flask (*Z*)-ethyl 2,2-difluoronon-3-enoate (0.05 g, 0.27 mmol, 1.0 eq) was added and dissolved in dry isopropanol (1.0 mL, 0.4 M), under inert atmosphere. To the solution was added sodium borohydride (0.034 g, 0.91 mmol, 4.0 eq). The reaction mixture was left to stir overnight, after which point methanol was added slowly to quench the reaction. To the resulting reaction mixture was added water and extracted with ether (×3), which was then washed with brine. The combined organic layers were dried using magnesium sulfate, filtered and concentrated under reduced pressure. The residue was purified by flash column chromatography on silica gel with 50% ether in hexanes (R_f= 0.57) to yield 0.025 g of a translucent and colourless oil (63% yield). ^{1}H-NMR [300 MHz; $CDCl_3$]: δ (ppm) 0.88 (t, *J* = 6.8 Hz, 3H), 1.20-1.42 (m, 6H), 2.21-2.27 (m, 2H), 3.78 (t, *J* = 13.4 Hz, 2H), 5.41-5.55 (m, 1H), 5.81-5.90 (m, 1H); ^{13}C-NMR [75 MHz, $CDCl_3$]: δ (ppm) 19.9, 22.5, 28.5, 29.1, 31.4, 65.3, 121.5, 121.8, 140.8; ^{19}F-NMR [282 MHz, $CDCl_3$] δ (ppm) -102.27 (dd, *J*=15 Hz, 30 Hz).

***(Z)-2,2-Difluoronon-3-ene-1,1-diol*. (2.18)** To a flame dried and argon filled flask, equipped with a stir bar, was added PCC (0.14 g, 0.66 mmol, 1.5 eq), which was suspended in dry dichloromethane (1.32 mL, 0.5 M). In a separate flame dried and argon filled flask was dissolved (*Z*)-2,2-difluoronon-3-en-1-ol (0.078 g, 0.44 mmol,

1.0 eq), in dry dichloromethane (0.1 mL, 5.0 M). The flask containing PCC was placed in an ice bath, at 0 °C and the alcohol mixture was added dropwise through a cannula. The reaction mixture was left overnight. Dry ether was added to the flask and the reaction mixture was run through a bed of celite and flushed with dry ether. The contents were dried using magnesium sulfate and the solvent was removed under reduced pressure, affording 0.09 g of a crude, colourless oil (68% yield). Shift change from starting alcohol indicated: ^{1}H-NMR [300 MHz; $CDCl_3$]: δ (ppm) 4.45 (t, J = 12.6 Hz, 1H), 5.41-5.66 (m, 1H), 5.85-6.00 (m, 1H). ^{13}C-NMR [75 MHz, $CDCl_3$]: δ (ppm) 13.9, 22.4, 28.5, 29.0, 29.6, 31.3, 65.4, 121.4, 140.9. ^{19}F NMR [282 MHz; $CDCl_3$] δ (ppm) -99.34 (dd, J = 15 Hz, 30 Hz).

***(Z)-1-Ethoxy-2,2-difluoronon-3-en-1-ol*. (2.19)** To a flame dried and argon filled flask, equipped with a stir bar was added (*Z*)-ethyl 2,2-difluoronon-3-enoate (0.05 g, 0.22 mmol, 1.0 eq). Dry ether was added (50 µL, 5.5 M) and the reaction flask was cooled to −78 °C. To a separate reaction flask at −78 °C was added LAH (0.0032 g, 0.75 mmol, 0.33 eq) and dry ether (100 µL, 0.8 M). The LAH and ether slurry was transferred to the first reaction flask via a cannula. The reaction mixture was maintained at a temperature of −78 °C, for 25 minutes, at which time the reaction was carefully quenched with ethanol. The reaction was slowly allowed to warm to room temperature. The contents were poured over a mixture of ice and sulfuric acid. The solution was extracted with ether (×3) and washed with brine. The solution was dried using magnesium sulfate, filtered and the solvent was removed under reduced pressure. The material was carried on crude due to hydrolysis/

degradation on silica column. ^{1}H-NMR [300 MHz; $CDCl_3$]: δ (ppm) 2.21-2.33 (m, 2H), 3.79 (t, *J* = 6Hz, 1H), 5.53-5.56 (m, 2H). ^{19}F NMR [282 MHz; $CDCl_3$] δ (ppm) -98.22 (dd *J* = 12 Hz, 300 Hz).

***(Z)-2,2-Difluoro-1-hydroxynon-3-en-1-yl 4-methylbenzenesulfonate*. (2.20)** To a flame dried and argon filled flask, equipped with a stir bar, was added (*Z*)-2,2-difluoronon-3-ene-1,1-diol (0.05 g, 0.25 mmol, 1.0 eq) and dry dichloromethane (1.3 mL, 0.2 M). To the solution was added dry pyridine (0.06 g, 0.75 mmol, 3.0 eq) dropwise, at 0°C, followed by tosyl chloride (0.051 g, 0.27 mmol, 1.05 eq). The reaction was left to stir overnight and slowly allowed to warm to room temperature. The reaction mixture was quenched with water and extracted with ether (×3), which was then washed with 1 M HCl and brine. The combined organic layers were dried using magnesium sulfate, filtered and the solvent was removed under reduced pressure. The material was carried on crude due to hydrolysis/ degradation on silica column. ^{1}H-NMR [300 MHz; $CDCl_3$]: δ (ppm) 0.88 (t, *J*= 6.2 Hz, 3H), 3.78 (t, *J*= 13.2 Hz), 5.35-5.47 (m, 1H), 5.55-5.89 (m, 1H), 7.30 (d, *J*= 5.9 Hz, 2H), 7.8 (d, J= 6 Hz, 2H). ^{19}F NMR [300 MHz; $CDCl_3$] δ (ppm) -99.00 (dd, *J*= 15 Hz, 251 Hz).

***(Z)-1-Bromo-2,2-difluorononon-3-ene*. (2.22)** To a flame dried and argon filled flask was added (*Z*)-2,2-difluoronon-3-en-1-ol (0.02 g, 0.11 mmol, 1.0 eq), triphenylphosphine (0.058 g, 0.22 mmol, 2.0 eq), tetrabromomethane (0.074 g, 0.22 mmol, 2.0 eq) and toluene (1.1 mL, 0.1 M). The flask was equipped with a reflux

condenser and the reaction was heated to 110 °C for several hours. The reaction mixture was cooled to room temperature and quenched with water. The mixture was extracted with hexanes (×3), which was then washed with brine. The combined organic layers were dried using magnesium sulfate, filtered and concentrated under reduced pressure. The material was carried on crude due to hydrolysis/ degradation on silica column. ^{1}H-NMR [300 MHz; $CDCl_3$]: δ (ppm) 0.88 (t, J = 6.8 Hz, 3H), 2.17-2.21 (m, 2H), 3.67 (t, J=8 Hz, 2H), 5.49-5.58 (m, 1H), 5.79-5.89 (m, 1H). ^{19}F NMR [282 MHz; $CDCl_3$] δ (ppm) -92.99 (dd, J=15Hz, 30Hz).

***(Z)-2,2-Difluoronon-3-en-1-yl 4-methylbenzenesulfonate*. (2.23)** To a flame dried and argon filled flask, equipped with a stir bar, was added (*Z*)-2,2-difluoronon-3-en-1-ol (0.05 g, 0.28 mmol, 1.0 eq) and dry dichloromethane (2.2 mL, 0.13 M). To the solution was added dry pyridine (0.088 g, 1.12 mmol, 4.0 eq) dropwise at 0 °C. The reaction mixture was cooled to −50 °C and a solution of tosyl chloride (0.093 g, 0.49 mmol, 1.8 eq), in dry dichloromethane (0.32 mL, 1.54 M), was added dropwise. The reaction was left to stir for two hours, after which it was quenched with methanol. Water was added to the reaction flask and the solution was extracted with ether (×3), which was then washed with 1 M HCl, sodium bicarbonate and brine. The combined organic layers were dried using magnesium sulfate, filtered and concentrated under reduced pressure. The material was carried on crude due to hydrolysis/ degradation on silica column. ^{1}H-NMR [300 MHz; $CDCl_3$]: δ (ppm) 0.88 (t, J = 6.8 Hz, 3H), 1.24-1.38 (m, 6H), 2.12-2.17 (m, 2H), 2.46 (s, 3H), 4.159 (t, J=11.7

Hz, 2H), 5.35-5.45 (m, 1H), 5.83-5.87 (m, 1H), 7.36 (d, *J*=8.7 Hz, 2H), 7.80 (d, *J*=8.7 Hz, 2H). ^{19}F NMR [282 MHz; $CDCl_3$] δ (ppm) -98.99 (dd, *J*=15 Hz, 30 Hz).

***(Z)-2,2-Difluorononon-3-en-1-yl trifluoromethanesulfonate*. (2.24)** To a flame dried and argon filled flask, equipped with a stir bar, was added (*Z*)-2,2-difluorononon-3-en-1-ol (0.05 g, 0.28 mmol, 1.0 eq) and dry dichloromethane (2.2 mL, 0.13 M). To the solution was added dry pyridine (0.088 g, 1.12 mmol, 4.0 eq), dropwise at 0 °C. The reaction mixture was cooled to −50 °C and a solution of trifluoromethanesulfonic anhydride (0.14 g, 0.49 mmol, 1.8 eq), in dry dichloromethane (0.32 mL, 1.5 M) was added dropwise. The reaction was left to stir for two hours, after which it was quenched with methanol. Water was added to the reaction flask and the solution was extracted with ether (×3), which was then washed with 1 M HCl, sodium bicarbonate and brine. The combined organic layers were dried using magnesium sulfate, filtered and concentrated under reduced pressure. The material was carried on crude due to hydrolysis/ degradation on silica column. ^{1}H-NMR [300 MHz; $CDCl_3$]: δ (ppm) 4.200 (t, *J*=11.5 Hz, 2H), 5.35-5.45 (m, 1H), 5.83-5.87 (m, 1H). ^{19}F NMR [282 MHz; $CDCl_3$] δ (ppm) -74.29 (s, 3F), -99.00 (dd, *J* = 15Hz, 30 Hz, 2F).

***Ethyl 2,2-difluoro-3-hydroxy-3-phenylpropanoate*. (2.32)** To a refluxing suspension of freshly activated zinc dust (0.05 g, 0.77 mmol, 1.1 eq) in dry THF (3.9 mL, 0.2 M), was added a solution of ethylbromodifluoroacetate (0.14 g, 0.7 mmol,

1.0 eq) and benzaldehyde (0.07 g, 0.7 mmol, 1.0 eq). After 30 minutes the reaction mixture was cooled to room temperature and quenched by the slow addition of ethyl acetate. The mixture was extracted with ethyl acetate (×3), which was then washed with brine and 1 M $NaHSO_4$. The combined organic layer was dried using $MgSO_4$, filtered and the solvent was removed under reduced pressure. The resulting yellow oil was purified by flash column chromatography on silica gel with 20% ethyl acetate in hexanes (R_f=0.2) to yield 0.09 g of a colourless oil (51% yield). ^{1}H-NMR [300 MHz; $CDCl_3$]: δ (ppm) 1.34 (t, J = 6.9 Hz, 3H), 4.12-4.25 (m, 2H), 2.82-2.85 (bs, 1H), 5.14-5.22 (m, 1H), 7.34-7.76 (m, 5H). Analytical data were in accordance with those reported in the literature.[7]

***(Z)-1,4-Bis(benzyloxy)but-2-ene*. (2.33)** To a solution of (*Z*)-butene-1, 4-diol (0.28 g, 3.1 mmol, 1.0 eq), in dry THF (dried by Na; 5.0 mL), was carefully added NaH (60% dispersion in mineral oil; 0.3365 g, 14.0 mmol, 4.4 eq) under inert atmosphere. The reaction mixture was heated to reflux for several hours and then cooled to room temperature. A solution of benzyl bromide (2.1 g, 12.1 mmol, 3.8 eq), in dry THF (dried by Na; 5 mL), was added dropwise to the stirred mixture, while maintaining room temperature. The reaction mixture was then heated again to reflux and left to stir for 2 hours, at which point it was cooled to room temperature and left to stir for several days. Water was added dropwise until all remaining NaH was destroyed. The THF was removed under reduced pressure and the resulting residue was taken up in dichloromethane and extracted (×3), which

was then washed with saturated ammonium chloride solution (×3), water (×3), and brine. The organic layers were dried using magnesium sulfate, filtered and concentrated under reduced pressure. The yellow residue was then purified by flash column chromatography on silica gel with 10% ethyl acetate in hexanes (R_f=0.3) to give the product in quantitative amounts. ^{1}H-NMR [300 MHz; $CDCl_3$]: δ (ppm) 4.07 (d, J = 4.4 Hz, 4H), 4.50 (s, 4H), 5.76-5.82 (m, 2H), 7.25-7.34 (m, 10H). Analytical data were in accordance with those reported in the literature.[8]

***2,3-Bis((benzyloxy)methyl)oxirane*. (2.34)** In a round bottom flask, equipped with a dropping funnel, magnetic stir bar and $CaCl_2$ drying tube, a solution of (*Z)*-butene-1, 4-diol (0.10 g, 0.37 mmol, 1.0 eq), in dry dichloromethane (1.32 mL, 0.3 M), was added. To this a solution of 80% mCPBA (0.29 g, 0.93 mmol, 2.0 eq), in dichloromethane (1.32 mL, 0.5 M) was slowly added. The resulting yellow solution was stirred at room temperature overnight. The reaction mixture was stirred with saturated sodium sulfite to reduce the excess mCPBA and then extracted with ether (×3), which was then washed with saturated sodium bicarbonate solution. The combined organic layers were dried using magnesium sulfate, filtered and concentrated under reduced pressure to give the epoxide as an oily semi-solid. ^{1}H-NMR [300MHz; $CDCl_3$]: δ (ppm) 3.21-3.25 (m, 2H), 3.49-3.52 (m, 2H), 3.60-3.67 (m, 2H), 4.45-4.50 (m, 2H), 7.25-7.35 (m, 10H). Analytical data were in accordance with those reported in the literature.[9]

***2-Benzyoxyaetaldehyde*. (2.27)** To a solution of (*Z*)-1,4-bis(benzyloxy)but-2-ene (1.0 g, 3.75 mmol, 1.0 eq), in 2.5 mmol/ml of dichloromethane/methanol mixture (7.0 ml:2.3 ml, 3:1), at −78 °C was bubbled a stream of ozone, until a blue colour was observed (times may vary). The excess ozone was removed by purging the solution with a stream of argon (disappearance of blue colour). The reaction flask was sealed with a rubber septum and dimethylsulfide (0.93 g, 15.0 mmol, 4.0 eq) was added at −78 °C, dropwise. The reaction mixture was warmed to ambient temperature and stirred over night. The solvents were removed under reduced pressure. After flash column chromatography on silica gel with hexanes (R_f=0.21), a faint yellow oil was obtained with a crude yield of 112%.

Crude ^{1}H-NMR, compared to those reported in the literature,[10] confirmed product formation with one co-eluting byproduct. Desired product: ^{1}H-NMR [300 MHz, $CDCl_3$] δ (ppm) 4.11 (s, 2H), 4.63 (s, 2H), 7.34-7.36 (m, 5H), 9.72 (s, 2H). Co-eluting byproduct: ^{1}H-NMR [300 MHz, $CDCl_3$] δ (ppm) 3.49 (s, 2H), 4.89 (s, 3H), 7.37 (m, 4H), 7.48 (m, 2H), 8.11 (d, J= 6.0Hz 2H).

***Ethyl 2,2-difluoro-3-hydroxynonanoate*. (2.30)** A schlenk flask equipped with a magnetic stir bar was flame dried under vacuo and flushed with argon. To the flask was added activated zinc (0.65 g, 1.0 mmol, 1.0 eq). The flask was resealed and vacuumed and placed under argon. To the flask was added dry THF (1.3 ml, 0.75 M, dried over Na). Ethyl bromodifluoroacetate (0.20 g, 1.0 mmol, 1.0 eq) was then

added dropwise at room temperature. The contents were left to stir for 15 minutes. Freshly distilled heptaldehyde (0.80 g, 0.7 mmol, 0.7 eq) was then added dropwise to the schlenk flask and left to stir overnight. The solution was quenched with 1 M HCl and extracted with ether (×3), which was then washed with brine. The combined organic layers were dried using magnesium sulfate, filtered and concentrated under reduced pressure. The residual oil was purified by flash column chromatography on silica gel with 30% ethyl acetate in hexanes (R_f= 0.51) to give 0.17 g of the alcohol (70% yield). ^{1}H-NMR [300 MHz; $CDCl_3$]: δ (ppm) 0.85-0.98 (m, 3H), 1.16-1.74 (m, 10H), 1.37 (t, J = 7.1 Hz, 3H), 1.97 (s, 1H), 3.93-4.13 (m, 1H), 4.36 (q, J = 7.1 Hz, 2H). Analytical data were in accordance with those reported in the literature.[11]

***Ethyl 2,2-difluoro-3-oxononanoate*. (2.31)** To a solution of ethyl 2,2-difluoro-3-hydroxynonanoate (0.06 g, 0.23 mmol, 1.0 eq), in dry dichloromethane (1.1 mL, 0.2 M), at room temperature, was added Dess-Martin reagent (0.15 g, 0.36 mmol, 1.5 eq) under inert atmosphere. After stirring for 2 hours, the reaction mixture was quenched with saturated sodium bicarbonate and saturated sodium thiosulfate. The mixture was extracted with ether (×3), which was then washed with brine. The combined organic layers were dried using magnesium sulfate, filtered and concentrated under reduced pressure. The residual oil was purified by flash column chromatography on silica gel with 20% ethyl acetate in hexanes (R_f=0.8) to yield 0.040 g of the desired ester (73% yield). ^{1}H-NMR [300 MHz; $CDCl_3$]: δ (ppm) 0.82-

1.01 (m, 3H), 1.21-1.49 (m, 6H), 1.36(t, *J*=7.1 Hz, 3H), 1.56-1.76 (m, 2H), 2.74 (m, 2H), 4.38 (q, *J*= 7.1 Hz, 2H). Analytical data were in accordance with those reported in the literature.[11]

Preparation of Dess-Martin Reagent

Step 1:

2-Iodobenzoic acid (1.0 g, 4.0 mmol, 1.0 eq) was added to a solution of oxone (3.2 g, 5.2 mmol, 1.3 eq) in deionized water (13.0 mL, 0.45 M). The reaction mixture was warmed to 75 °C over a period of 25 minutes. It was stirred at this temperature for 3 hours. The suspension was cooled to 0 °C and left to slowly stir overnight. The mixture was filtered and washed thoroughly with water and acetone. The residue was then dried under high vacuum for several hours.

Step 2:

A slurry of IBX (from above: 0.71 g, 2.53 mmol, 1.0 eq) in acetic anhydride (2.3 g, 23.5 mmol, 9.3 eq) and acetic acid (2 mL) was heated to 100 °C. After 40 minutes the solid had dissolved. The solvent was removed under vacuum at room temperature until a thick slurry remained. The slurry was filtered and washed with ether to give Dess-Martin reagent in an overall 82% yield from iodobenzoic acid. ^{1}H-NMR [300 MHz; $CDCl_3$]: δ ppm 1.99 (s, 6H), 2.32 (s, 3H), 7.91 (t, J= 7.1 Hz, 1H), 8.09 (t, J=8.1 Hz, 1H), 8.29 (d, J= 8.1 Hz, 2H). Analytical data were in accordance with

those reported in the literature.[12]

***Styrene glycol dimesylate*. (2.39)** To a round bottom flask, equipped with a stir bar, thermometer and dropping funnel, was added styrene glycol (0.5 g, 3.8 mmol, 1.0 eq) and freshly distilled pyridine (1.35 mL). The solution was cooled to −5 °C using an ice salt bath. Methanesulfonyl chloride (0.66 g, 8.5 mmol, 2.24 eq) was added dropwise over a period of several hours. The reaction mixture was stirred with ice, until a white precipitate formed. The solution was acidified to a pH of 3 using 1 M HCl. The contents were extracted using DCM (×3), which was then washed with brine. The combined organic layers were dried using magnesium sulfate, filtered and concentrated under reduced pressure. Pentane was slowly added until a cloudy appearance was observed, at which point the flask was placed in the freezer overnight. The resulting solid was collected and washed with cold pentane and dried for several hours under vacuum. White solid carried onto next step.

***1-Amino-2-phenylaziridine*. (2.40)** To a round bottom flask, equipped with a magnetic stir bar, was added hydrazine hydrate (0.31 g, 9.9 mmol, 14.7 eq). The finely powdered styrene glycol dimesylate (0.2 g, 0.7 mmol, 1.0 eq) was then added, with gentle stirring, at room temperature. To the resulting slurry was added 3 mL of pentane. The stirring speed was adjusted so that two phases (somewhat mixed) could be observed. After 24 hours of stirring at room temperature, two distinct layers were observed. The excess hydrazine hydrate was separated from the

pentane using a separatory funnel. The organic layer was filtered through cotton. No further isolation and purification as performed and contents were used immediately in the next step.

***1-Amino-2-phenylaziridinium acetate*. (2.41)** The pentane solution containing 2-phenylaziridine-1-amine (from above), at 0 °C was stirred and 0.04 mL of acetic acid was added dropwise. Stirring was continued until a white precipitate was observed. While maintaining the temperature at 0 °C, the salt was filtered and washed with cold pentane. The solid was dried in vacuo. Recrystallization can be performed using DCM, at no warmer than 20 °C. The turbid solution was filtered through celite and washed with DCM. The clear solution was then treated with pentane until crystallization began. The solution and crystals were kept cool in order to avoid the formation of a yellow byproduct. Crystallization yielded 0.46 g of 1-amino-2-phenylaziridinium acetate (63% yield). ^{1}H-NMR [300 MHz; $CDCl_3$]: δ (ppm) 1.95-2.20 (m, 5H), 2.67-2.95 (m, 1H), 6.50-6.70 (m, 3H), 7.28-7.40 (m, 5H). Analytical data were in accordance with those reported in the literature.[13]

4.3 Preparation of Compounds Described in Chapter 3

***5-Iodopyridin-2-amine*. (3.7)** To a flask, was added 2-aminopyridine (2.4 g, 25.0 mmol, 1.0 eq), periodic acid dehydrate (0.86 g, 3.75 mmol, 0.15 eq), iodine (3.2 g, 12.5 mmol, 0.5 eq) and a mixture of acetic acid (60 mL, 0.42 M), water (3.0 mL, 8.3 M) and sulfuric acid (0.5 mL, 50.0 M), under inert atmosphere. The mixture was heated to 80 °C for 4 hours. The reaction mixture was then cooled to room temperature and poured into a sodium thiosulfate solution to quench any unreacted iodine. The solution was extracted with ether (×3), which was then washed with 1 M NaOH and brine. The combined organic layers were dried using magnesium sulfate, filtered and concentrated under reduced pressure. The crude material was purified by flash column chromatography on silica gel with 25% ethyl acetate, 0.01 % triethylamine in hexanes (R_f=0/31) to afford 3.3 g of a yellow solid (60% yield). ^{1}H-NMR [300 MHz; $CDCl_3$]: δ (ppm) 7.16 (d, *J* = 8.6 Hz, 1H), 7.36 (d, *J* = 3.2 Hz, 1H) 8.36 (d, *J* = 3.1 Hz, 1H). Analytical data were in accordance with those reported in the literature.[14]

***2-(2,5-Dimethyl-1H-pyrrol-1-yl)-5-iodopyridine*. (3.8)** To 2-amino-5-bromopyridine (1.3 g, 5.8 mmol, 1.0 eq) and p-toluene sulfonic acid (0.46 g, 0.08 mmol, 0.005 eq), in toluene (5.0 mL, 1.2 M), was added 2,5-hexanedione (0.83 mL, 7.0 mmol, 1.2 eq). The mixture was refluxed using a Dean Stark apparatus overnight. The toluene was removed and the resulting product was extracted with ether (×3), which was then washed with water several times and brine. The

combined organic layers were dried using magnesium sulfate, filtered and concentrated under reduced pressure. The crude product was purified by flash column chromatography on silica gel with 35% ethyl acetate, 0.01 triethylamine in hexanes (R_f=0.25) to afford 1.3 g of a white solid (73% yield). ^{1}H-NMR [300 MHz; $CDCl_3$]: δ (ppm) 2.16 (s, 6H), 5.92 (s, 2H), 7.04-7.06 (d, *J* = 8.5 Hz, 1H), 8.11-8.15 (dd, *J* = 8.5, 2.5 Hz, 1H), 8.84 (d, *J* = 2.0 Hz, 1H). Analytical data were in accordance with those reported in the literature.[14]

***5-(Benzyloxy)-2-(2,5-dimethyl-1H-pyrrol-1-yl)pyridine*. (3.9)** To a dried and argon filled schlenk flask was added a mixture of CuI (0.045 g, 0.23 mmol, 0.1eq), 1,10-phenathroline (0.083 g, 0.46 mmol, 0.2 eq), cesium carbonate (1.1 g, 3.5 mmol, 1.5 eq) and 2-(2,5-dimethyl-1*H*-pyrrol-1-yl)-5-iodopyridine (0.69 g, 2.3 mmol, 1.0 eq), in toluene (3.0 mL, 0.8 M). To this reaction mixture was added benzyl alcohol (10 eq) and heated in an oil bath, at 110 °C, overnight. The reaction mixture was cooled to room temperature and filtered through celite. The solvent was removed under reduced pressure. The resulting brown mixture was purified by flash chromatography on silica gel with 35% ethyl acetate, 0.01% triethylamine in hexanes (R_f=0.6) to yield 0.49 g of a brown solid (76% yield). ^{1}H-NMR [300 MHz; $CDCl_3$]: δ (ppm) 2.16 (s, 6H), 5.17 (s, 2H), 5.89 (s, 2H), 7.16 (d, *J* = 8.6 Hz, 1H), 7.38-7.47 (m, 6H), 8.36 (d, *J* = 3.1 Hz, 1H). Analytical data were in accordance with those reported in the literature.[14]

***5-(Benzyloxy)pyridine-2-amine*. (3.10)** To a mixture of hydroxylamine hydrochloride (0.26 g, 4.2 mmol, 10 eq) and 5-(benzyloxy)-2-(2,5-dimethyl-1*H*-pyrrol-1-yl)pyridine (0.1 g, 0.39 mmol, 1.0 eq) in ethanol/water (2:1, 0.3 M), was added triethylamine (0.086 g, 0.86 mmol, 2.0 eq). The reaction mixture was heated to reflux overnight and the resulting product was quenched with cold HCl. The mixture was washed with ether, which was then adjusted to a pH of 10 using 6 M NaOH. The product was extracted with dichloromethane (×3), which was then washed with brine. The combined organic layers were dried using magnesium sulfate, filtered and concentrated under reduced pressure. The crude material was recrystallized with ethanol to yield 0.06 g of a yellow solid, in (78% yield). ^{1}H-NMR [300 MHz; $CDCl_3$]: δ (ppm) 5.17 (s, 2H), 5.89 (s, 2H), 7.16 (d, *J* = 8.6 Hz, 1H), 7.38-7.47 (m, 6H), 8.36 (d, *J* = 3.1 Hz, 1H). Analytical data were in accordance with those reported in the literature.[14]

***N-(5-(benzyloxy)pyridin-2-yl)acetamide*. (3.5)** To a solution of 5-(benzyloxy)pyridine-2-amine (0.024 g, 0.12 mmol, 1.0 eq), in dry dichloromethane (0.8 mL, 0.15 M) was added DMAP (0.0025 g, 0.024 mmol, 0.2 eq) and triethylamine (0.03 g, 0.24 mmol, 1.5 eq), followed by the dropwise addition of acetyl chloride (0.019 g, 0.242 mmol, 1.5 eq), at 0 °C. The reaction mixture was stirred overnight, quenched with brine. The mixture was then extracted with ether (×3), which was then washed with brine. The combined organic layers were dried using magnesium sulfate, filtered and concentrated under reduced pressure. The crude product was recrystallized from ethyl acetate, to yield 0.022 g of a yellow solid (78% yield). ^{1}H-

NMR [300 MHz; $CDCl_3$]: δ (ppm) 2.19 (s, 3H), 5.10 (s, 2H), 7.28-7.44 (m, 5H), 8.01 (d, *J* = 8.0 Hz, 1H), 8.14 (d, *J* = 3.2 Hz, 1H), 8.25 (d, *J* = 3.1 Hz, 1H). Analytical data were in accordance with those reported in the literature.[14]

***5-Bromopyrimidin-2-amine*. (3.17)** To a solution of 2-aminopyrimidine (10 g, 105 mmol, 1.0 eq) in acetonitrile (225 mL, 0.5 M) was added a catalytic amount of ammonium formate (0.65 g, 10.5 mmol, 0.1 eq). To this vigorously stirred solution was added in portions *N*-Bromosuccinamide (19 g, 105 mmol, 1.0 eq). The solution was left to stir for one hour. The white precipitate was filtered and washed thoroughly with copious amounts of water. Product was then placed under vacuo for 24 hours to remove any remaining solvents. No further purification was required and a quantitative amount product was obtained. ^{1}H-NMR [300 MHz; $CDCl_3$]: δ (ppm) 5.03 (bs, 2H), 8.42 (s, 2H). Analytical data were in accordance with those reported in the literature.[14]

***5-Bromo-2-(2,5-dimethyl-1H-pyrrol-1-yl)pyrimidine*. (3.18)** To a flame dried, argon filled, round bottom flask, equipped with a stir bar was added 2-amino-5-bromopyrimidine (2.0 g, 12 mmol, 1.0 eq) and p-toluenesulfonic acid (0.023 g, 0.08 mmol, 0.006 eq), dissolved in toluene (100 mL, 0.1 M). The solution was heated to reflux and all solids fully dissolved. 2,5-Hexanedione (1.6 g, 14 mmol, 1.2 eq) was added dropwise. The solution was left to reflux overnight. Once the reaction was complete, it was cooled to room temperature and water was added to the reaction

flask. The solution was extracted with ethyl acetate (×3), which was then washed with water (×3) and brine. The solution was dried using magnesium sulfate and filtered. The crude material was purified by flash column chromatography on silica gel with 20% ethyl acetate, 0.01% triethylamine in hexanes (R_f= 0.22) to afford 2.5 g of a white solid (86% yield). ^{1}H-NMR [300 MHz; $CDCl_3$]: δ (ppm) 2.40 (s, 6H), 5.50 (s, 2H), 8.00 (s, 2H). Analytical data were in accordance with those reported in the literature.[14]

***5-(Benzyloxy)-2-(2,5-dimethyl-1H-pyrrol-1-yl)pyrimidine*. (3.19)** To a flame dried, argon filled schlenk flask was added a mixture of copper iodide (0.23 g, 1.2 mmol, 0.1 eq), 1,10-phenathroline (0.27 g, 2.4 mmol, 0.2 eq), cesium carbonate (2.5 g, 18 mmol, 1.5 eq) and 5-bromo-2-(2,5-dimethyl-1*H*-pyrrol-1-yl)pyrimidine (3.0 g, 12 mmol, 1.0 eq), in toluene (20 mL, 0.5 M). Benzyl alcohol (12.3 mL, 119 mmol, 10 eq) was added and reaction was heated to 110 °C using an oil bath, overnight. The reaction mixture was cooled to room temperature and filtered through celite. The solvent was removed under reduced pressure. The resulting brown mixture was purified by flash chromatography on silica gel using a gradient mobile phase. The excess BnOH was removed with 5% ethyl acetate, 0.01% triethylamine in hexanes, followed by isolation of product using 10 % ethyl acetate, 0.01% triethylamine in hexanes, to afford 2.7 g a yellow solid (81% yield). ^{1}H-NMR [300 MHz; $CDCl_3$]: δ (ppm) 2.26 (s, 6H), 5.19 (s, 2H), 5.87 (s, 2H), 7.43-7.45 (m, 5H), 8.49 (s, 2H).

Analytical data were in accordance with those reported in the literature.[14]

***5-(Benzyloxy)pyrimidin-2-amine*. (3.20)** To a mixture of hydroxylamine hydrochloride (6.1 g, 100 mmol, 10 eq) and 5-(benzyloxy)-2-(2,5-dimethyl-1*H*-pyrrol-1-yl)pyrimidine (2.8 g, 10 mmol, 1.0 eq) in ethanol/water (2:1, 0.3 M), was added triethylamine (3.1 mL, 20 mmol, 2.0 eq). The reaction mixture was heated to reflux for two days, at which point it was quenched with cold HCl. The mixture washed with ether (×3), which was then adjusted to a pH of 10 with 6 M NaOH. The product was extracted with dichloromethane (×3), dried using magnesium sulfate, filtered and concentrated under reduced pressure. The crude material was recrystallized from ethanol, to afford1.5 g of a yellow solid (75% yield). ^{1}H-NMR [300 MHz; $CDCl_3$]: δ (ppm) 5.13 (s, 2H), 7.37-7.44 (m, 5H), 8.07 (s, 2H). Analytical data were in accordance with those reported in the literature.[14]

***N-(5-(benzyloxy)pyrimidin-2-yl)acetamide*. (3.6)** To a solution of 5-(benzyloxy)pyrimidin-2-amine (0.14 g, 0.67 mmol, 1.0 eq), in dry dichloromethane (3.0 mL, 0.4 M), was added DMAP (0.014 g, 0.13 mmol, 0.2 eq) and dry pyridine (81 µL, 1.0 mmol, 1.5 eq), followed by the dropwise addition of acetyl chloride (66 µL, 0.94 mmol, 1.4 eq), at 0 °C. The reaction mixture was stirred overnight and slowly quenched with brine. The mixture was extracted with ether (×3), which was then washed with brine. The combined organic layers were dried using magnesium

sulfate, filtered and concentrated under reduced pressure. The product was recrystallized from ethyl acetate, to afford 0.15 g of a white solid (91% yield). ^{1}H-NMR [300 MHz; $CDCl_3$]: δ (ppm) 2.39 (s, 3H), 5.12 (s, 2H), 7.36-7.42 (m, 5H), 8.04 (bs, 1H), 8.31 (s, 2H). Analytical data were in accordance with those reported in the literature.[14]

***N-(5-(benzyloxy)pyrimidin-2-yl)butyramide*. (3.12)** To a solution of 5-(benzyloxy)pyrimidin-2-amine (0.50 g, 2.49 mmol, 1.0 eq), in dry dichloromethane (6.2 mL, 0.4 M), was added DMAP (0.051 g, 0.5 mmol, 0.2 eq) and dry pyridine (0.3 mL, 3.7 mmol, 1.5 eq), followed by the dropwise addition of butyryl chloride (0.36 mL, 3.5 mmol, 1.4 eq), at 0 °C. The reaction mixture was stirred overnight and slowly quenched with brine. The mixture was extracted with ether (×3), which was then washed with brine. The combined organic layers were dried using magnesium sulfate, filtered and concentrated under reduced pressure. The product was recrystallized from ethyl acetate, to afford 0.61 g of a white solid (90% yield). ^{1}H-NMR [400 MHz; $CDCl_3$]: δ (ppm) 1.01 (t, *J* = 7.4 Hz, 3H), 1.73-1.79 (m, 2H), 2.57-2.59 (t, *J* = 7.4 Hz, 2H), 5.12 (s, 2H), 7.37-7.41 (m, 5H), 8.04 (bs, 1H), 8.32 (s, 2H). ^{13}C-NMR [75 MHz; $CDCl_3$]: δ (ppm) 14.3, 19.1, 39.8, 71.9, 128.1, 129.2, 129.4, 135.9, 146.0, 149.7, 152.0, 172.1. HRMS (EI) calculated ($C_{15}H_{17}N_3O_2$): 271.1321, observed: 271.1323.

***N-(5-(benzyloxy)pyrimidin-2-yl)hexanamide*. (3.14)** To a solution of 5-(benzyloxy)pyrimidin-2-amine (0.11 g, 0.55 mmol, 1.0 eq), in dry dichloromethane

(6.2 mL, 0.4 M), was added DMAP (0.011 g, 0.1 mmol, 0.2 eq) and dry pyridine (66.5 µL, 0.83 mmol, 1.5 eq), followed by the dropwise addition of hexanoyl chloride (107 µL, 0.77 mmol, 1.4 eq), at 0 °C. The reaction mixture was stirred overnight and slowly quenched with brine. The mixture was extracted with ether (×3), which was then washed with brine. The combined organic layers were dried over magnesium sulfate, filtered and concentrated under reduced pressure. The product was recrystallized from ethyl acetate, to afford 0.15 g of a white solid (91% yield). ^{1}H-NMR [400 MHz; $CDCl_3$]: δ (ppm) 0.88 (t, *J* = 7.4 Hz, 3H), 1.32-1.36 (m, 4H), 1.69-1.73 (m, 2H), 2.56 (t, *J* = 7.4 Hz, 2H), 5.10 (s, 2H), 7.24-7.38 (m, 5H), 8.18 (bs, 1H), 8.31 (s, 2H). ^{13}C-NMR [75 MHz; $CDCl_3$]: δ (ppm) 13.9, 22.4, 24.8, 31.4, 37.4, 71.3, 127.6, 128.6, 128.8, 135.3, 145.4, 149.1, 151.4, 172.1. HRMS (EI) calculated ($C_{17}H_{21}N_3O_2$): 299.1634, observed: 299.1635.

***N-(5-(benzyloxy)pyrimidin-2-yl)octanamide*. (3.16)** To a solution of 5-(benzyloxy)pyrimidin-2-amine (0.11 g, 0.55 mmol, 1.0 eq), in dry dichloromethane (6.2 mL, 0.4 M), was added DMAP (0.011 g, 0.11 mmol, 0.2 eq) and dry pyridine (66.5 µL, 0.83 mmol, 1.5 eq), followed by the dropwise addition of octanoyl chloride (133 µL, 0.77 mmol, 1.4 eq), at 0 °C. The reaction mixture was stirred overnight and slowly quenched with brine. The mixture was extracted with ether (×3), which was then washed with brine. The combined organic layers were dried using magnesium sulfate, filtered and concentrated under reduced pressure. The product was recrystallized from ethyl acetate, to afford 0.18 g of a white solid (92% yield). ^{1}H-NMR [400 MHz; $CDCl_3$]: δ (ppm) 0.87 (t, *J* = 6.9 Hz, 3H), 1.26-1.38 (m, 8H), 1.70-1.74

(m, 2H), 2.59 (dq, J = 1.3, 0.4 Hz, 2H), 5.12 (s, 2H), 7.36-7.41 (m, 5H), 8.12-8.16 (bs, 1H), 8.32 (s, 2H). ^{13}C-NMR [75 MHz; $CDCl_3$]: δ (ppm) 14.0, 22.6, 25.1, 29.0, 29.2, 31.6, 37.3, 71.3, 127.6, 128.6, 128.9, 135.3, 145.4, 149.1, 151.6, 172.7. HRMS (EI) calculated ($C_{19}H_{25}N_3O_2$): 327.1947, observed: 327.1940.

***N-(5-hydroxypyrimidin-2-yl)acetamide*. (3.4)** A solution of *N*-(5-(benzyloxy)pyrimidin-2-yl)acetamide (0.03 g, 0.12 mmol, 1.0 eq) in methanol (3.5 mL, 0.04 M), was treated with 10% Pd/C (0.003 g, 10 mol%) and the resulting black suspension was stirred at room temperature under H_2 atmosphere overnight. The catalyst was removed by filtration through a pad of celite and the filtrate was concentrated under reduced pressure. The residue was purified by flash column chromatography on silica gel with 20% ethyl acetate, 1% triethylamine in hexanes (R_f=0.18) to quantitatively afford a white solid. ^{1}H-NMR [300 MHz; DMSO-d_6]: δ (ppm) 2.08 (s, 3H), 8.13 (s, 2H), 10.20 (bs, 1H), 10.28 (s, 1H). Analytical data were in accordance with those reported in the literature.[14]

***N-(5-hydroxypyrimidin-2-yl)butyramide*. (3.11)** A solution of *N*-(5-(benzyloxy)pyrimidin-2-yl)butyramide (0.03 g, 0.11 mmol, 1.0 eq) in methanol (3.2 mL, 0.04 M) was treated with 10% Pd/C (0.003 g, 10 mol%) and the resulting black suspension was stirred at room temperature under H_2 atmosphere overnight. The catalyst was removed by filtration through a pad of celite and the filtrate was concentrated under reduced pressure. The residue was purified by flash column

chromatography on silica gel with 20% ethyl acetate, 1% triethylamine in hexanes (R_f=0.18) to quantitatively afford a white solid. ^{1}H-NMR [300 MHz; DMSO-d_6]: δ (ppm) 0.93 (t, J = 7.4 Hz, 3H), 1.61 (q, J = 7.4 Hz, 2H), 2.36-2.41 (m, 2H), 8.24 (s, 2H), 10.25 (s, 1H). ^{13}C-NMR [75 MHz; DMSO-d_6]: δ (ppm) 14.1, 18.7, 38.3, 145.3, 148.6, 150.7, 171.3. HRMS (ESI$^+$) calculated ($C_8H_{11}N_3O_2$): 181.0850, observed: 181.0844.

***N-(5-hydroxypyrimidin-2-yl)hexanamide*. (3.13)** A solution of *N*-(5-(benzyloxy)pyrimidin-2-yl)hexanamide (0.03 g, 0.10 mmol, 1.0 eq) in methanol (3.0 mL, 0.04 M) was treated with 10% Pd/C (0.003 g, 10 mol%) and the resulting black suspension was stirred at room temperature under H_2 atmosphere overnight. The catalyst was removed by filtration through a pad of celite and the filtrate was concentrated under reduced pressure. The residue was purified by flash column chromatography on silica gel with 20% ethyl acetate, 1% triethylamine in hexanes (R_f=0.18) to quantitatively afford a white solid. ^{1}H-NMR [300 MHz; DMSO-d_6]: δ (ppm) 0.86 (t, J = 6.8 Hz, 3H), 1.23-1.28 (m, 4H), 1.53 (m, 2H), 2.35 (t, J = 7.4 Hz, 2H), 8.22 (s, 2H), 10.21 (s, 1H). ^{13}C-NMR [75 MHz; DMSO-d_6]: δ (ppm) 14.3, 22.3, 25.0, 31.3, 36.3, 145.3, 148.6, 150.6, 171.5. HRMS (ESI$^+$) calculated ($C_{10}H_{15}N_3O_2$): 209.1164, observed: 209.1132.

***N-(5-hydroxypyrimidin-2-yl)octanamide*. (3.15)** A solution of *N*-(5-(benzyloxy)pyrimidin-2-yl)octanamide (0.03 g, 0.09 mmol, 1.0 eq) in methanol (0.003 g, 0.04 M) was treated with 10% Pd/C (0.003 g, 10 mol%) and the resulting black suspension was stirred at room temperature under H_2 atmosphere overnight.

The catalyst was removed by filtration through a pad of celite and the filtrate was concentrated under reduced pressure. The residue was purified by flash column chromatography on silica gel with 20% ethyl acetate, 1% triethylamine in hexanes (R_f=0.18) to quantitatively afford a white solid. ^{1}H-NMR [300 MHz; DMSO-d_6]: δ (ppm) 0.88 (t, J = 6.8 Hz, 3H), 1.22-1.230 (m, 8H), 1.53-1.56 (m, 4H), 2.33 (t, J = 7.4 Hz, 2H), 8.20 (s, 2H), 10.18 (s, 1H). ^{13}C-NMR [75 MHz; DMSO-d_6]: δ (ppm) 14.4, 22.5, 25.3, 28.9, 29.0, 31.6, 36.3, 145.3, 148.5, 150.7, 171.4.

***2-(2,5-Dimethyl-1H-pyrrol-1-yl)-5-methoxypyrimidine*. (3.22)** To a seal tube, equipped with a stir bar and flushed with argon was added toluene (5.0 mL, 0.8 M). A stream of argon was bubbled through the toluene. To the reaction vessel was added copper iodide (0.019 g, 0.1 mmol, 0.1 eq), 1,10-phenathroline (0.072 g, 0.4 mmol, 0.4 eq), cesium carbonate (0.48 g, 1.5 mmol, 1.5 eq) and 5-bromo-2-(2,5-dimethyl-1*H*-pyrrol-1-yl)pyrimidine (0.25 g, 1.0 mmol, 1.0 eq). To the seal tube sodium methoxide was quickly added via syringe (0.6 mL, 10 mmol, 10.0 eq) and the seal tube was capped. The mixture immediately turned a bright orange and the reaction was left to heat at 90 °C overnight. The mixture was allowed to cool down to room temperature and the contents were filtered over a bed of celite. The solvent was removed under reduced pressure. The resulting brown mixture was purified by flash column chromatography on silica gel with 20% ethyl acetate, 0.01% triethylamine in hexanes (R_f= 0.22) to afford 0.16 g of a white solid (80% yield). ^{1}H-NMR [400 MHz; $CDCl_3$]: δ (ppm) 2.26 (s, 6H), 3.96 (s, 3H), 5.87 (s, 2H), 8.44 (s, 2H).

^{13}C-NMR [75 MHz; $CDCl_3$]: δ (ppm) 14.0, 69.2, 107.6, 129.2, 144.5, 150.9, 151.4. HRMS (EI) calculated ($C_{11}H_{13}N_3O$): 203.1059, observed: 203.1023.

***5-Butoxy-2-(2,5-dimethyl-1H-pyrrol-1-yl)pyrimidine*. (3.23)** To a flame dried and argon filled schlenk flask was added a mixture of copper iodide (0.19 g, 0.1 mmol, 0.1 eq), 1,10-phenathroline (0.072 g, 0.4 mmol, 0.4 eq), cesium carbonate (0.49 g, 1.5 mmol, 1.5 eq) and 5-bromo-2-(2,5-dimethyl-1*H*-pyrrol-1-yl)pyrimidine (0.25 g, 1.0 mmol, 1.0 eq), in toluene (5.0 mL, 0.8 M). Butanol (1.0 mL, 10 mmol, 10.0 eq) was added and heated to 110 °C, using an oil bath, overnight. The reaction mixture was filtered through celite and the solvent was removed under reduced pressure. The resulting brown mixture was purified by flash chromatography on silica gel with 20% ethyl acetate, 0.01% triethylamine in hexanes (R_f= 0.22) to afford 0.20 g of a clear, colourless oil (80% yield). ^{1}H-NMR [400 MHz; $CDCl_3$]: δ (ppm) 0.99 (t, J = 7.4 Hz, 3H), 1.50-1.52 (m, 2H), 1.79-1.81 (m 2H), 2.23 (s, 6H), 4.08 (t, J = 6.4 Hz, 2H), 5.84 (s, 2H), 8.40 (s, 2H). ^{13}C-NMR [75 MHz; $CDCl_3$]: δ (ppm) 13.7, 13.8, 19.0, 31.0, 68.8, 107.5, 129.2, 144.5, 150.9, 151.3. HRMS (EI) calculated ($C_{14}H_{19}N_3O$): 245.1528, observed: 245.1504.

***2-(2,5-Dimethyl-1H-pyrrol-1-yl)-5-(hexyloxy)pyrimidine*. (3.24)** To a flame dried and argon filled schlenk flask was added a mixture of copper iodide (0.019 g, 0.1 mmol, 0.1 eq), 1,10-phenathroline (0.072 g, 0.4 mmol, 0.4 eq), cesium carbonate (0.48 g, 1.5 mmol, 1.5 eq) and 5-bromo-2-(2,5-dimethyl-1*H*-pyrrol-1-yl)pyrimidine (0.25 g, 1.0 mmol, 1.0 eq), in toluene (5.0 mL, 0.8 M). Hexanol (1.25 mL, 10 mmol,

10.0 eq) was added and heated 110 °C, using and oil bath, overnight. The reaction mixture was filtered through celite and the solvent was removed under reduced pressure. The resulting brown mixture was purified by flash chromatography on silica gel with 20% ethyl acetate, 0.01% triethylamine in hexanes (R_f= 0.22) to afford 0.22 g of a clear, colourless oil (79% yield). ^{1}H-NMR [400 MHz; $CDCl3_3$]: δ (ppm) 0.94 (t, J = 7.0 Hz, 3H), 1.37 (dq, J = 7.1, 3.5 Hz, 4H), 1.48-1.52 (m, 2H), 1.82-1.86 (m, 2H), 2.26 (s, 6H), 4.09 (t, J = 6.5 Hz, 2H), 5.87 (s, 2H), 8.42 (s, 2H). ^{13}C-NMR [75 MHz; $CDCl_3$]: δ (ppm) 13.8, 14.0, 22.5, 25.5, 29.0, 31.4, 69.2, 107.5, 129.2, 144.5, 150.9, 151.4. HRMS (EI) calculated ($C_{16}H_{23}N_3O$): 273.1841, observed: 273.1849.

***2-(2,5-Dimethyl-1H-pyrrol-1-yl)-5-(octyloxy)pyrimidine*. (3.25)** In a flame dried and argon filled schlenk flask was added a mixture of CuI (0.019 g, 0.1 mmol, 0.1 eq), 1,10-phenathroline (0.072 g, 0.4 mmol, 0.4 eq), cesium carbonate (0.48 g, 1.5 mmol, 1.5 eq) and 5-bromo-2-(2,5-dimethyl-1*H*-pyrrol-1-yl)pyrimidine (0.25 g, 1.0 mmol, 1.0 eq), in toluene (5.0 mL, 0.8 M). Octanol (1.57 g, 10 mmol, 10.0 eq) was added and heated to 110 °C, using an oil bath, overnight. The reaction mixture was filtered through celite and the solvent was removed under reduced pressure. The resulting brown mixture was purified by flash chromatography on silica gel with 20% ethyl acetate, 0.01% triethylamine in hexanes (R_f= 0.22) to afford 0.20 g of a clear, colourless oil (67% yield). ^{1}H-NMR [400 MHz; $CDCl_3$]: δ (ppm) 0.90 (t, J = 6.5 Hz, 3H), 1.26-1.35 (m, 10H), 1.85 (m, 2H), 2.26 (s, 6H), 4.09 (t, J = 6.4 Hz, 2H), 5.87 (s, 2H), 8.42 (s, 2H). ^{13}C-NMR [75 MHz; $CDCl_3$]: δ (ppm)13.8, 14.0, 14.8, 22.6, 25.8, 29.1,

29.1, 31.7, 69.2, 107.5, 129.2, 144.5, 150.9, 158.5. HRMS (EI) calculated ($C_{18}H_{27}N_3O$): 301.2154, observed: 301.2170.

***5-(Hex-1-yn-1-yl)pyrimidin-2-amine*. (3.26)** A solution of 2-amino-5-bromo (0.50 g, 2.9 mmol, 1.0 eq), in distilled DMSO (3.8 mL, 0.75 M) and dry triethylamine (2.5 mL, 1.15 M) was deoxygenated with a stream of argon. To this solution the addition of 1-hexyne (0.26 g, 0.38 mL, 3.2 mmol, 1.11 eq), followed by the addition of $(Ph_3P)_4Pd$ (0.1712 g, 0.148 mmol, 0.05 eq) and CuI (0.044 g, 0.22 mmol, 0.08 eq) was performed. The mixture was left to stir overnight, at 55 °C, after which point all volatiles were evaporated under reduced pressure. The resulting residue was suspended in hot MeOH and filtered using paper. Water was added to the solution and a yellow filtrate was collected. Further purification of the material was performed by recrystallization from methanol, to afford 0.40 g of a yellow solid (80% yield). Note: Do not place on column. ^{1}H-NMR [400 MHz; $CDCl_3$]: δ (ppm) 0.95 (t, J = 6.4 Hz, 3H), 1.42-1.62 (m, 4H), 2.40 (t, J = 6.9 Hz, 2H), 5.30 (bs, 2H), 8.31 (s, 2H). Analytical data were in accordance with those reported in the literature.[15]

***5-Hexylpyrimidin-2-amine.* (3.27)** A solution of 5-(hex-1-yn-1-yl)pyrimidin-2-amine (0.20 g, 1.1 mmol, 1.0 eq) in ethanol (10 mL, 0.11 M) was hydrogenated at 1200 psi and 60 °C, using 20% Pd/C (0.04 g), and H_2 gas. The solution was cooled to room temperature and filtered through filter paper. All volatiles were evaporated.

Further purification was performed from ethyl acetate, to quantitatively afford a yellow to white solid. ^{1}H-NMR [400 MHz; $CDCl_3$]: δ (ppm) 0.95 (t, *J*= 6.4 Hz, 3H), 1.42-1.72 (m, 6H), 1.73-1.81 (m, 2H), 2.42 (t, *J*= 6.9 Hz, 2H), 5.30 (bs, 2H), 8.29 (s, 2H). Analytical data were in accordance with those reported in the literature.[15]

***N-(5-hexylpyrimidin-2-yl)acetamide*. (3.28)** To a solution of 5-hexylpyrimidin-2-amine (0.020 g, 0.11 mmol, 1.0 eq), in dry dichloromethane (3.0 mL, 0.035 M), was added DMAP (0.0024 g, 0.022 mmol, 0.2 eq) and dry pyridine (13 μL, 0.17 mmol, 1.5 eq), followed by the dropwise addition of acetyl chloride (11 μL, 0.154 mmol, 1.4 eq), at 0 °C. The reaction mixture was stirred overnight and slowly quenched with brine. The mixture was extracted with ether (×3), which was then washed with brine. The combined organic layers were dried using magnesium sulfate, filtered and concentrated under reduced pressure. The product was recrystallized from ethyl acetate, to afford 0.02 g of a white solid (82% yield). ^{1}H-NMR [300 MHz; $CDCl_3$]: δ (ppm) 0.93 (t, *J* = 6.4 Hz, 3H), 1.30-1.36 (m, 6H), 1.63-1.65 (t, *J* = 6.9 Hz, 2H), 2.53 (s, 2H), 2.61 (m, 2H), 8.49 (s, 2H), 9.10 (s, 1H). ^{13}C-NMR [75 MHz; $CDCl_3$]: δ (ppm) 14.0, 22.5, 25.1, 28.6, 29.7, 30.8, 31.5, 130.0, 156.0, 157.8, 171.4. HRMS (EI) calculated ($C_{12}H_{19}N_3O$): 221.1528, observed: 221.1524.

***N-(5-hexylpyrimidin-2-yl)butyramide*. (3.29)** To a solution of 5-hexylpyrimidin-2-amine (0.020 g, 0.11 mmol, 1.0 eq), in dry dichloromethane (3.0 mL, 0.035 M) was added DMAP (0.0024 g, 0.022 mmol, 0.2 eq) and dry pyridine (13 μL, 0.17 mmol, 1.5 eq), followed by the dropwise addition of butyryl chloride (16 μL, 0.154 mmol, 1.4

eq), at 0 °C. The reaction mixture was stirred overnight and slowly quenched with brine. The mixture was extracted with ether (×3), which was then washed with brine. The combined organic layers were dried using magnesium sulfate, filtered and concentrated under reduced pressure. The product was recrystallized from ethyl acetate, to afford 0.022g of a white solid (81% yield). ^{1}H-NMR [300 MHz; $CDCl_3$]: δ (ppm) 0.86-0.90 (t, J = 6.4 Hz, 3H), 1.01 (t, J = 6.9 Hz, 3H), 1.25-1.35 (m, 6H), 1.57-1.61 (m, 2H), 1.73-1.81 (m, 2H), 2.52-2.57 (m, 2H), 2.63-2.68 (m, 2H), 8.34-8.37 (s, 1H), 8.41 (s, 2H). ^{13}C-NMR [75 MHz; $CDCl_3$]: δ (ppm) 13.7, 22.2, 24.8, 28.2, 28.3, 29.3, 29.4, 30.5, 31.1, 129.7, 155.7, 157.5, 171.1. HRMS (EI) calculated ($C_{14}H_{23}N_3O$): 249.1841, observed: 249.1847.

4.4 Spectrophotometric Determination of pK_a Values

A solution of 10 mM potassium phosphate and 200 mM KCl was adjusted to the desired pH using 1-5 M KOH or 1 M HCl in the range of pH 2-14. The buffer solution (2 mL) was transferred to a cuvette and a blank UV spectrum was recorded on an Agilent 8453 diode array spectrophotometer. To this solution, a concentrated solution of inhibitor in absolute ethanol (25 mmol) was added and the UV spectrum was recorded and the pH was measured.

4.5 Inhibition of sLOX-1

To a final concentration of 20 μM LA (in ethanol) in 100 mM borate buffer (pH 9.2) was added inhibitor as a concentrated solution in ethanol or DMSO (to a final concentrations of 2.5-1000 μM depending on the inhibitor and less than 5% ethanol

and 3% DMSO, by volume), and the sLOX-1 (Lipoxidase from *Glycine max)* to a final concentration of 3 nM. The initial rates were then plotted as a function of added inhibitor concentration relative to the initial rates measured under identical experimental conditions, but without added inhibitor.

4.6 Oxidative Stability Experiments

4.6.1 Under Air

A solution of 100 mM borate buffer (pH 9.2) was transferred to a cuvette and a blank UV spectrum was recorded on an Agilent 8453 diode array spectrophotometer. To this solution, a concentrated solution of inhibitor in absolute ethanol (to a final concentration of 25 μM) was added and the UV spectrum was recorded every five minutes for 1 hour.

4.6.2 Under Argon

A solution of 100 mM borate buffer (pH 9.2) purged with argon was transferred to a cuvette, under inert atmosphere and a blank UV spectrum was recorded on an Agilent 8453 diode array spectrophotometer. To this solution, a concentrated solution of inhibitor in absolute ethanol (to a final concentration of 25 μM) purged with argon was added, under inert atmosphere and the UV spectrum was recorded every five minutes for 1 hour.

4.7 References

(1) Zhang, T.; Ma, W.-L.; Li, T.-R.; Wu, J.; Wang, J.-R.; Du, Z.-T. *Mol. Cells* **2013**, *18*, 5201.

(2) Tranchepain, I.; Le Berre, F.; Duréault, A.; Le Merrer, Y.; Depezay, J. C. *Tetrahedron.* **2001**, *45*, 2057.

(3) Kyi, S.; Wongkattiya, N.; Warden, A. C.; O'Shea, M. S.; Deighton, M.; Macreadie, I.; Graichen, F. H. M. *Bioorg. Med. Chem. Lett.* **2010**, *20*, 4555.

(4) Seyferth, D.; Heeren, J. K.; Singh, G.; Grim, S. O.; Hughes, W. B. *J. Organomet. Chem.* **2000**, *5*, 267.

(5) Kellersmann, C.; Steinhart, H.; Francke, W. *Lipids.* **2006**, *41*, 777.

(6) Denmark, S. E.; Wang, Z. *Org. Synth*. **2004**, 42.

(7) Hallinan, E.; Fried, J. *Tetrahedron Lett.* **2000**, *25*, 2301.

(8) Nishizono, N.; Akama, Y.; Agata, M.; Sugo, M.; Yamaguchi, Y.; Oda, K. *Tetrahedron.* **2011**, *67*, 358.

(9) Garner, P.; Park, J. M. *Synth. Commun.* **1987**, *17*, 189.

(10) Pollex, A.; Millet, A.; Müller, J.; Hiersemann, M.; Abraham, L. *J. Org. Chem.* **2005**, *70*, 5579.

(11) Fukuda, H.; Kitazume, T. *J. Fluorine Chem.* **2003**, *74*, 171.

(12) Dess, D. B.; Martin, J. C. *J. Org. Chem.* **1983**, *48*, 4155.

(13) Müller, R. K.; Joos, R.; Felix, D.; Schreiber, J.; Wintner, C.; Eschenmoser, A. *Org. Synth.* 114.

(14) Nam, T.-G.; Nara, S. J.; Zagol-Ikapitte, I.; Cooper, T.; Valgimigli, L.; Oates, J. A.; Porter, N. A.; Boutaud, O.; Pratt, D. A. *Org. Biomol. Chem.* **2009**, *7*, 5103.

(15) Robins, M. J.; Nowak, I.; Rajwanshi, V. K.; Miranda, K.; Cannon, J. F.; Peterson, M. A.; Andrei, G.; Snoeck, R.; De Clercq, E.; Balzarini, J. *J. Med. Chem.* **2007**, *50*, 3897.